Design Improvement of the Front End Shape and Headroom to Reduce Drag and Improve Stability in a Modified ISUZU Bus

Alemshet Lemi Hirpo

A Thesis Submitted to the Department of Mechanical Engineering

College of Mechanical, Chemical and Materials Engineering

Office of Graduate Studies

Adama Science and Technology University

May, 2025

Adama, Ethiopia

Design Improvement of the Front End Shape and Headroom to Reduce Drag and Improve Stability in a Modified ISUZU Bus

Alemshet Lemi Hirpo

Advisor:

Alemayehu Wakjira Huluka (PhD)

A Thesis Submitted to the Department of Mechanical Engineering

College of Mechanical, Chemical and Materials Engineering

Office of Graduate Studies

Adama Science and Technology University

May, 2025

Adama, Ethiopia

DECLARATION

I hereby declare that this thesis entitled “Design Improvement of the Front End Shape and Headroom to Reduce Drag and Improve Stability in a Modified ISUZU Bus” is my own work and has not been submitted to any university for similar purpose. The references used in this thesis are duly recognized by proper citations.

Alemshet Lemi Hirpo ______	________________________	________________
Name of student	Signature	Date

RECOMMENDATION

I, the advisor of this thesis, hereby certify that we have read the revised version of the thesis entitled "Design Improvement of the Front End Shape and Headroom to Reduce Drag and Improve Stability in a Modified ISUZU Bus" prepared under my guidance by Alemshet Lemi Hirpo. Therefore, recommend the submission of a revised version of the thesis to the department following the applicable procedures.

Alemayehu Wakjira Huluka (PhD) ___________________________ ______________________

Major Advisor Signature Date

APPROVAL PAGE

I, the advisor of the thesis entitled "Design Improvement of the Front End Shape and Headroom to Reduce Drag and Improve Stability in a Modified ISUZU Bus" and developed by Alemshet Lemi Hirpo, hereby certify that the recommendation and suggestions made by board of examiners are appropriately incorporated into the final version of the thesis.

Alemayehu Wakjira Huluka (PhD) ______________________ ____________________

Major Advisor Signature Date

We, the undersigned, members of the Board of Examiners of the thesis by Alemshet Lemi Hirpo have read and evaluated the thesis entitled "Design Improvement of the Front End Shape and Headroom to Reduce Drag and Improve Stability in a Modified ISUZU Bus" and examined the understanding of the candidate during open defense. This is, therefore, to certify that the thesis is accepted for partial fulfillment of the requirement of Master of Science in Automotive Engineering

___________________________ ____________________ __________________

Chairperson Signature Date

___________________________ ____________________ __________________

Reviewer 1 Signature Date

___________________________ ____________________ __________________

Reviewer 2 Signature Date

Final approval and acceptance of the thesis is contingent upon submission of its final copy to the Office of Postgraduate Studies (OPGS) through the Department Graduate Council (DGC) and School Graduate Committee (SGC).

__________________________ ____________________ __________________

Department Head Signature Date

___________________________ ____________________ __________________

School Dean Signature Date

___________________________ ____________________ __________________

Office of Postgraduate Studies, Dean Signature Date

ACKNOWLEDGEMENT

First of all, I would like to thank my teacher and Advisor Alemayehu Wakjira (PhD) for his insight and greatly advised starting from proposal development to the end my thesis work. I am extremely grateful for his all contribution to my thesis. Also I would like to thank Mr. Addis Tefera he helps me on ANSYS software and some other related information which gives great shape for my thesis. He is a great hearted person that he did all this through phone calling and telegram contact and I had a great respect for him. I would also thank Mr. Sintayehu he plays the main role during my experimental test. During the lab test he was with him from the first day up to the end of lab tests and he assists me with full of his energy for that I had grateful thanks for him. Finally I would like to thank my teacher Getachew Alemayehu (PhD) for his knowledge contribution, my friends Mr. Pawulos Barud and my families for their significant contribution.

TABLE OF CONTENTS

LIST OF FIGURES

LIST OF TABLES

ACRONYMS

CFD…………………….Computational fluid dynamics

CLC…………………….Corrected lift coefficient

CLM……………………Measured lift coefficient

RANS…………………..Reynolds Average Navier stokes

DNS…………………….Direct numerical simulation

SST……………………..Shear stress transport

FEA…………………….Finite element Analaysis

suv……………………...Sport utility vehicle

CAD…………………...Computer Aieded Design

AMES………………....ANTA metal engineering solution

TNL……………………Total number of luggage

RHS……………………Rectangular hollow section

NOMENECLATURE

CD…………………….....Drag coefficient

CL…………………….....Lift Coefficient

F_D……………………….Drag Power

FL……………………….Lift Force

V_{RR}……………………..Volume of roofrack

V_L………………………Volume of luggage

A_T………………………Working section area

A_{CS}……………………...Cross sectional area

W_T……………………..Total weight

Ext……………………..existing

Mdf ……………………modified

ABSTRACT

Aerodynamics is a study of the Air Force on the surface of the body when moving along the highway. Most bus that is locally modified is rectangular body shape. However body shape is one of the predetermined parameter in aerodynamic performance of bus. Drag, being one of the aerodynamic forces, greatly affects the performance of a vehicle. Reducing fuel consumption of transportation vehicle especially those who's their aerodynamically shape is inefficient in fuel consumption such as bus important due fuel economy of one country. Because fuel economy, emission, stability, drag and others effects of poor aerodynamic design shape are the main criteria to be considered during design of vehicle body shape. Design improvement of the overall body shape increase vehicle performance. This work focused on the design improvement of frontal body shapes and headroom to reduce the drag and improve stability of locally modified ISUZU bus. Two models are designed under this study: existing bus model and modified bus model. These models are designed using CATIA software V5 R19.existing and modified bus model conduct CFD simulation with scaled down model 1:20 scale with 120km/h, 100km/h and 80km/h respectively. According to the results of numerical analysis the drag coefficient of modified bus at speed of 80km/h, 100km/h and 120km/h is improved by 27.46%, 27.24%and 26.97% respectively. The average percentage of fuel consumption reduction and lift force reduction is 16.33% and 88.5% respectively. The wind tunnel test model conduct experiment with scale of 1:35 under three speed 90km/h, 70km/h and 50km/h respectively. The experimental results show that the drag coefficient deviate by 10.9%, 9% and 7% at speed of 14m/s, 19.6m/s and 25.2m/s respectively. However according to the past study this results is optimum.

Keywords: Aerodynamics, CFD, front shape, headroom, stability, fuel consumption and drag

CHAPTER ONE

INTRODUCTION

1.1 Background of the Study

Aerodynamics studies the behavior of airflow around the object. Aerodynamic studies cover three main branches-theoretical, numerical, and experimental. This terminology must be accounted for with respect to design modifications accomplished by researchers and manufacturers. Aerodynamics are a large contributor in reducing drag, fuel consumption, and improving stability of vehicle thus saving cost and reducing emission.

Fuel consumption, speed and safety are an important issue related to aerodynamic design. (Mirmahdi et al, 2021) If resistance reduces fuel consumption and minimizes emissions Automobile industries face challenges in both the performance and design of vehicles. The primary challenges of modern automobiles are the high costs of fuel and the adverse effects of emissions on the environment. With this, design enhancement measures and weight improvement can at least help in controlling drag and fuel consumption at certain levels.
The stream management system is introduced actively or passively to add an increase in efficiency by delaying or preventing the separation of the flow.

Approximately 80% of fuel consumption inefficiencies are related to drag force due to the shape of the vehicle moving at higher speeds. Ground vehicles are also responsible for about 30% of CO_2 and greenhouse gas emissions. Various techniques have been researched to decrease these concerns. (Mukut & Abedin, 2019).

Aerodynamics is involved with the study of air flow about the object. Aerodynamic studies are further classified into three branches-theoretical, numerical, and experimental. This terminology must always be taken into consideration with the design modification carried out by researchers and manufacturers. Aerodynamics is highly beneficial in reducing drag, fuel-saving, and improving the stability of vehicles and thereby saving cost and saving the environment from hazards. All three are necessary for the fuel-consumption metrics; speed, and safety are dependent on aerodynamic manipulation.

(Mirmahdi et al, 2021). Basically, the drag force reducing would minimize fuel consumption, which eliminates emissions. Buildings of modern automotive aerospace face challenges in performance and design. The macro perspective problems for modern automobiles are the high cost of fuel and the ecological impact caused by emissions. Design optimization and, to a lesser extent, weight optimization may contribute to the mitigation of drag and fuel consumption. In addition, flow control systems, either actively or passively, are employed to delay or prevent flow separation, which further improves efficiency.

Approximately 80% of fuel consumption inefficiencies are related to drag force due to the shape of the vehicle moving at higher speeds. Ground vehicles are also responsible for about 30% of CO2 and greenhouse gas emissions. Various techniques have been researched to decrease these concerns. (Mukut & Abedin, 2019).

Aerodynamic drag constitutes 16% of the total energy consumption in transportation system in the United States. Thus, refining aerodynamics is one of the most viable solutions to enhance fuel economy. In this study, we can conclude that when the angle of the vehicle diffuser increases, the first case will be directly reduced, while the additional resistance increases. Similarly, the overall aerodynamic lift coefficient decreases. Residual treatment associated with additional devices is reported to increase the decrease in aerodynamic resistance by 8%.

(Arabaci, 2022).

In Ethiopia, some few vehicle manufacturing industries modify ISUZU trucks by converting them into buses for transportation purposes. These modified vehicles own several factors that influence their driving behavior and performance. Those factors include air resistance and the moment (or torque) which acts counter on stability, maneuverability, and handling. Crosswinds are one more of the external effects that could affect the performance of these modified vehicles with respect to Management. Crosswind Effects on Some Imported bus models in Ethiopia: Safety and Fuel Consumption Aspects (Tirfe et al., 2021). The subjective assessment of a vehicle by test drivers is that the test drivers are experienced drivers who assess reduced vehicle performance by their own observations and practical experience. This appraisal concerns handling, comfort, noise, and driving experience in general. Take into consideration how aerodynamic factors, such as crosswind effect, influence vehicle stability and performance. Smooth operation throughout many conditions is not just important. Direct control could possibly be made low because of strip wrong storage and other sulky factors like interruption of treatment. Side-kick aerodynamic devices generate flow separation at the rear of the vehicle, thereby improving stability and ride quality. This study aims at enhancing ride comfort in straight-line driving, one approach is to enhance the comfort by reducing the traction produced between tires and the road surface. (kamur et al., 2019). Crosswind effects on vehicle stability, cornering, and wind noise (Mcarthur et al., 2018). An automotive engineers' prime task is to reduce the fuel consumption of the vehicle on the road. Considerable friction drag within the atmosphere extracts a considerable portion of the fuel consumed by a vehicle because it has to be supplied with power to overcome this drag force to push things along. Therefore, drag reduction against shape modification for aerodynamics is carried out to obtain better fuel efficiency. Tests of the computing mechanics (CFD) of the liquid to evaluate the overall effects of such deformation can take much less time, so classical foot and acceptance methods are not so effective. Usually, the accepted range of engineering error lies within 5%. The roof panel surface significantly affects the wake region, which in turn influences the airflow around the vehicle. An air moving across concave, circular surfaces creates low-speed rotating airflows into concavity. conical forms integrated into the car housing can be used to reduce resistance. Resistance decreases whenever there is lower airflow at the distance between concave surface and roughness of the roof panel. Out of all methods considered, the method with rectangular arrangement has been proven to have the best drag reduction effect. (yang et al., 2021).

Vehicle aerodynamics aims at drag and fuel consumption minimization. For heavy vehicles, up to 80% of fuel consumption is attributed to air resistance. Vortices are formed enabling the application of different drag reduction devices giving 9% drag reduction without yaw and 15% with yaw. Front-end modifications seem to work better without yaw, while spoilers are utilized for stability. Change in front add-ons along with yaw would reduce drag by spoiling rear vortices thereby enhancing fuel economy and stability. The results are validated through CFD analysis while flow is visualized in areas that cannot be tested in wind tunnels. (Ribeiro et al., 2022).

Design refinement of the outer body shape of modified ISUZU buses in a bid to reduce aerodynamic drag. (Grandemange et al., 2015). When one vehicle passes another, particularly during turns, acceleration, or deceleration, the change in airflow around the two vehicles fluctuates and so do the aerodynamic forces. These changes in the flow field are triggered when two vehicles are traveling in the same direction and one overtakes the other, resulting in dynamic disturbance in the surrounding air. Crosswinds pose extreme challenges to vehicle stability with regard to speed, direction, position, and overall handling, which is particularly concerning on highways. The automotive industry now pushes to improve fuel efficiencies for cars that consume less material in the making of lighter and faster vehicles; This means, the aerodynamic forces of drag, lift, and sideways are now under consideration when vehicles pass each other. Sidewind effects are typically assessed at varying speeds using a wind tunnel test. Yawing moments directly correlate to crosswind speed while the pressure coefficient drops with the increase of airspeed (Iresha et al., 2021).

(a)

(b)

Figure 1. 1 a, b Existing bus (ANTA Metal Engineering Solution)

Installing a cargo compartment can increase aerodynamic drag and affect vehicle stability by obstructing airflow over the body from the side. The existing cargo space in the roof, completely covered with the rack of the roof, raises the profile of the bus to gain further side surface area. 1.

the primary objective of the present study is to modify the exterior of the bus to reduce drag and improve stability. Various parameters in the optimization process include aerodynamics, center gravity, weight distribution, materials, costs, safety, production and environmental effects. The stabilization of the movement of the vehicle contains further parameters such as tires, car body, fitting, and weather and road conditions. The design of luggage compartments must account for factors such as clearance height, door size, and ease of access. Inside the compartment, the layout should be carefully organized to efficiently accommodate a variety of bag sizes. The distributor can optimize space access, to prevent item over-stacking or difficulty of access.

1.2 Statement of the Problem

Waste of energy and environmental pollution are among the major global concerns for all scientific discipline. Isuzu is locally manufactured. This locally manufactured Isuzu bus front face inclined by around 9^0 which is not enough to penetrate air resistance. During the motion of the bus due to frontal area of the bus more energy need to accelerate the bus. When bus uses more fuel it releases more emission which leads environmental impact. Due to the height of bus crosswinds also significantly impact its stability and performance of bus. These sideways gusts disrupt the bus's movement, pushing it around and making it harder to control. Previous studies have been done to solve this problem by adding a luggage compartment away from unlimited loading height. That increase the front area and height of bus. However, as a result of increase in a bus's frontal area and height of the bus significantly impacts both its fuel efficiency and stability. Due to instability of bus rollover accident was faced. Instability is also affecting the comfort of travellers. Therefore, the aims this thesis is to improve the frontal section to reduce resistance, enhance stability.

1.3 Objectives

1.3.1 General Objective

The general objective of this proposed thesis work is to reduce drag and improve stability in a modified ISUZU bus.

1.3.2 Specific Objectives

The specific objectives of the proposed thesis are

- ✓ Drag coefficient reduced and stability (lift coefficient) improved
- ✓ Frontal air resistance and stability of modified ISUZU bus analyzed
- ✓ Drag and lift force test conducted at three speeds and numerical result validated (At ASTU Thermal Lab).

1.4 Significance of the Study

The output of this proposal is to give better contribution to modified Isuzu bus manufacturers in terms of aerodynamic aspects and stability. Enhanced stability leads to a reduced risk of rollovers and accidents, especially on highways or during sudden maneuvers. This isn't just about protecting the passengers on board; it also plays a crucial role in safeguarding other road users, greatly contributing to overall road safety. Since improvement will reduce fuel consumption, it brings market competitive advantage for manufacturers.

1.5 Scope of the Study

The study will focus on design improvements of the front-end shape and headroom to reduce drag and improve stability in a modified ISUZU bus. The effect of air flow on frontal surface and driving stability was analyzed using ANSYS software and validated using wind tunnel testing (At ASTU Thermal Lab). The design is modeled using CATIA V5 R19 software. The effects will be analyzed within a specific range of wind speeds.

1.6 Organization of the Study

The thesis consists of five chapters. Chapter one is the introduction which contains the background, statement of the problem, objectives, scope of the study and Organization of the study. Chapter two includes overview of literature review, a summary of the review and the research gap. Chapter three focuses on materials and methods and material selection. Chapter four discusses modeling, analysis of existing and modified buses and experimental set up. Chapter five: results and discussion computational data and validation of drag and lift force test results with numerical results and conclusions, recommendation, references and appendix is included at the end.

CHAPTER TWO

LITERATURE REVIEW

2.1 Introduction

Previous study plays an important role in supporting this study with understanding of some specific topics and reference information. This work provides a more informed perspective on the issues that have been mentioned, summarizing the main results and placing those results in contrast with this study. Beyond mere reviews or citations of important literature, the nature of this work puts the study in an entire field and draws from known work, even hinting at what is missing or what is an opportunity for some exploration. Of these references are studies that will attack similar problems, use similar methods, or align similar topics, which all will comment on and support the present investigation.

2.2 Overview of Aerodynamics

Understanding aerodynamics is the study of air motion and its interaction with objects in motion. The way air flows around and over an object greatly influences the forces acting upon that object. So in racing, the knowledge and handling of aerodynamic forces become vital parameters for a vehicle's performance optimization (S.Nath et al, 2021).

One may say that aerodynamics and vehicle dynamics are intrinsically related. The drag, down force, and side forces that aerodynamics exerts on the vehicle body are important aspects in determining vehicle behavior. Aerodynamics is, in short, a study of the interaction of gas fluids with moving bodies. Primarily, this specific field investigates the drag and lift forces that occur when air flows about an object. Most critical, affecting nearly every object that moves through the air (Thakur et al., 2020). Aerodynamics plays a vital role in how well vehicles perform. The main forces at play are drag, which pushes against the vehicle's movement, and lift, a force that acts perpendicularly (and is intentionally designed to be negative, or downforce, in vehicles to enhance grip). Components like wings create the most downforce when angled at 90 degrees and the least drag when aligned with the airflow at 0 or 180 degrees. While the front splitter is used, the side skirt helps control the air pressure around the car. The rear diffuser is important for controlling the air flow and increasing the clamping power (Agarwal, 2020).

2.3 Aerodynamic Force

The focus of the aerodynamic components design of a commercial truck is to help reduce enormous drag forces thereby improving fuel efficiencies. The main ideas are to reduce resistance coefficients and reduce air resistance and fuel consumption The increasing cost of fuel and the rapidly depleting supply of fossil fuels are making aerodynamics a progressively crucial factor in vehicle design, pushing the need for fuel-efficient transportation. However, drag is not the sole aerodynamic force influencing vehicle performance.

Lift force opposes the weight of the vehicle and its direction is upwards. Downforce pushes the vehicle downwards towards the road surface, increasing traction (Mirmahdi et al, 2021).

2.3.1 Drag force

Locally built ISUZU buses are inefficient in terms of fuel consumption because of their body design and other add-on devices. One of the add-on devices which spoil the aerodynamic profile of the bus is the roof rack which is used to load luggage. Installation of roof rack increases resistance coefficient (CD) as well as designed frontal area (A), which increase the components of aerodynamic drag. The authors were modified roof rack with an aerodynamic-efficient rooftop cargo compartment to study an aerodynamic-efficient bus in reducing drag. (Tirfe et al., 2021).

$F_d = 0.5\, \rho\, Cd\, A\, V^2$ A = frontal surface area

V = velocity of air F_d = Drag power

ρ = density of air Cd = Drag coefficient

2.3.2 Lift Force

Lift forces are a big problem for automobile engineers. If, at high speeds, excessive lift forms due to air traveling over its body, it will lose traction. This can be fatal because of an accident that can be accidents of rollover. Hence the design consideration has to be designed with precision to ensure generated lift stays within limits increasing stability and safety of the vehicle overall (S.Nath et al, 2021).

Fl= 0.5 $CL\ \rho\ A\ V$^2

Fl = Lift Force CL = Lift Coefficient ρ = Air Density A= Frontal Area of Body V = Velocity of Body

Lift is an upward force that takes away grip and stability but is called downforce when applied purposely, creating a strong grip, better handling, and advancing a vehicle's performance. It all depends on playing out the currents of air opposite to the motion of the vehicle (Manigandan, 2024).

Aerodynamic lift greatly affects vehicle stability at higher speeds. The lift coefficient and balance play significant roles in ensuring corner stability at high speeds, lane changes and straight-line stability.

Lift also influences crosswind sensitivity and braking. Lift will adversely affect braking performance through reduction of the normal force acting on the tires. The normal force is the force that presses tires against the road surface and this is directly proportional to maximum frictional force tires can generate for braking. Although front end shape has little effect on total lift, rear shape is quite weighty. Roof curvature combined with tangent increases lift. For optimal stability, the front-rear lift coefficient difference should be less than 0.1. The diffuser can reduce the overall lift, especially in the rear axle. The parameters affecting chugging will equally affect the stability conditions under which lift is obtained (Howell et al, 2021). The adjusted lift coefficient C L TC is obtained by multiplying the measured lifting coefficient (C L T m) by multiplying the coefficient (C L T m) by the factor C L c = C L m × $(1\text{-}B)^2$.

Corrected Lift Coefficient (CLC)
Measured Lift Coefficient (CLM)
Blockage Ratio (B)

2.4 Aerodynamics of automobiles and its effects on fuel consumption

Aerodynamics of the vehicle design plays a decisive role in saving the fuel and energy consumption of the vehicle. Modified changes in the ISUZU bus typically include modifications of the body shape. Making changes to the body's exterior-frame, such as adding more seats or maybe expanding the cabins, detracts from the aerodynamic configuration of the vehicles resulting to a greater workload by the engine and increased drag. Thus, one ends up with more fuel, more power, and greater operational costs accompanied by a negative impact on the environment (Damissie et al., 2017).

In terms of fuel consumption, an important factor to consider is reducing drag. An important consideration in the design process is the optimization of drag against height and speed. Thrust, drag, and lift are the three fundamental parameters in the performance of a streamlined vehicle. The vehicle's drag is a function of the airflow speed around it. Height and roof size which is aerodynamically inefficient associated with poor fuel economy or more environment damage when it comes to vehicles. Rounded shapes with, possible, tight and smooth coverings will reduce aerodynamic drag. Smoothing the body surface will further reduce drag and save fuel at any given speed. Drag force itself is a function of speed, frontal surface area, and the vehicle's drag coefficient (Abdullah., 2021).

The most crucial aspect for improving vehicle efficiency and performance in fuel consumption is the design of vehicles for reduced drag. The transition from the original design to the tapered rear design, the front spoiler, and the streamline bodies are very important drag-cutting measures in the quest for fuel economy saving 1 to 4 liters in fuel consumption.

Unfortunately, additional components can increase drag, mainly at other yaw angles. Lines and wires should be prepared so that they do not violate the soft flow of the air under the vehicle.

Effective designs of windshields have very significant influences on the appropriate management of airflow and lift and drag characteristics. There is a smooth air flow along the front glass in a larger curvature radius and a slope of more than 12 degrees. Smooth body surfaces are markedly important, whereas rough body surfaces and edges lead to disturbed airflow and drag increase. Strategically placed slots may also guide the air well in the vortex area and providing both good air circulation and total drag reduction.

(R. Jadhav & P. Chorage, 2020).

For the automobile industry, reducing fuel consumption is one of its major directives in minimizing aerodynamic drag. Among others, one of the major direct environmental-detrimenting mandates for the automobile industry involves reducing aerodynamic drag for fuel economy. An area of vehicle performance that drag touches upon-fuel consumption, acceleration, handling, noise, and, most importantly, environmental impact-is very important. Ideally, more drag reduction will proceed by optimizing the shapes at the front and rear of the bus body. About a 2% drag coefficient (Cd) decrease can be equated into 1% fuel savings at highway speed.

Lower emissions and less environmental impact accompany this. Vehicle drag minimization consists of two aspects: decreasing frontal area and shaping the vehicle aerodynamically.

Streamlining the bus design and incorporating features like spoilers and diffusers could significantly reduce drag and improve fuel economy. Minor shape modifications could reduce drag up to 20% and hence save about 10% of fuel. Yaw angle is the deviation of the vehicle from its forward path due to lateral motion and contributes essentially to drag; hence 0-yard yaw (straight travel) usually minimizes drag. An increase in speed means increased drag force for each base model and modified model.

In industry, terms drag force and drag coefficient directly influence fuel consumption. Fuel system efficiency and operational cost are essential parameters in determining the overall efficiency of a vehicle. Therefore, a number of technologies and advancements have been crafted with the principal aim of minimizing fuel consumption in vehicles (Sikder & Abedin, 2023). Vehicle shape optimization in aerodynamics still matters to emission reduction. Considerations mainly along the drag and lift characteristics become prime areas of research and development by manufacturers. Simulations of airflow around vehicles at experimental benchmarks and computed drag and lift coefficients have been validated. More than 50% of fuel consumption at highway speeds is accounted for by aerodynamic drag; therefore, improvement of vehicle shape to reduce drag becomes paramount in fuel economy and emission reduction. Increasingly with speed, drag increases to a square amount, and therefore the area of focus is the drag coefficient (UI Hoque et al, 2018).

2.5 CFD (Computational Fluid Dynamics) simulation

Its definition refers to numerical techniques that provide approximate solutions for fluid movement and heat transfer. CFD is not an independent science by itself, but an applied numerical analysis for fluid mechanics and heat transfer according to that definition: Example: The most basic write-up would be the core mathematical equations, generally in partial differential equations, for relating physics with fluid movement.

The governing equations are defined for engineering and science in the context of Computational Fluid Dynamics (Reddy and R. Locanadham, 2017).

The applications of computer simulation in computational fluid dynamics include airflow surrounding the bus modeled in specialized software that produces very accurate mesh grids and boundary conditions. This has been done in conjunction with wind tunnel experimentation but validated previously so that CFD is used for redesign.

The analysis of the CFD focuses on the most important aerodynamic features, front shapes and movements to minimize the resistance and to detect the structure that contributes to the stability of the vehicle. The three most important processes in the CFD procedure include preliminary processing, solutions and post -processing. This procedure has been applied to modified design sequences, including two tire configurations, that is, the basic interodal tires, and some aerodynamic changes (kapote, 2024).

Definition of preprocessor in mesh generation its geometry of the computational domain and mesh generation for control volume of calculation usually, fine mesh in regions of rapid change Since the application of numerical methods to capture gradients and complexities would be best by fine grids applied to areas of rapid flow change or temperature changes, a finer grid will give more accurate solutions. Choice of grids also defines the software you can use, along with the computer-processing time of calculations.

Thus, they will give more accurate and precise simulation of the physical behavior in that area. More computing performance and increased processing time require the above. However, this detail of such a grid also indicates how to use the computer power and calculate time required for the calculations. The solver of Computational Fluid Dynamics performs calculations based on numerical solution techniques such as finite difference or finite element methods. The post-processor in CFD refers to the last stage where the result of numerically calculating output from the simulation solver is processed or interpreted and distributed. One of the primary objectives of post-processing is to present the geometry behind and the mesh generated, allowing users to visualize their computational domain and how discretization was applied in the simulation. (Kapote, 2024).

2.6 Turbulence Modeling

Air or fluid flow over blunt bodies like buses is characterized by motion known as turbulence. The turbulence occurs in various forms, like regions of separated flow known as separation bubbles, thin liquid film on the surface known as boundary layers, and the region of disturbed flow at the rear of the body known as the wake. To accurately model and predict the complex patterns of turbulent flow from bluff bodies, engineers would rather employ the computational method of the RANS equations. With proper turbulence models added to them, these equations give a good enough description of how turbulence affects the mean flow field on average. Selection of a turbulence model for computational fluid dynamics (CFD) RANS equations is a highly critical task with various parameters. The desired accuracy and the computational space required as well as the time available for running the simulation. The modeling of turbulence in fluid dynamics broadly consists of three methods.

(Tirfe et al., 2021).

- **Classical Turbulence Models** or **Reynolds-Averaged Navier-Stokes (RANS)** relies on averaging the governing equations to predict mean flow behavior with modeling the impact of the turbulent fluctuations.
- **Direct Numerical Simulation**, or **DNS**, seeks to simulate turbulence by directly solving for the energy scales of swirling motion within the fluid without using any models or approximations. It calls for very high-powered computers for such accuracy.
- **Large Eddy Simulation (LES)** is between these two extremes, solving the large-scale turbulent eddies explicitly but simulating the effects of the smaller, sub-grid scale motions.

four common types of turbulence models that fall under the Reynolds-Averaged Navier-Stokes (RANS**)** approach:– Algebraic (Zero-Equation) Models**,** One-Equation Models (like Spalart-Allmaras), Two-Equation Models (such as k-epsilon, k-omega, and SST), and Second-Order Closure Models – are all categorized under the umbrella of RANS turbulence models **.**

- **k- Epsilon Turbulence Model**

The K-epsilon turbulence model can guarantee a decent accuracy of various types of turbulence and shows the reliability and effects proven in the calculation. This limit has made a lot of improvement to improve predictive opportunities in the standard K-epsilon model.

Two such notable variants available in the fluent software are the RNG (renormalization group) K-Epsilon model and the realizable K-Epsilon model. These differences are trying to improve the initial defects in the start model and further expand the applicability with the turbulence of more level. The two equations are solved regardless of information about the characteristics and scales of turbulent fluctuations in the flow.

Standard k- Epsilon Turbulence Model in the K-Epsilon turbulence model, the equation used to describe the transport of turbulent kinetic energy (k) is derived directly from the fundamental, exact fluid dynamics equations.

A. RNG k-epsilon Turbulence Model The RNG (Renormalization Group) K-Epsilon model is also derived from the fundamental, time-dependent Navier-Stokes equations, as is the standard K-Epsilon model, but it does so through a sophisticated mathematical technique known as renormalization group theory.
B. Realizable K-Epsilon Turbulence Model the Realizable K-Epsilon model represents the latest advancement among the three common variations of the K-Epsilon turbulence model.

- **K-Omega Turbulence Model**

The K-Omega turbulence model is also a technique used to simulate turbulent flows. The model has two main versions: the basic K-Omega model and the Shear Stress Transport (SST) K-Omega model. The main models of K -Omega and its analog SST determine the transmission equation for turbulent kinetic energy (K) and certain dissipation speed along the same mathematical configuration.

The SST model introduces dramatic changes with respect to the base model. The SST model continues to deliver between the K-omega base model near the outer wall and the K-epsilon model on the outer boundary.

Secondly, for better capture of the transport of the most crucial turbulent shear stresses, the SST model employs a new turbulent viscosity equation.

A. **Standard K-Omega Turbulence Model** Turbulence Model fluent employs a standard K-Omega turbulence model that was specifically installed to improve the calculation of phenomena such as low Reynolds number effects, compressibility, and shear flow spreading. The standard model is based on empirical correlations and employs transport equations for the turbulent kinetic energy (k) and its specific dissipation rate (ω)
B. **SST K- Omega Turbulence Model** in FLUENT, the Shear Stress Transport (SST) K-Omega model is the sole accessible variation of the standard K-Omega model. The SST K-Omega model was created by merging features of the standard K-Omega model alongside a transformed form of the K-Epsilon model.

2.7 Overview of Interior Headroom

The interior of any vehicle is built for seating and standing passengers for a safe and a more comfortable journey.

2.7.1 Headroom for Standing

It is a first between male and female passengers in the headroom analysis in the vehicle. The example improves according to Figure 2. In this case, both standing male and female passengers have enough headroom with males attaining 25mm clearance. Comfort must include both passengers seated or standing when the vehicle considers interior arrangement. Headroom is an important consideration concerning passenger freedom and ease of movement (Fridman & Napper, 2016).

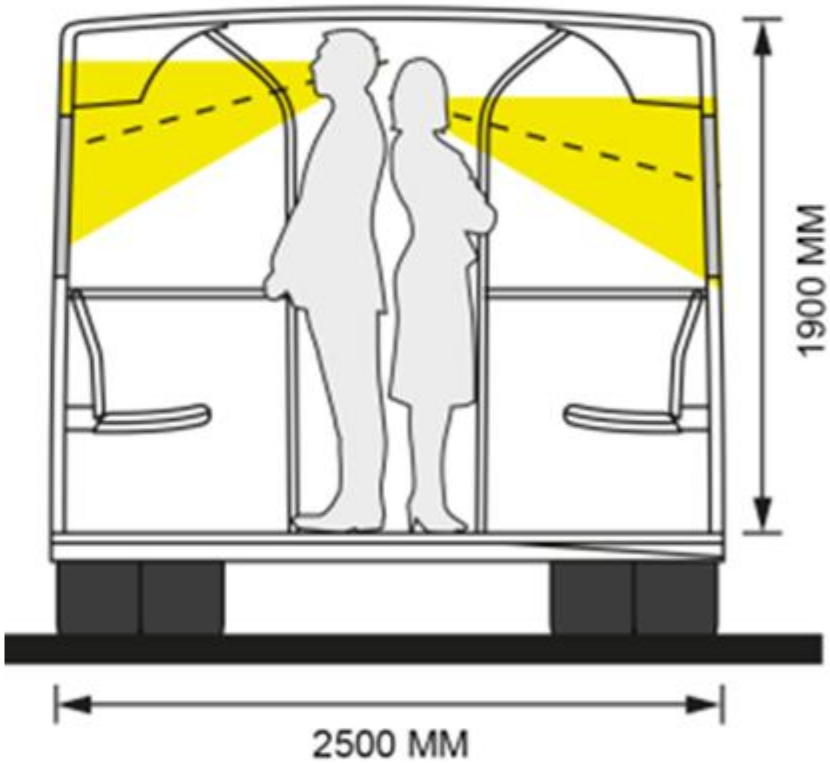

Figure 2. 1 Bus Design for Standing (Fridman & Napper, 2016).

2.7.2 Headroom for Standing

According to past research data observed study were done on developing equation for estimating body height on Ethiopian Adults at Jimma University. According to 2015/2016, report of the registrar, there are a total of 38,862 in both gender. Among these students 22,298 were regular students in both undergraduate and postgraduate programs. A total number of 660 students were participating in research study equally from both genders. From that person response rate was 96.7%. (97.0% male and 96.4% Female).   The data was collected from 638 students (320 males, 318 females).the age of the students in which study carried on is between 18 to 40 years. Data were gathered using questionnaire and measurement of anthropometric parameters. Prediction from arm span, half arm span and knee height is taken when not possible take measurements. Among this Arm span is best prediction (Digssie et al, 2016).

Table 2. 1 Mean (SD) anthropometric measurements of study participants in Jimma University, March 2016

Variables	Male	Female	Total
Height	174.29 ((± 5)	161.08 ((± 4.6)	167.71 ((± 8.2)

Increased stability and decreased drag through frontal shape and adequate height according to seated passengers are the key issues in research.

2.7.3 Ergonomics Assessment of passenger seats

The survey research done in mekele city (Ethiopia) on the ergonomics assessment of passenger seat (minibus). The main aim of its study is to gather anthropometric data necessary for design and manufacture of passenger seats. According to this survey 50% and 95% of passenger height is 171cm and 183cm respectively. Also the seat height and seating height data are 40.4cm and 82.4 cm respectively (G/yesus et, al, 2013).

Table 2. 2 Passenger and seating height status

Seat sections (cm)	**Percentile**		
	5%	**50%**	**95%**
Passenger height	162	171	183
Seat height	37.5	38.7	40.4
Seating height	76.5	74.4	82.4

2.7.4 National head clearance regulation ADR 58.6:

Australian rules for ADR 58.6 design are mainly applied to the appropriate vertical space or spray for passenger cars for the comfort of passengers, especially for high passengers. For example, it will be determined with respect to seating positions above this raised floor, not for the vehicle's interiors, in vehicles with elevated an area of the floor. The main goal of ADR 58.6

is to ensure a convenient place for human residents in the car. It must be said that there must be safety between the head of a passenger and any nearby rigid surface-the bus is a dynamic system exposed to vary forces while operating. Moreover, performance of the vehicle could also be improved further by lowering the center of gravity of the vehicle and by reducing the overall mass of a vehicle (Fridman and Napper , 2016).

2.8 General Overview of Bus Body skeleton Structure

Bus structure under unnecessary weight will affect speed, fuel consumption, and overall performance. To analyze the bending and torsional load of the structure, this was done. A model of a bus made in CATIA has been imported into ANSYS Workbench with proper boundary conditions. The dimensions and thickness of structural metal components were optimized for structural weight reduction and then structural strength was evaluated. The model of Isuzu passenger bus which existed for 33 passenger capacity. The bus structure has rectangular hollow steel sections of varied sizes.

Finite Element Analysis (FEA) simulates structural behavior under different conditions and processes. The first part of the action in FEA involves discretizing the structure into a mesh of smaller elements. For this bus structure analysis, tetrahedral elements were utilized because their shape is adaptable to complex shapes. Mesh refinement (element size and count) affects result accuracy. The second step of FEA deals with the inputs: the absolute forces and restrictions which the bus encounters in reality. This analysis is made up of self-weight from the bus, passenger weight, and fuel weight. Thus, all those loads will be a combination of causing stresses and strains inside the structure. The last step of the FEA is to solve the model. Through numerical methods, the software simulates how each element under the defined loads reacts and predicts overall structural response (deflections, stresses, strains), which indicates integrity of structures, weak parts, and inform merits in future design optimization for safety and performance, improving the bus ability to mobilize passengers and fuel safely (Tafesse et al, 2018).

Today's passenger bus manufactured in different industry according to local need. To maintain the market in competition weight reduction by keeping existing facilities take more attention. The design of internal bus skeleton structure develops in different industries. Internal bus framework forms a basis for further bus advancements in the industry. The strength of bus body frame comes from the manufacturing used strength. Type of welding used the result of our strength. The top and bottom frames must be strong because it is under different load such as: load of interior parts, load of passengers and aerodynamic load. Front and back frame are also needed to be strong and beauty. The design of the bus body should conform to the chosen chassis. Dimension such as: Length, Width and height must balance each other so that the vehicle can maintain stability (Chinta & Rao , 2014).

The structural design depends on the passenger capacity with regard to the different types of user and the nature of operation. Bus body design parameters are the shape, stability purpose, and strength, in general (Reddy et al, 2016).

2. 9 Cab roof fairing

The comparison between the model fitted with cab roof fairing and the model without roof fairing was made by testing the scale truck model under wind tunnel tests and numerical simulations. The result showed a 15.05% reduction in drag when compared to the model without cab roof fairing (Kim et al., 2017).

2.10 Crosswind Aerodynamic and Stability

Crosswind-related effects on performance refer to a condition of wind coming from the side of the vehicle which consequently creates lateral force effects on vehicle stability, handling, and aerodynamics. It is most critical in vehicles with large exposed surfaces such as trucks, buses, SUVs, or in-case with roof-mounted cargo. Aerodynamic forces produced by the crosswinds and effects on vehicle stability are mainly aspects integrated into the design of vehicles for improved safety and efficiency (Zhang et al., 2020).

2.11 Crosswinds and Crosswind Sensitivity

A cross wind is one that blows across the path of a moving vehicle instead of from the front or rear; that is, its effects on the vehicle are due primarily to its force acting perpendicular to the travel direction. This lateral pressure then causes significant force to act upon the vehicle, pushing it in a sideways direction. The absolute force and what that force can do depend on the wind's speed and angle, the size and shape of the vehicle, and the speed at which it is moving. In essence, strong crosswinds bring in a considerable lateral force, which could substantially disrupt the vehicle's intended path and bring even greater challenge to the driver. Crosswind sensitivity concludes by how effectively a vehicle can resist destabilizing forces induced by lateral wind gusts. Therefore, it measures how prone a vehicle is to movement in two relevante modes:

• Sideslip: The assessment by which the vehicle slips out of track produced along the horizontal plane due to the lateral force brought about by crosswinds.

• Yawing: The result of vehicle spinning around the vertical axis. These two motions could significantly complicate a driver's effort to maintain control and stability under windy conditions (Kapote, 2024).

2.12 Instability in Crosswind Conditions

Long-sized and far-traveling buses are most susceptible to violent instability due to strong crosswinds. These accidents can be broadly classified into three types: rollover when the bus tilts excessively and may fall over; sideslip when the bus slides laterally and cannot control; and rotation when the bus spins through yaw. The factors affecting stability include; a center of gravity, road conditions, speeds, steering, and braking. To estimate the severity of an accident, the engineers used criteria such as a rapid drop in wheel-road contact force, large displacement states, and a rapid increase in yaw angle. Engineers adopted simulation approaches involving dynamic models with six equations of motion at the bus's center of gravity: three translational and the remaining three rotational. (Minh Hoang Trinh et al., 2022).

2.13 Stability and Vehicle Aspects

The aerodynamic property of the vehicle can be modified and can greatly affect its handling. Vehicle dynamics play a very important role in accurate prediction of vehicle behavior. Some of the important parameters concerning vehicle dynamics are aerodynamics, power transfer to wheel, tire characteristics, weight distribution of the vehicle, and suspension system. Parameters of aerodynamics considered in handling would be aerodynamic forces like down and drag forces, side forces and how these forces distribute over the four wheels. Aerodynamics can lead to two types of changes in vehicle behavior: positive changes that enhance handling and negative changes that impair it. Vehicle handling is measured through four main parameters: Grip, Balance, Control, and Stability. Grip refers to the maximum lateral acceleration generated by the tires. Balance is the yaw moment associated with this maximum lateral acceleration. Control indicates the yaw moment produced when the driver adjusts the steering angle by one degree. Finally, Stability is defined as the anti-yaw moment generated by the vehicle (Roy & Sharma, 2021).

Research on the aerodynamic effects of vehicle additions such as spoilers, roof racks, and taxi signs has been limited, with the earliest studies dating back to Faerber's work in the 1950s. The aim of this research is to examine how these additions influence fuel efficiency and vehicle safety. The primary concern is that these add-ons lead to increased fuel consumption and higher greenhouse gas emissions. They can also compromise directional stability and safety, particularly rooftop additions that generate considerable side forces and rolling moments in crosswinds. The study shows that these add-ons can sometimes increase aerodynamic drag by as much as 5-30%, depending on the yaw angle, resulting in greater fuel use and CO_2 emissions with blunt body style add-ons. On the contrary, removing these add-ons from the vehicles leads to decreased fuel consumption and emissions. All included, these vehicle add-ons dramatically change the aerodynamics, leading to increased drag and fuel consumption, whereas taking them away can improve efficiency and decrease emissions (Chowdhury et al., 2012).

The major disadvantages associated with buses and other commercial vehicles are high fuel consumption, exhaust emissions and stability against crosswinds. Current issues facing the FSR Isuzu Bus in Ethiopia include its locally constructed external body, which has poor aerodynamics, and a flat front surface that increases drag and air resistance. The objectives of the study are to reduce aerodynamic drag by improving the bus's exterior shape, examine the impact of surface roughness (strips) on aerodynamic performance in crosswinds, and enhance both crosswind stability and fuel efficiency. Design modifications include creating a new aerodynamic body shape, adding roof strips, improving diffuser angles, and smoothing the front and rear edges with a curved front design. The results of the study showed a reduction in the drag coefficient of approximately 45%, an overall decrease in aerodynamic drag by 60%, improved crosswind stability, reduced side force and rolling moment, and enhanced fuel economy and road stability (Kahsay and Zeleke, 2024).

The impact of perpendicular wind on drag losses in city buses, focusing on constant travel and wind speeds while excluding factors like acceleration, deceleration, and wind gusts. It found that steady side winds increase aerodynamic drag, primarily affecting the bus's rear and wake regions. By segmenting the bus into seven sections, the analysis revealed that the rear surface generates the most drag, with side forces being minimal but more pronounced at lower speeds. A 2 m/s side wind resulted in a fivefold increase in drag. Moreover, side wind reduced the size of the rear wake and caused flow instability, particularly at lower speeds. The study highlights that the interaction between cruising speed and side wind creates a total velocity vector, which is crucial for accurate drag loss calculations (Szodrai., 2022).

Two side wind simulation methods for SUVs, referred to as "partial car" and "partial wind," were evaluated to understand their impact on flow fields under varying side wind intensities. The "partial car" method replicates the Tongji wind tunnel test by tilting the vehicle at an angle α, while the "partial wind" method adjusts vehicle and side wind speeds at the inlet. Both approaches yielded similar results, indicating that aerodynamic drag, lateral force, and lift increase with higher yaw angles. An analysis of pressure maps and comparison of test results reveal that the SUV's aerodynamic performance is significantly influenced by its underbody design and side wind conditions, with yaw angles of -2°, -5°, and -10° being specifically assessed (Zhou et al., 2022).

Stability of a vehicle is very essential while cornering safely. Instability manifests in two forms, either oversteer or understeer. One of the factors in cornering stability is downforce, which results from the combination of surface area, aspect ratio, and cross-section of a vehicle and its angle of attack. The low pressure generated under the vehicle by maximizing airflow generates downforce through the difference in pressure. In comparison, double-decked buses have a larger frontal area and height but still produce less downforce than regular passenger cars and make them more susceptible to the instabilities brought about by their weight and cornering forces. While lift, due to the lower pressure on top of the vehicle, greatly influences stability and performance, vehicle height, in and of itself, does not directly factor in; the difference in pressure ultimately becomes the major point of contention. Cornering results from the combined centripetal and centrifugal forces, which are perpendicular and unequal. Observed vibrations in the model during testing likely stemmed from the lightweight construction material and insufficiently rigid connections (Nizom, 2011)**.**

2.14 Handling and Influence Factors of Stability

The active vehicle safety level is determined by vehicle stability in handling, as it influences maneuverability and safety at high speeds. It has two facets, namely, handling and stability. Poor handling makes a vehicle skid, turn excessively, or rollover, thereby compromising its stability. On the other hand, insufficient stability results in uncontrollability, thereby endangering the occupants and the vehicle. Therefore, a good driving stability is essential for safe vehicle operation. The driver and vehicle form a complex intertwined system. It is further influenced by several factors such as tire stiffness, mass distribution in the vehicle, and steering input. Reduction of the moment of inertia improves handling characteristics at low speeds. Rearward shifting of the center of mass increases the high-speed stability of vehicles. Handling stability is evaluated by analyzing a vehicle's responses to steering input, especially lateral acceleration; roll angle, and yawing angular velocity. The study simulates how the vehicle responds to changes in driving conditions (Chen et al, 2019).

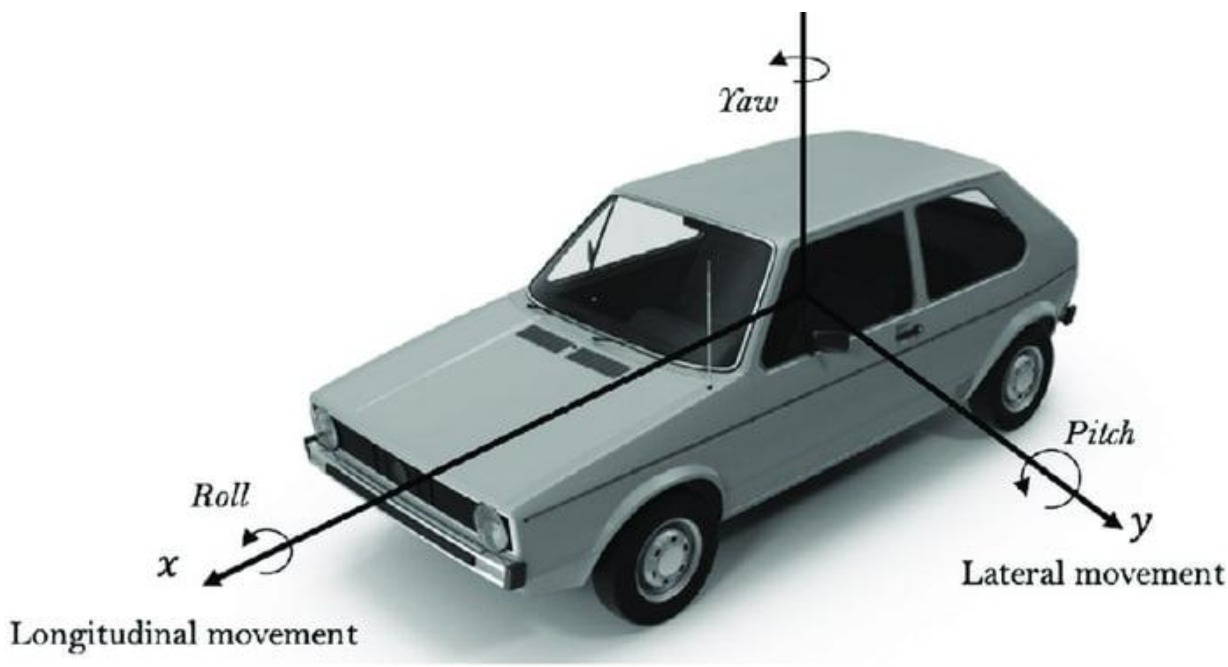

Figure 2. 2 of moment on a vehicle (Chen et al, 2019)

2.15 Weight Addition and Costs

The vehicle manufacturing industry has been focusing on incorporating lightweight and high-strength components. There is a close relation of weight with fuel consumption and emissions, and the latter should be reduced in a vehicle through its weight to achieve improvement in acceleration, braking, and stability (P Chirinda & Matope., 2020).

There are two broad approaches to achieve vehicle weight reductions, i.e. by material reduction existing materials with lighter alternatives or by improving performance through part redesign. Lightweight materials such as aluminum, magnesium, titanium, and composite material, among others, are preferred in place of conventional heavier materials such as steel. Aluminum could, for instance, be more preferable because it is lighter, recyclable, and absorbs twice as much crash energy as mild steel (Khademian et al., 2020) However, adopting new materials often involves trade-offs. While these substitutions can result in benefits like lighter, stronger, and more efficient products, they may also lead to increased production costs, which represent the trade-off or disadvantage of these advantages (Hagnell et al, 2020)

2.16 Review Summary

Aerodynamics plays an important part in vehicle performance, fuel economy, and safety through the reduction of the air resistance or drag that oppose motion. Since drag minimization is one of the most crucial parts of vehicle design for the purposes of better fuel saving and lessening environmental pollution, hence streamlining the shape of the vehicle is one of the best means of reducing drag, allowing air to pass by the vehicle without turbulence. Other means such as chamfering, corner rounding, and edge smoothing further reduce drag by decreasing turbulence around the vehicle. The design of the front and rear of the vehicle has quite significant effects on the overall aerodynamic efficiency of the vehicle. Aerodynamic devices such as spoilers or diffusers control the airflow to enhance down force and reduce lift to stabilize the vehicle at high speeds, increase traction, and prevent lift, especially for performance vehicles. Lowering the height of the vehicle minimizes the wind area and drag resistance and enhances stability. Engineers progressively design, through iterations and modern simulations, a vehicle body that balances drag reduction with down force or lift depending upon the performance requirement. By using streamlined, curved designs and smart material placement, vehicles can become more fuel-efficient, handle better, and be safer, leading to a more enjoyable and environmentally friendly driving experience.

2.17 Research Gap

In previous studies, researchers focused on enhancing the aerodynamic performance of locally modified ISUZU buses through various methods. Their primary approach involved modifying the roof racks of existing bus bodies and incorporating add-on devices to streamline airflow, underbody modification, weight reduction, diffuser angle and others. Loading luggage compartment onto the roof rack increases both the exposed area and the drag coefficient of the bus; particularly affecting its aerodynamics both from the sides and front. Reducing the bus's overall height lowered its center of gravity, which in turn improved its stability. The head shape of bus also adversely impacting drag coefficient. Previous research data indicates that the existing ISUZU bus has a flat front shape, which results in poor aerodynamic performance**.** The previous research study on front part modification was done on other model of bus numerically but not on headroom and experimental validation. Further design improvements are necessary to increase the aerodynamic performance and stability of the bus and validation of drag and lift force was carried on.

CHAPTER THREE

MATERIALS AND METHODS

3.1 Introduction

The section indicates the materials and methods to be used in evaluating the effects of front end shape and headroom on aerodynamic drag and stability in a modified Isuzu. The analysis combines computational fluid dynamic (CFD) simulation with wind tunnel tests to evaluate the vehicle's aerodynamic characteristics under various speeds. Small 3D Model designed using CATIA and analysis will be done with ANSYS Fluent software. Validation of numerical results will be through experimental investigation.

3.2 Materials

In a research study, materials refer to the resources and instruments used to conduct the investigation. According to this thesis, the materials required to carry out this study are listed as follows: the material used for this thesis are:

To conduct this research effectively, a range of essential tools and software will be utilized. A personal computer (PC) will serve for organizing document, capable of running various operating systems and applications necessary for data analysis and design. Meters will be used to gather precise data from existing buses. For design and modeling, advanced Computer-Aided Design (CAD) software such as CATIA V5R19 will be employed for detailed 3D modeling and engineering applications. Additionally, AutoCAD will be used for creating precise 2D drawing. The **ANSYS Fluent** software, a powerful computational fluid dynamics (CFD) tool, will be crucial for simulating fluid flow.

Finally, for physical prototyping and small-scale aerodynamic research, a Creality K2 Plus 3D printer will be used to create prototypes. HM 170 Educational Wind Tunnel, providing a practical environment for testing drag lift force and validating with numerical results.

3.3 Methods

Methods refer to the organized strategies and techniques employed for data collection and analysis. They encompass the specific procedures and instruments used to address research questions or hypotheses. To effectively achieve the general and specific goals of this project, a carefully crafted methodology must be implemented. The following steps outlining the components of this methodology.

3.3.1Flow Chart

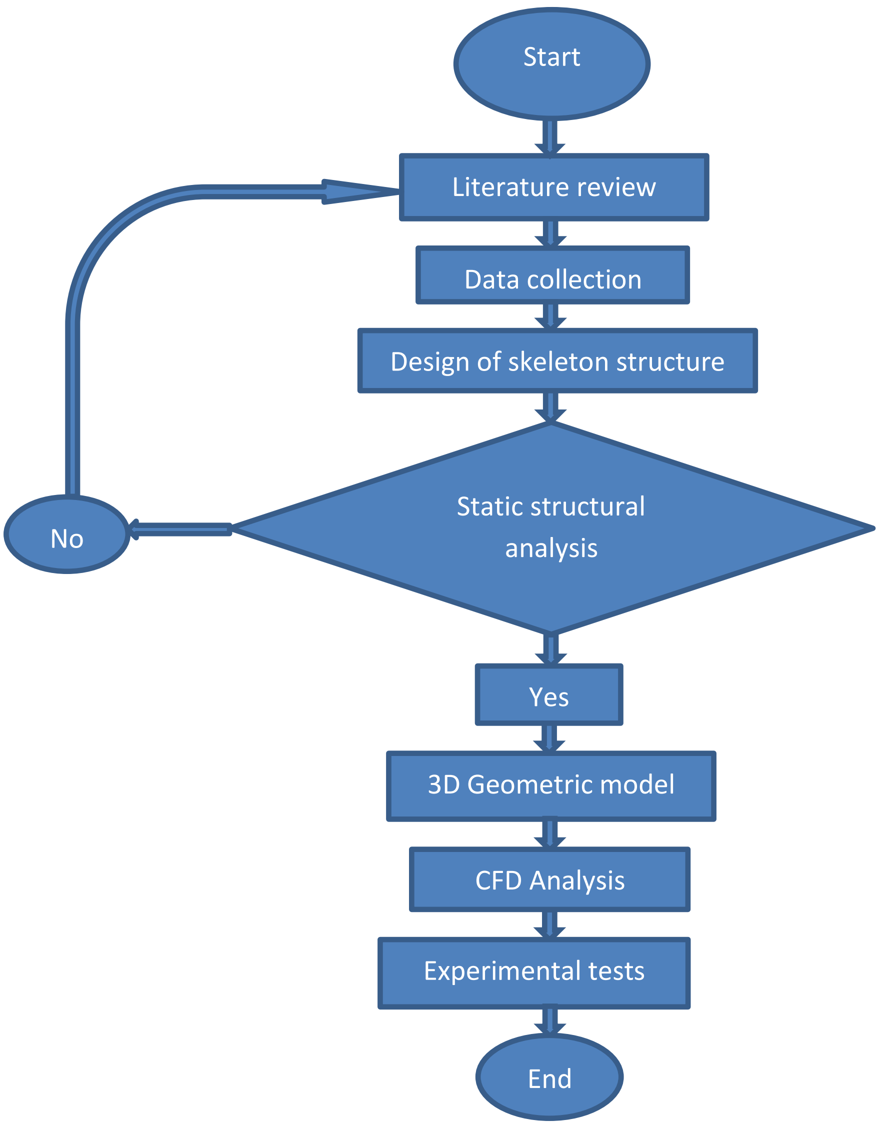

Figure 3. 1Flow of Research methodology

3.3.2 Literature Review

A literature review is a thorough examination of existing research on a particular topic. Its main goals are to summarize, analyze, and synthesize relevant studies, theories, and findings to provide context for a specific research question or project.

3.3.3 Data Collection

Data collection is the organized process of gathering information to answer research questions, test hypotheses, or evaluate results. Data can be gathered both as primary and secondary data collecting to answer research question.

A. Survey Observations (AMES)

ANTA Metal Engineering Solution. AMES Established before 30 years E.C. this company is found in Addis Ababa around Gelan condominium. This company manufactures different body of vehicle such as: Bus body building, Van (Container), Tanker Truck and Track Back Carry. The data is collected through interviewee questioner from. For further improvement and modification important data regarding area of study should be collected. This data is collected from locally modification of bus company leader and direct measurement of both skeleton structure and final body of bus. Carrying capacity of this bus is 33 passengers. The main company found in Addis Ababa (Akaki kality sub-city wereda 12) industry zone.

B. Data taken from company in questionnaire's form

This research aims to investigate the production of locally modified ISUZU buses in Ethiopia, focusing on the operations of ANTA Metals Engineering Solution PLC. The study will examine the weight characteristics of these modified buses, analyze the company's production status and challenges, and explore the evolution of their production processes over time. According to data from the company the total weight of the bus is 19000kg before construction structure and up to 41000kg after body construction. Materials used for construction of the bus body are: RHS, U-channel, Angle iron and sheet metal. They use Steel material (mild steel). The company stays on production for 30 years and with the past five years the company reorganizes itself with the name of ANTA Metal Engineering Solution. Currently the company production is customer based.

According to information taken in the past five years the companies manufacture 160 pcs of buses.

C. Dimension of Bus

The Isuzu bus is a widely used compact model, mainly designed for public transportation. Although the exact dimensions can vary based on the specific model or configuration, the following is dimensions of one Isuzu bus taken from ANTA Metals Engineering Solution.

Table 3. 1 Specification of locally modified bus

Parameter	Values(meter)
Length	7.500
Height	2.76
Width	2.160
Internal height	1.910
Seat height	0.430
Internal height at the back seat	1.780
Wheelbase	3.820
Front overhang	1.200
Rear overhang	2.480

Dimension of luggage compartment

The luggage compartment of a bus is designated storage area for passenger items. It is located at the rear, side and top of the bus.

Rear luggage compartment

L = 1.25m H = 0.73m D = 0.83m

Side luggage compartment

L = 0.87 H = 0.435 D = 0.42

Survey at Bus Station (Bishoftu Bus Station)

Survey conducting at bus station is to gather dimension of luggage. This data is needed because of the part is exposed to air which is under effect of aerodynamics.

Dimension of roof rack

Bus roof racks are essential component for buses. It provides additional storage space for carrying luggage and cargo.

L = 3.0m, H = 0.6m W = 1.3m,

The above data collected from bus from the bus station. This data goes beyond mere facts. It provides helpful and meaningful information that can significantly impact our decision-making. By examining this information, we can reveal trends concerning the bus's performance, passenger usage, and scheduling efficiency. Recognizing these patterns will enable us to pinpoint areas that need improvement.

Figure 3. 2 Locally modifies structural and body ISUZU bus

3.3.4 Design

The design concept serves as the central idea guiding the development of the modified Isuzu bus. It is articulated through a collection of sketches, images, and a written statement. The design focused on creating an aerodynamically efficient and stable bus. This design has been developed using CATIA V5 software.

3.3.5 Numerical Analysis

The numerical analysis of both the baseline model and the modified model was performed using ANSYS.

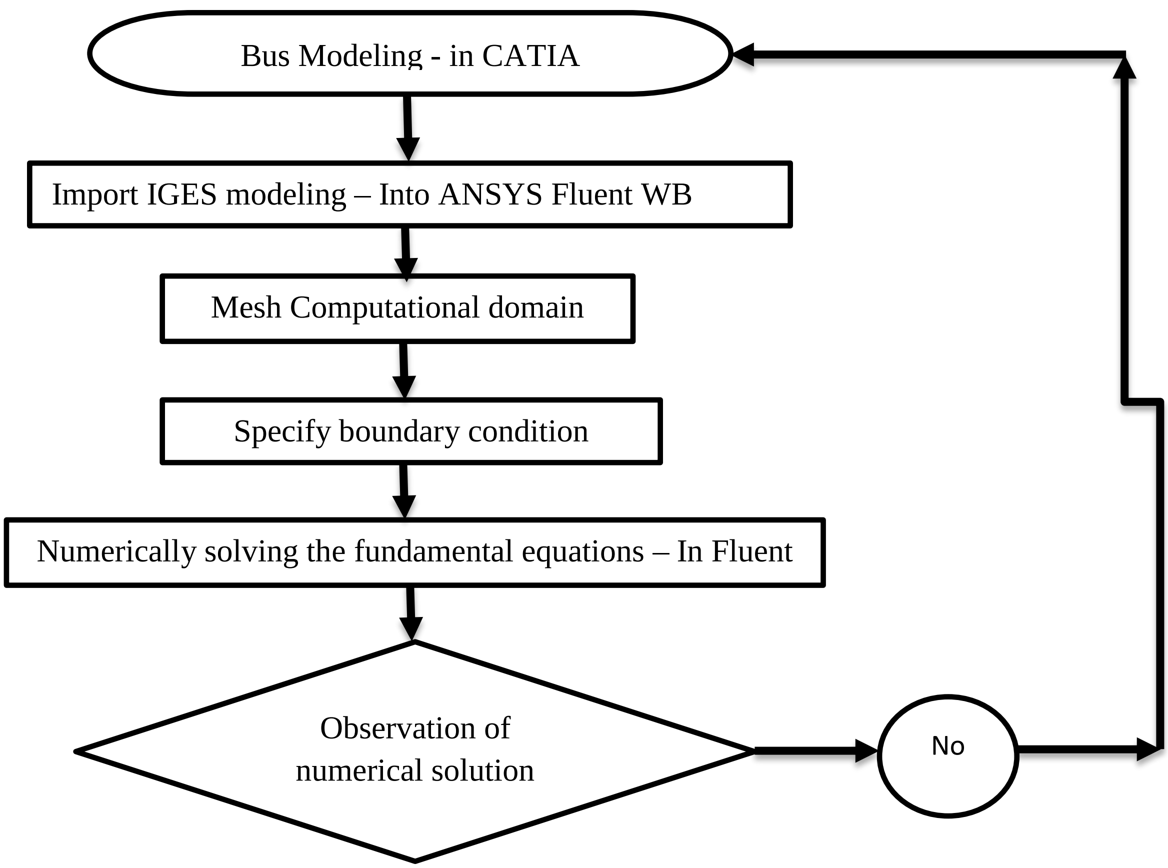

Figure 3. 3 Fluent Methodology Flow chart

3.3.6 Experimental Test (wind tunnel)

An experimental investigation was conducted in a wind tunnel to validate the results obtained from the software, using a scaled model of the newly modified bus.

3.4 Material selection

The material used to construct the structure of the bus is steel RHS. The material form of the structural steel used to construct the structure is RHS rectangular and square hollow section form.

CHAPTER FOUR

MODELING AND ANALYSIS OF ISUZU BUS

4.1 Introduction

This section will present the modeling and analysis of the Isuzu bus. Such analyses as fluid dynamics will be performed extensively and performance of the bus evaluated on different Speeds (80km/h, 100km/h, 120km/h).This analysis would give important information on things like reducing drag, fuel efficiency, stability, and passenger comfort. Ultimately, these results would lead to design improvements and optimization strategies in reducing drag as well as enhancing the whole performance and stability of the Isuzu bus.

4.2 Modeling

Simplified version of vehicle underwent modifications and CFD analysis in ANSYS. The Ahmed Body benchmark was used to validate the CFD methodology. Airflow analysis showed a deceleration of air velocity at the front of the vehicle followed by acceleration. High-pressure concentrations were observed in the front windshield and wing mirrors which were significantly reduced by multiple geometrical modifications, such as removal of mirrors and smoothing of the frontal curves. Mesh refinement achieved by reducing cell element size thus resulted in high accuracy of drag and lift coefficient calculations, indicating that further refinement may yield results even closer (UI Hoque et al., 2018). The current bus design has a flat front profile; hence it does confront quite a very serious air resistance problem, especially on high speed where the drag force becomes significantly higher and stability is reduced. Addressing these with a breath of fresh air, this study identifies external body designs where the current model serves as benchmark for comparison. Modeling of bus body structures was done by CATIA in a three-dimensional model, and the target was to investigate the effects of varied design parameters on drag force. The goal was to find some effective solutions in terms of improving both aerodynamics and overall stability. Two bus models were included in this study: the existing bus,and a bus with a modified front-end shape and height (A. Muthuvel et al., 2013). The models are designed initially using CATIA and then further export the geometric data into ANSYS Fluent software for analysis on aerodynamic drag (Cd). Create the computational mesh during the CFD simulation process. The mesh created has been assigned unique names for each part of the model (for example, ground, wind tunnel walls, and different bus components) to facilitate the analysis. This is notable because the dimensions, design features, and data of the models are directly scaled down from the existing vehicles. This means that the ratio remains 1:1 with the reference vehicle. The same scaling rule is also adopted to the baseline and modified models.

4.2.1 Existing bus modeling

The ISUZU bus is locally modified in our country. Many study showed that this model has poor aerodynamic shape and very poor fuel consumption. This bus is mainly used for intercity travel and long distance travel. Existing bus is a bus which is already in use.

Case 1 existing bus model without roof rack

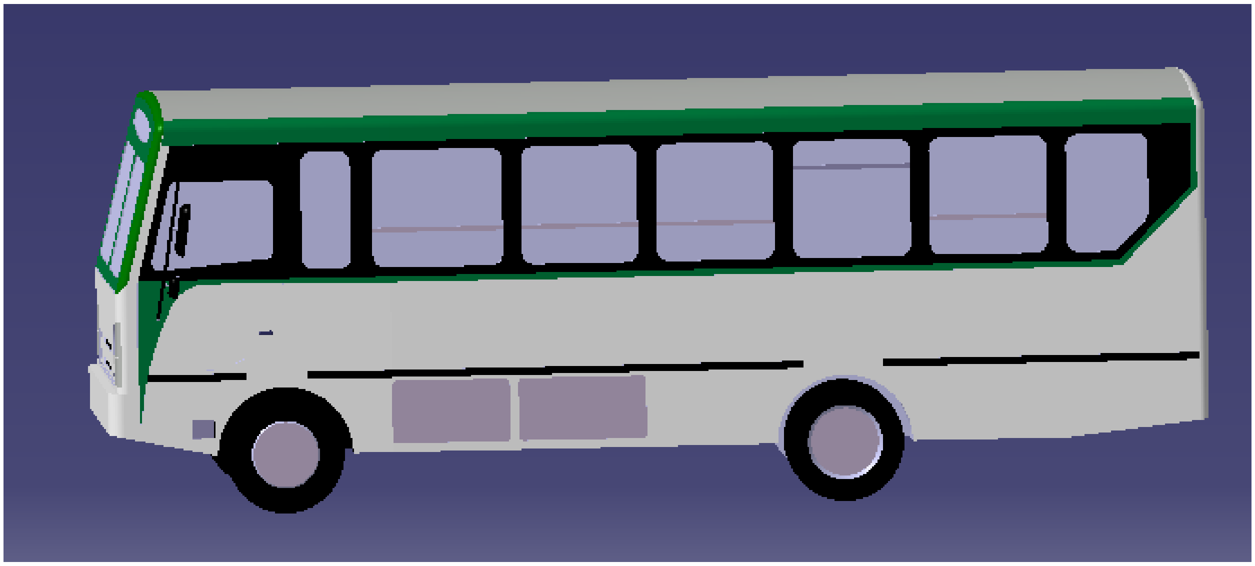

Figure 4. 1 Existing bus model

4.2.2 Modeling of Modified Bus

Locally modified existing ISUZU bus model is aerodynamically insufficient due to its external body shape appearance. These increase the amount of fuel consumption and lead its instable which is economically disadvantage. Environmentally the amount of emission increases. For this reason aerodynamically efficient ISUZU bus has to be preferable.

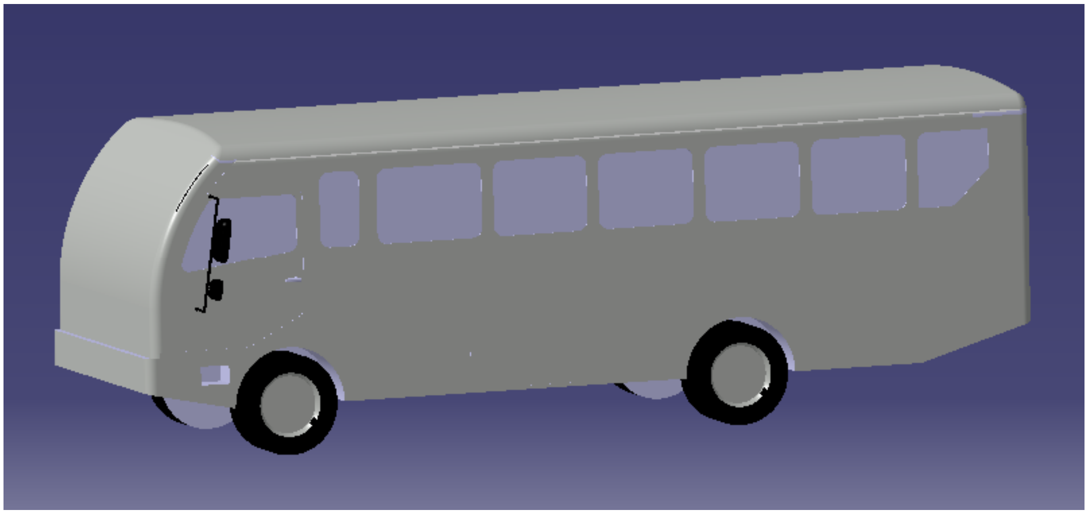

Figure 4. 2 Modified bus model

4.3 Static structural skeleton

4.3.1 Modeling of Existing and modified Bus Skeleton structure

Reducing the total impact energy in bus accidents can be achieved through several key methods: decreasing the bus's mass, mitigating the effects of gravitational acceleration during a fall, or, most promisingly in the short term, minimizing the vertical distance the bus's center of gravity falls. This reduction in fall height is also intrinsically linked to the prevention of rollover accidents, a significant concern for passenger bus safety. The stability of passenger buses is a major design consideration, influenced by various factors. Among these, height is critical because it determines the position of the center of gravity. A higher center of gravity increases the instability of the bus, hence increasing the chance of a rollover accident, and in case of a fall, increases the impact energy. It therefore means that strategies directed towards lowering the center of gravity and preventing rollovers will be central in improving buses' safety and reduced impact energy (Reddy et al 2016).

Bus structure consists six main parts. This are: top and floor frame, left and right side frame, back and front frame. The body design parameter contains height and stability. The dimension of the structure is taken from ANTA metals engineering solution with direct measurement. All structural dimensions are measured by meter. The structure is made by steel material. The material form is rectangular and square hollow section. The modeling of the structure is made by CATIA V5 R19 software. The scope of this structural design is to improve stability by reducing the internal height of the bus to the minimum suitable seating purpose. This is concluded depending on the prediction of the height of Ethiopian people study before.

- ✓ **Load carrying capacity of the skeleton structure**

There are two different loaded on the top of the structure. These are load due to pressure of air and weight of the luggage (sheet metal cover, roof rack structure and luggage). Different types of luggage is loaded on the on the top of the roof rack. Among this bag is one of the luggages. The dimension of single luggage is length, width, and height 0.47m, 0.26m and 0.6m respectively. Mass of luggage allowable load for one the passengers 25kg (Tirfe et al., 2021). The bus holding capacity of 33 passengers.

- ✓ **Volume of roof rack**

The amount of load to be loaded on the top of roof rack is calculated from the volume of the roof rack. The volume of roof rack is taken from the dimension of roof rack which are length, width and height. The measured value of this dimension is 3m, 1.3m and 0.3m respectively. But the height of luggage is 0.6 m, therefore this height should be considered in volume of roof rack.

$$V_{RR} = L \times W \times H \text{ -------------------------------equ (4. 1)}$$

L =length ----------- (3m)

W = width------------- (1.3m)

H = height------------- (0.6m)

V_{RR} = 3m x 1.3m x 0.6m

V_{RR} = $\mathbf{2.34m^3}$

Therefore the volume of roof rack is 2.34m^3.

Volume of luggage compartment

$$V_L = l \times w \times h \text{------------------------------------equ (4. 2)}$$

L=0.47m w = 0.26m   h = 0.6m   L (length), w (width), h (height)

V_L = 0.47m x 0.26m x 0.6m

V_L = **0.07332m^3**

The total numbers of luggage accommodated by roof rack are calculated from the V_{RR} and $V_{L.}$

$$TNL = \frac{\mathbf{VRR}}{\mathbf{VL}} \text{--equ (4. 3)}$$

$$TNL = \frac{2.34m3}{0.07332m3} = \mathbf{32}$$

- ✓ **Load on skeleton structure**

Load on the structure are load due to pressure of air and load due to loaded items

- ✓ **Load due to luggage**

The luggage load is calculated by multiplying the number of luggage suited at available space and mass per each luggage. The available space holds 32 luggage's'. The number of passenger bus carry is 33 passengers. 25kg luggage is allowed for one passenger. The total mass of luggage is 25kg x32 = 800kg

$$W = mg \text{ ---equ (4. 4)}$$

W = weight , m = mass, g = acceleration due to gravity

W =800kg x 9.81m/s^2

W = **7848 N**

- ✓ **Load due to roof rack and sheet metal**

The material of roof rack is RHS 25 x 25 x 1.5. The total length of the RHS used for manufacturing the structure is 39915mm and sheet metal cover the roof rack structure is

7500mm x 1.5mm the sum of their length are 300mm. the length of both roof rack structure and support are 40215mm

The weight of square RHS is: weight = density x volume

$$W \text{ (weight)} = \rho \times V \text{--equ (4. 5)}$$

$\rho = 7850 kg/m^3$

$$V = A_{CS} \times L \text{--equ (4. 6)}$$

L_T = **40215mm**

$$A_T = (W_O \times H_O) - (w_i \times h_i) \text{ --------------------------------------equ (4. 7)}$$

W_O= Outer width (25mm) H_O = outer height (25mm)

w_i = inner width (22mm) h_i = inner height (22mm)

$A_{CS} = (25 \times 25) - (22 \times 22)$, $A_{CS} = 625mm^2 - 484mm^2$

A_{CS} = **141mm²**

$V = 141$ mm2 $\times 40215mm = 5670315mm^3 \approx V =$ **0.005670315m³**

$W = \rho \times V$

$W = 7860kg/m^3 \times 0.005670315m^3$, $W = 44.5119kg \approx$ **44.57kg**

Therefore the weight of roof rack structure is 44.51kg the load of the roof rack are:

$W = mg = 44.57kg \times 9.81m/s^2$

W = **437.23N**

The weight of sheet metal cover the top of the structure which are curved at the end taken from CATIA software calculation which is 160.91kg load of sheet metal cover is:

$W = mg = 160.91kg \times 9.81m/s^2$

W = **1569.6N**

The total load the skeleton structure carry are the sum of the luggage load, roof rack RHS structure load and sheet metal cover load

W_T = 7848N + 437.23N +1569.6N

W_T = **9854.83N**

- ✓ **Load due to air pressure**

To know maximum air pressure load on that implied on the structure we have to conduct ANSYS fluent simulation at ideal speed 150km/h (Tirfe et al., 2021). From the following graph we have the pressure contour results that shows maximum pressure on exposed parts at considered speed is 1100 pa.

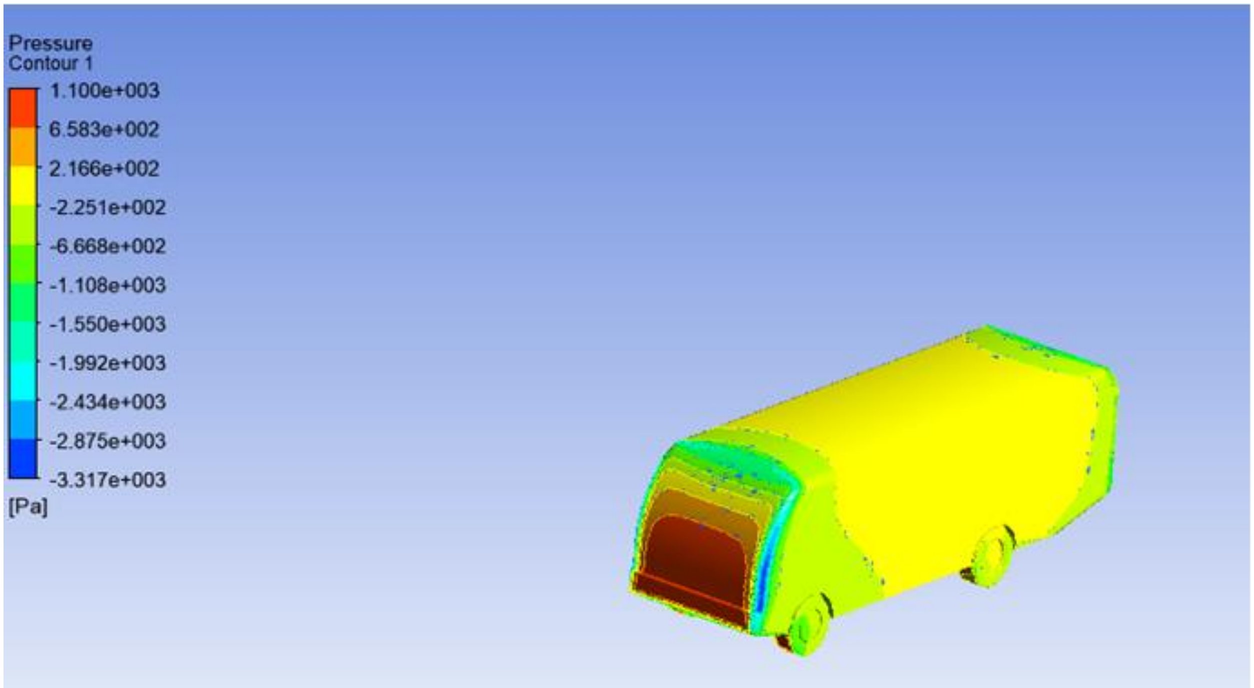

Figure 4. 3 pressure contour of modified bus at 150km/h

Table 4. 1 Load of air pressure and above roof structure of bus

Load above roof structure of bus	Weight (N)
Luggage	7848
Roof rack	437.22
Sheet metal cover	1569.6
Total load = 9854.83	
Air pressure load	1100 Pa

4.4 Stress analysis of skeleton structure

The previous research that optimized bus frame design for structural integrity, weight reduction, and noise/vibration mitigation through numerical and experimental method. Existing shape and size optimizations of frame components lay the groundwork for a more detailed investigation. And simulation of structural model was developed to evaluate the impact of beam thickness and roof cross rail end corner radius on the bus's load-bearing capacity. This previous study reveals that increasing beam thickness will directly correlate with enhanced stress strength and contributing to a reduction in the bus body skeleton's overall weight., characterized by critical parameters: a tensile and compressive yield strength of 360MPa, a yield stress of 220MPa, a density of 7850 kg/m³, a tensile strength of 386 MPa, a Young's modulus of 200 GPa, and a Poisson's ratio of 0.3, as documented by (yang & deny, 2015).

The structural analysis of bus is manufacture from different parts; top, floor, right, left, back and front frame members. To withstand load coming from air against to motion and load due to item on roof rack. In order to know the strength of the skeleton analysis load from two directions need to be studied. For the load from air pressure CFD analysis through optimal seed is studied. Load due to roof rack structure, luggage loaded and sheet coverage should be calculated.

Table 4. 2 material property of structural steel

Parameter of steel	Their value
tensile yield strength of	360MPa
compressive yield strength of	360MPa
yield stress	220MPa
density	7860 kg/m³
tensile strength	386 MPa
Young's modulus	200 GPa
Poisson's ratio	0.3

4.4.1 Material of skeleton

The material used for the construction of the structure is steel. The material forms are rectangular and square hollow section RHS, sheet metal u-channel and angle iron.

4.4.2 Geometry creation of structure

The skeleton structure of the Isuzu bus is the foundation of vehicle integrity and safety, and is made from the various forms of high-strength steel. This frame, an interconnected network of beams, columns, and bracing interconnected through weldments, has been designed to last under operational stresses and loads such as passenger and luggage, road vibration, and occasional impact. This skeletal framework cannot be neglected as per safety regulations and the bus should be dependable and continue to remain in service for a longer time. In order to cater to the optimization of the bus height design for structural analysis, a 3D model was created using CATIA V5 R19 software, and the same was imported into ANSYS Workbench. ANSYS Workbench inherently recognizes the assembly members as being in contact. The accuracy, convergence, and solution speed are mesh-dependent. Elements is 50mm. The steel material used for manufacturing the skeleton, with specific properties defined for the analysis, ensures the structural strength of the assembly.

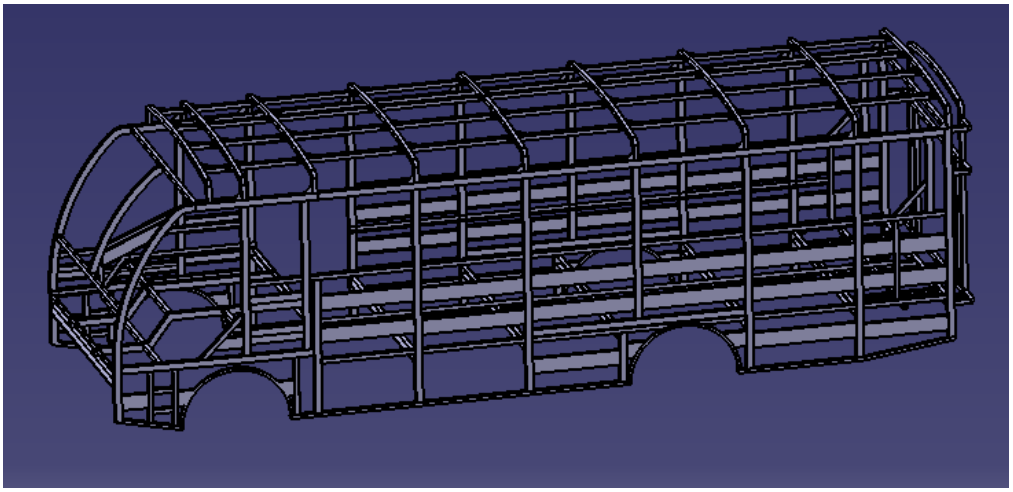

Figure 4. 4 Structural skeleton of existing bus

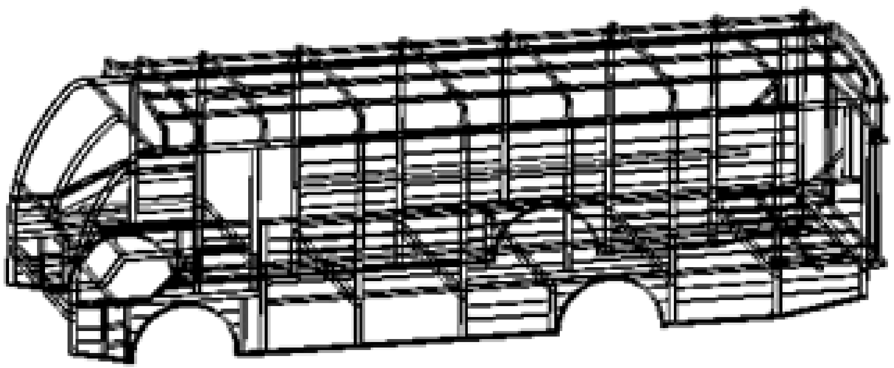

Figure 4. 5 Geometry Structural skeletons after imported into ANSYS workbench.

4.4.3 Stress analysis Results of skeleton

A. Equivalent (von- mises) stress of skeleton

This image shows the results of a static structural analysis performed on a bus skeleton using ANSYS. it visualizes the Equivalent (von-Mises) Stress distribution across the structure. Because complex loading conditions exist, such a tool is useful for predicting the yield of ductile materials. It combines all the different components of stresses (normal and shear) into a single value which is then compared with the yield strength of the material in question. The color distribution on the bus skeleton pinpoints the most and least stressed areas under the applied static loads. The analysis indicates a maximum equivalent stress of 154.28 Mpa and a minimum of 0 Mpa within the skeleton structure under the simulated static conditions. The structure is made of structural steel (mild steel) its yield strength are 360 Mpa. The von mises stress results of structure on the figure 154.28 Mpa which is less than yield strength of the structure material 360Mpa. Therefore the skeleton structure withstands the applied load.

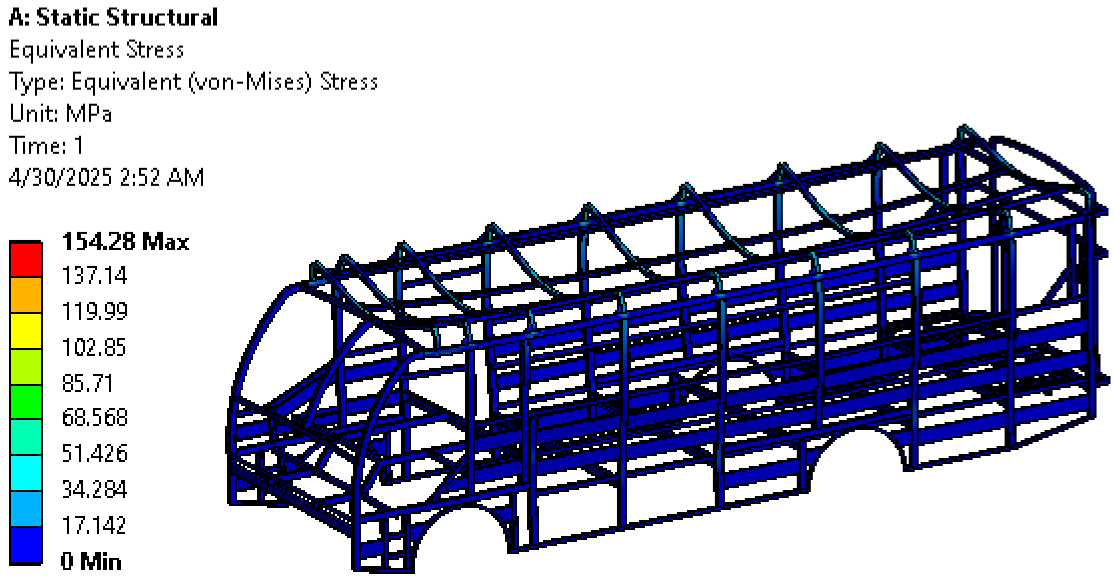

Figure 4. 6 Equivalent (von mises) stress of skeleton

B. Maximum shear stress

Maximum shear stress is the highest magnitude of shear stress experienced at any point within the material under the given loading conditions. Maximum shear stress is also a crucial parameter. Maximum shear stress is a direct indicator of potential failure. The analysis indicates a maximum shear stress of 83.815 MPa and a minimum of **0** MPa within the skeleton structure for this static load case. The allowable shear stress for the material 360Mpa used in the bus skeleton is a critical parameter for evaluating these results. The maximum calculated shear stress should be well below the material's shear strength which is 83.815Mpa.

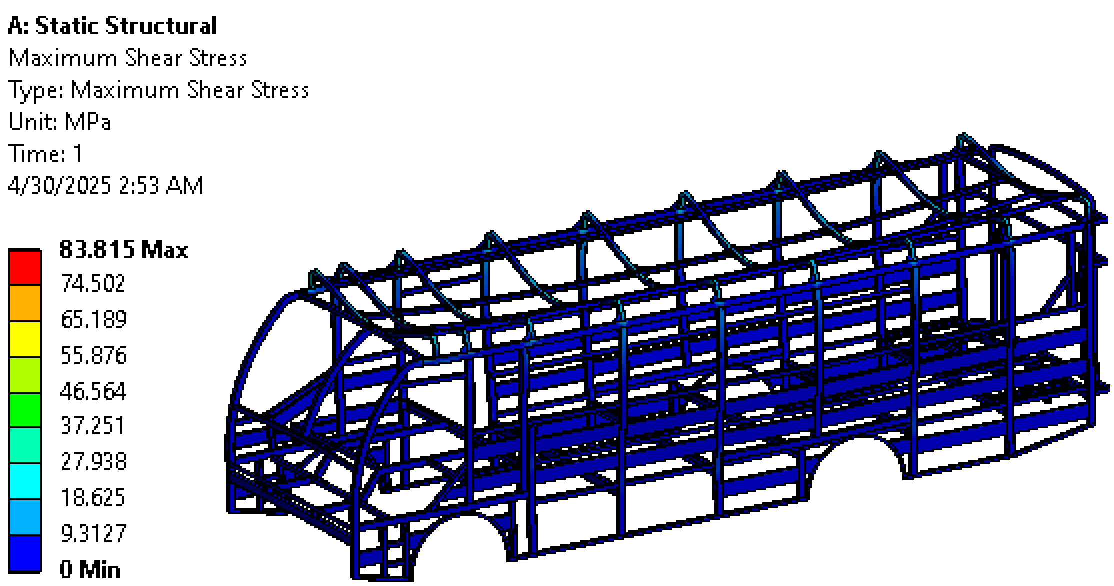

Figure 4. 7 Maximum shear stress of skeleton

C. Total Deformation

Total deformation in a structural analysis refers to the displacement of each point on the structure from its original, unloaded position under the applied loads. It's a vector quantity. The Total Deformation result typically ANSYS is the magnitude of this displacement vector. It essentially tells you how much each part of the structure has moved. High Deformation Areas have undergone the most significant displacement. In this image it appears that the highest deformation is concentrated in the central roof structure and possibly some of the upper side rails. According to the previous study the maximum deformation of the structure is 4mm which is safe regarding the deformation (Tam et al, 2023).

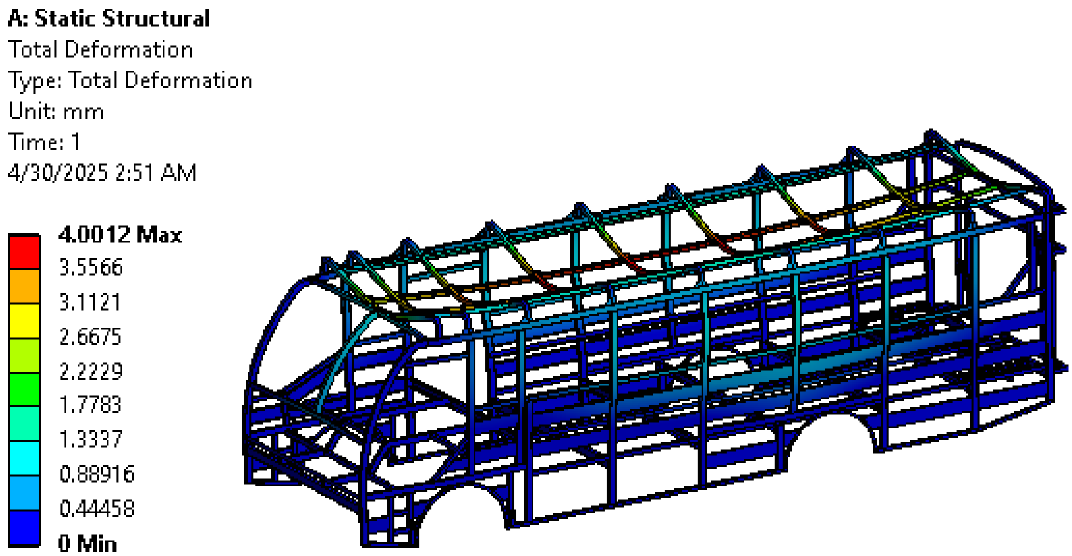

Figure 4. 8 Total deformation of skeleton

4.5 CFD Analysis

4.5.1 Geometry creation

The scaled geometry of the bus is modeled using CATIA V5 R19 software. The model converts into IGS forms which are used as an input data during analysis. The scale is 1:20. ANSYS Fluent software are used for CFD analysis. The model that converted into IGS format imported into ANSYS workbench. The dimension for the model design was taken from ANTA Metal Engineering Solution.

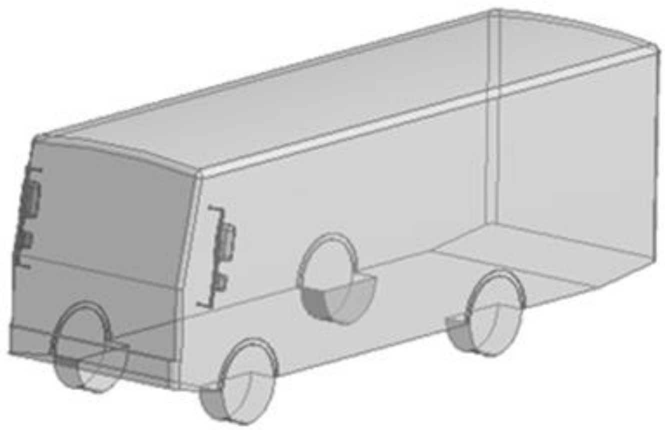

Figure 4. 9 Geometry Existing bus after imported into ANSYS workbench.

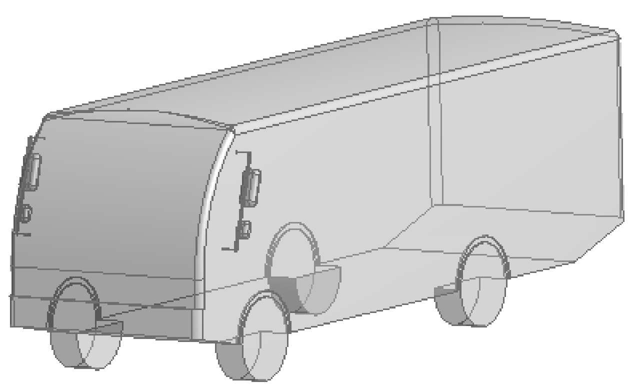

Figure 4. 10 Geometry modified bus after imported into ANSYS workbench.

After importing geometry that is converted into IGES format to refine the computational grid in the nearest of the bus model, the geometry of the physical domain and the enclosure created around it for the simulation play fundamental roles in the accuracy and efficiency of the results. According to the previous study the dimensions of the domain size are 3times of bus in upstream, 5 times length in downstream because wake region need more space for flow behavior, the side plane and height is about 2times length and finally the road attached to the wheel of the model. Wake region need more space for flow behavior. Boolean operation used to subtract volume of bus from volume of enclosure which represents volume of air (Tirfe et al., 2021).

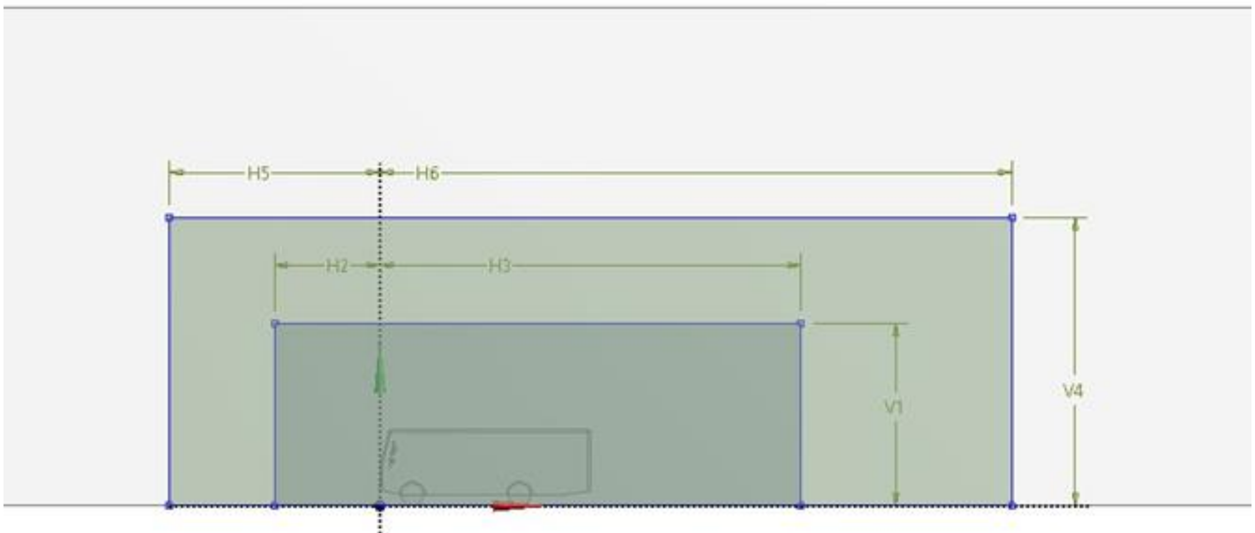

Figure 4. 11 Geometry of existing bus inside enclosure and two inner box

4.5.2 Mesh generation

A refinement zone was introduced to further investigate in mode detailed mesh around Bus. Mesh generation is one of the preprocessing stages next to geometry during analysis. Element sizing is should be considered during mesh that govern our results and operational time of analysis. The relevance used during meshing describes the finesses of the analyzed model. The relevance of 100 is high accuracy and time delay running time, while -100 means low accuracy and fast processing time. High smoothing method increases the number of iteration and element quality. (yudianto et al, 2021). Surface meshes are generated for both the bus itself and the outer boundary of the simulation area. Computational grid generated between body surfaces and enclosure. The computational cells need to be sufficiently small. For flow near the bus finer mesh is recommended on the boundary. At a distance from the bus flow are the same and mesh are coarse. Solver time and cell depends on element sizes. (Damissie et al., 2017).

In this study zero relevance method are used. The mesh used for the simulation is fine cells close to the surface of the bus to ensure accurate results in that critical area. Coarse mesh is used for area away from the bus body. Overall, the entire simulation area was composed of approximately1.4 million with tetrahedral element were used.

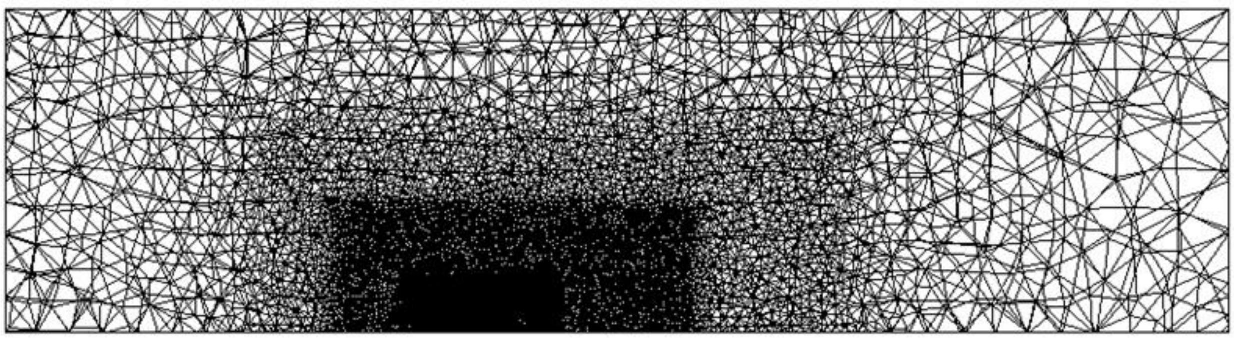

Figure 4. 12 Mesh of existing bus

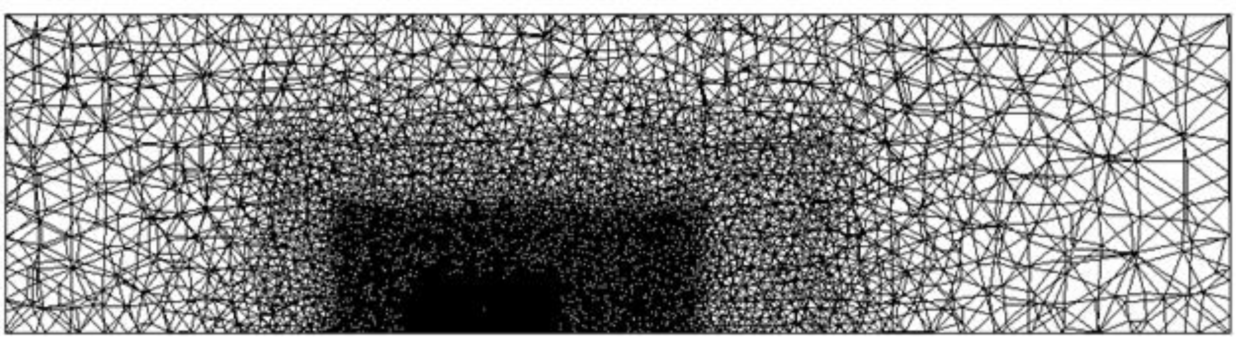

Figure 4. 13 Mesh modified on bus

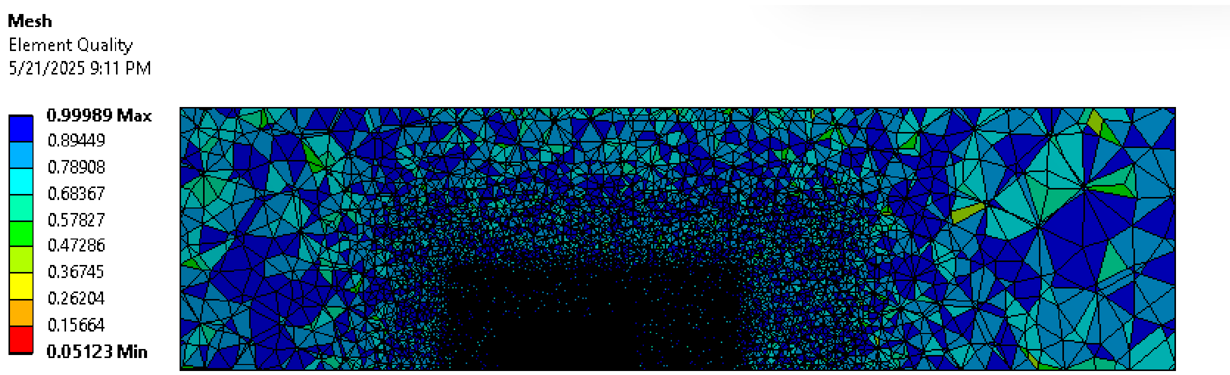

Figure 4. 14 Mesh quality of existing of bus

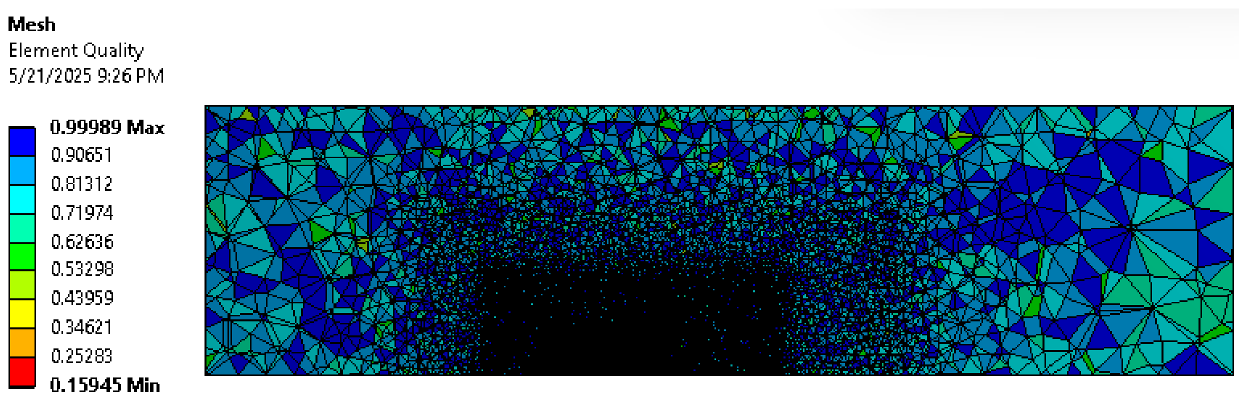

Figure 4. 15 Mesh quality of modified of bus

4.5.3 Grid independence test

A fundamental aspect of any reliable Computational Fluid Dynamics (CFD) study, was conducted to ensure the simulation results' independence from the computational grid. This process involves systematically refining the grid until further refinement yields negligible changes in the solution, that gives accuracy results and reliability (Kahsay and Zeleke, 2024). For the modified bus and modified bus, the grid independence study was performed using computational grids with the following number of elements:

Table 4. 3 Grid independence test for modified bus

Mesh	Nodes	Elements	Drag coefficients	Lift coefficients
1	148773	839772	0.4629	-0.2901
2	182435	1021806	0.4661	-0.2838
3	246633	1410411	0.4617	-0.3001
4	235784	1355669	0.4612	-0.3327
5	254145	1452820	0.4610	-0.3037

The drag and lift coefficient of the modified bus model was done for computational grids made of 839772, 1021806, 855819 and 1355669, 1410411 and 1452820 elements. The drag coefficients results in the above is nearly the same and the lift coefficient at mesh four is better improve stability. Therefore the mesh size of 5mm and element count of 1355669 was applied for all analysis.

4.5.4 Boundary Conditions

A full range of boundary conditions was utilized in the Computational Fluid Dynamics (CFD) simulation to adequately describe the flow around the bus. A constant-velocity boundary condition was assigned at the inlet in order to replicate the experimental test velocity, with three different wind velocities (80 km/h, 100 km/h, and 120 km/h) simulated. The outlet was defined as a pressure outlet at atmospheric pressure (zero gauge pressure). The two sides and the roof of the computational domain were defined as symmetry boundaries, which effectively functioned as no-slip boundaries. The bottom boundary represented the moving ground, and the analysis included the rotational effects of the bus wheels. A complete prescription of the flow was made with the specification of values for all flow properties within the computational domain.

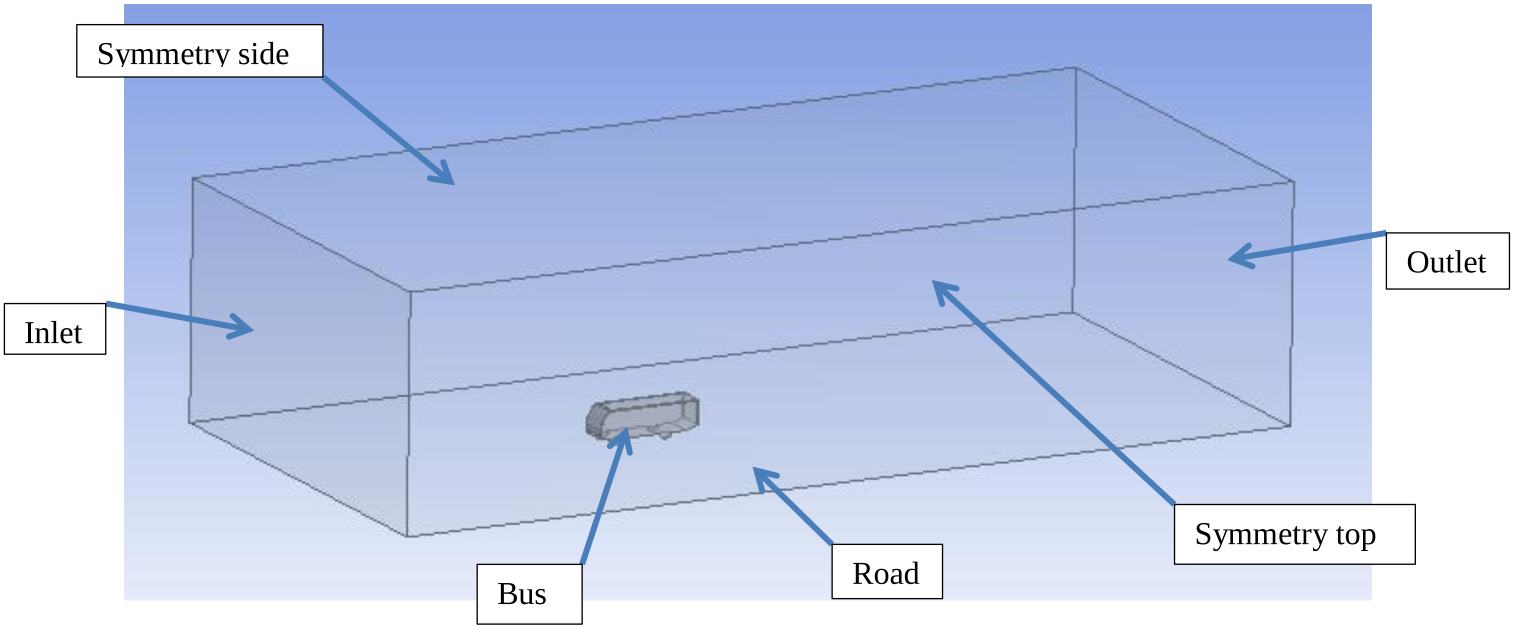

Figure 4. 16 Name selection

4.5.5 Fluent stage

To obtain trustworthy CFD predictions for turbulent flow, careful attention must be paid to the quality of the turbulence model. The ANSYS Fluent manual highlights the SST k-ω model as a strong choice when capturing boundary layer details is crucial, especially in involving flow separation or when precise heat transfer profiles are needed. Furthermore, numerous studies have demonstrated the SST k-ω model's ability to yield CFD results that closely align with experimental observations across a diverse set of applications. Given the importance of accurately resolving turbulent flow, particularly near walls, the SST k-ω turbulence model was selected for this analysis. The simulations were conducted across three distinct speeds: 80 kmph, 100 kmph, and 120 kmph. At the outlet of the computational domain, a zero gauge pressure condition was applied, with the operating pressure set to atmospheric levels. To ensure numerical stability and control convergence, a Courant number of 20 and relaxation factors of 0.25 were employed. For external aerodynamics of a bus, the "free stream" inlet might be considered low turbulence, e.g., 0.5% to 1% if it's "clean" air. Flows downstream of grilles, screens, or other significant flow conditioners. If the bus is operating in the wake of another vehicle, the incoming turbulence could be very high which is >5% up to 20%. At the inlet, the turbulent flow characteristics were defined by setting the turbulence intensity to 1% and the turbulent viscosity ratio to 10. Correspondingly, at the outlet, the turbulence intensity was specified as 5%, and the turbulent viscosity ratio as 10 (Tirfe et al., 2021).

Table 4. 4 Boundary conditions

Boundary	Boundary condition		values
Inlet	Constant velocity turbulent intensity viscosity ratio		V=80, 100 &120kmh 1% 10%
Outlet	Gauge pressure turbulent intensity viscosity ratio		O Pa 5% 10%
Road	Moving wall		V=80, 100 &120kmh
Bus	No slip stationary wall		________
Symmetry top and symmetry side	Wall is stationary with no slip		________

4.6 Experimental tests and methods

This chapter emphasize on the validation of numerical results of modified model through experimental in wind tunnel tests. The wind tunnel experiments are done in adama science and Technology University by using HM 170 open wind tunnel. Scaled modification test model is located in a fixed plan and the fluid flow is maintained in the state of movement
(Tirfe et al., 2021).

Wind tunnel testing is essential in aerodynamic design. It simulates the air flow around the vehicle or object in a controlled environment. The object does not move and the air turns to different speed and angle to repeat the actual phenomenon. Through this, engineers provide the opportunity to study the dynamic of air interactions that the air flows into an object and separates it from it. Knowing the way these forces act is necessary for understanding the aerodynamic characteristics of the object and determining where it can be improved in design. (M. Palanivendhan et al. ,2021).

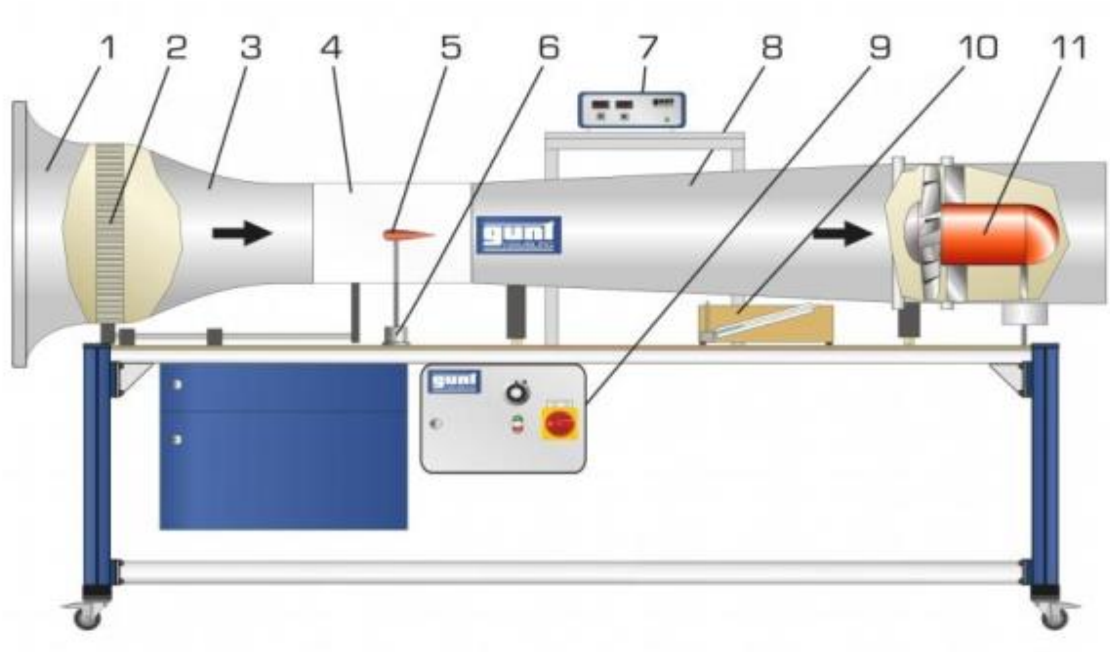

Figure 4. 17 HM 170 educational wind tunnel **(Tirfe et al., 2021)**

1. Inlet
2. Flow straightener
3. Jet
4. Measurement
5. Model
6. Electronic two component force transducer

7. Measurement amplifier with force display
8. diffuser
9. Switch box with fan speed control
10. Inclined tube nanometer for air speed
11. Axial fan

4.7 Specification of wind tunnel

Table 4. 5 specification of HM 170 wind tunnel (Lab manual)

General data	Value
Dimension	L x W x H: 2860 x 860 x 1700mm, Weight: 250kg Power supply: 230 VAC, 50 Hz, 1ph
Measurement section	Cross section 292 x 292 mm Length approx. 420mm
Force measurement	Model holder L to center of model 225mm
Measurement range	Lift 10 N, Drag 10 N Resolution: 0.1 N
Air flow	Air velocity -28m/s
Fan	Head 500 Pa Max. air flow 2.5m3/s , motor power 2.25kw Speed (frequency control)up to 2800RPM

4.8 Wind Tunnel Testing

The model ISUZU fluid flow tests are performed so far at speeds of 80 km/h, 100 km/h, and 120 km/h. The resistance for various speeds was measured to study the effect of the forward form and the deformation of the area of the aerodynamic characteristics (M. Palanivendhan et al, 2021). The obtained fluid mechanics results are compared to those of the attained experiments. The maximum error margin of 5% in the modeling and empirical results thereby confirm that the model reflects the basic physics quite well. Most of the inherent errors in a computational model arise from general approximations associated with meshing the geometry and the imposition of boundary conditions that may perfectly correspond to those in real life, leaving much room for inaccuracies. The experimental setup brings with itself a different set of errors whereby it is due to precision in manufacturing the test article, accuracy of installation within the wind tunnel, and the internal uncertainty in the measurement process Calibration is then conducted twice yearly, thereby eliminating or tapering off the gradual and unwanted changes or inaccuracies of just these force measurements being attained from the wind tunnel balance. The drag forces continually remain almost constant with increased speeds. One of the most basic tenets to minimize aerodynamic drag is to steer airflow so that it stays attached to the object surface and avoids the formation of large energy-dissipating wakes due to the separation of flow (Yuan and Wang, 2017).

The implications of wind tunnel tests regarding the reduction of wind speed upon wind showed that there may be a small difference between the experimental and simulation conditions. this difference has been considered unimportant as it stemmed from an unavoidable constraint in wind tunnel models and setups. (Sikder & Abedin, 2023).

The wind tunnel has the most accurate control of the air flow so far. One is able to test things definitely among other objects in the bus. When air flows over an uneven surface, like the underside of a bus with its mechanical parts (wheel axles, transmission, differential), it creates turbulence – a chaotic mix of pressure and speed changes. To deal with the strongest turbulence at the rear of the bus, an additional wing is often installed there. Furthermore, Placing a front wing creates increased pressure on the upper surface of the bus. There are more clamping power or negative rise, so the buses are increasingly stable among other objects on the bus (Arteaga et al, 2020).

4.9 3D Model Preparation

To study how air moves around a bus small 3d scaled down model of the bus should be constructed to validate CFD results. The materials used for the production of 3D models can be wood, metal or plastic. The scaled-down model is placed in the wind tunnel, generally attached to a special tool, the force balance. While air flows over the model, the force balance gives a precise reading of aerodynamic forces acting on it, such as drag and lift. A critical parameter for wind tunnel testing is the blockage ratio (B) defined by the frontal area of the model (A) divided by the cross-sectional area of the wind tunnel (AT); the blockage ratio indicates how much the airflow in the tunnel is disturbed by the presence of the test model. In experiments with aerodynamic fluid, the model must take place in the test section. The blocking coefficient is essentially determined by the ratio of the tunnel cross -sectional area to be involved in the model when viewed directly from the upward trend. This obstruction will alter the natural free flow of air that would exist if the tunnel were empty. Consequently, the air accelerates around the model, changing its pressure distribution. Thus, the blockage ratio can be taken as an indicator of the magnitude of these interference effects that the tunnel walls impose on the measurements. (Howell et al, 2021).

$$B = A/A_T \quad \text{-----equ (4.8)}$$

Where B – Blockage Ratio

A – Frontal Area

A_T – Working Section Area

The area of the cross section is 0.292m x 0.292m = **0.085264** m^2

It is very important to consider how the test model prevents the air flow when testing for aerodynamic tunnels. This closure is determined in relation to the lock, which compares the frontal area of the model with the intersection -section area of the wind tunnel.

Findings indicate that for square-shaped models occupying no more than 10% of the tunnel's area. (Tirfe et al., 2021).

In order to get the blockage ratio less than 10% the frontal area of the modified bus should be less than:

$$A_m = A_T \times \frac{10}{100} \quad \text{-----equ (4.9)}$$

$$A_m = A_T \times \frac{10}{100} = 0.085264 \times \frac{10}{100} = \mathbf{0.0085264}\ m^2$$

The frontal area of modified model should be less than 0.0085264 m^2 to get the blockage ratio less than 10%, according to data taken from ANSYS reference value reading the frontal area of the scaled modified bus is 0.0043473208 m^2 which is less than 0.0085264 m^2. The blockage ratio of the scaled modified model is:

$$B.R = \frac{A_m}{A_T} = \frac{0.0043473208}{0.085264} = 0.0509$$

The percentage of blockage ratio is 5.1% which is less than 10%.

The 3D scaled modified model was printed in Addis Ababa (wesen). The model is printed with scale of 1:35 scaled down. The following figure is the feature of machine when printed.

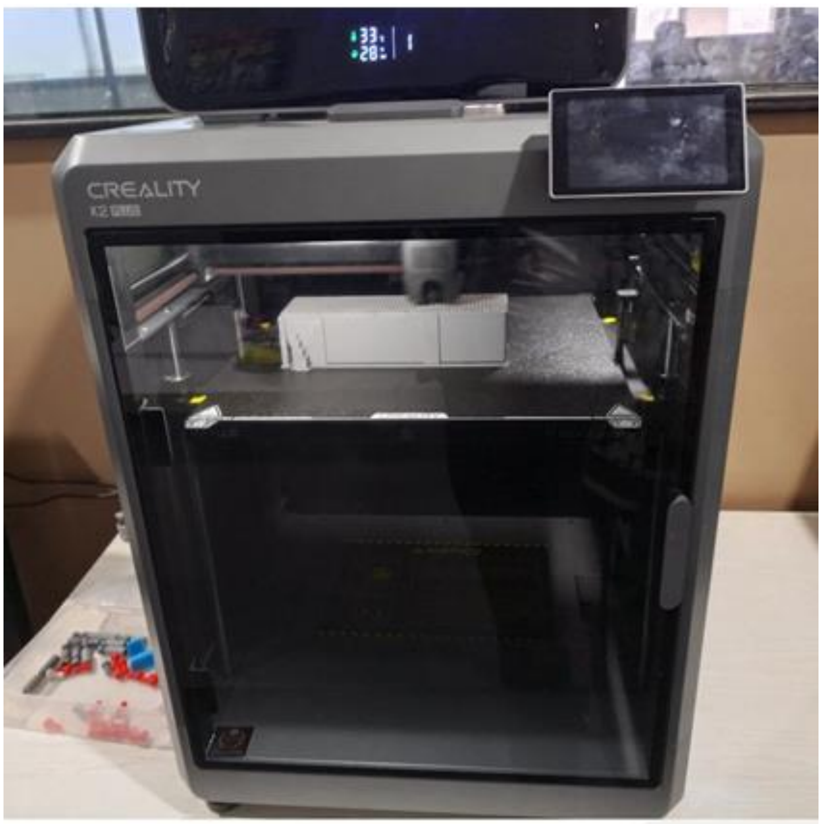

Figure 4. 18 Creality K2 plus 3D printer

4.10 Geometry creation

The geometry of scaled 3D modified model with scale of 1:35 is modeled using CATIA R 19 V5 software. After the modeling the model is converted into STL format and taken into the printer machine and printed. The material used to print this model is plastic materials. The 3D model is divided into thin layers or slicing technique which take into coding method. This machine melt this plastic material with high temperature.

Figure 4. 19 Printing time of modified bus model

4.11 Test procedure

After scaled 3D modified model is printed the experimental was conducted on HM 170 educational wind tunnel at Adama science and Technology University.

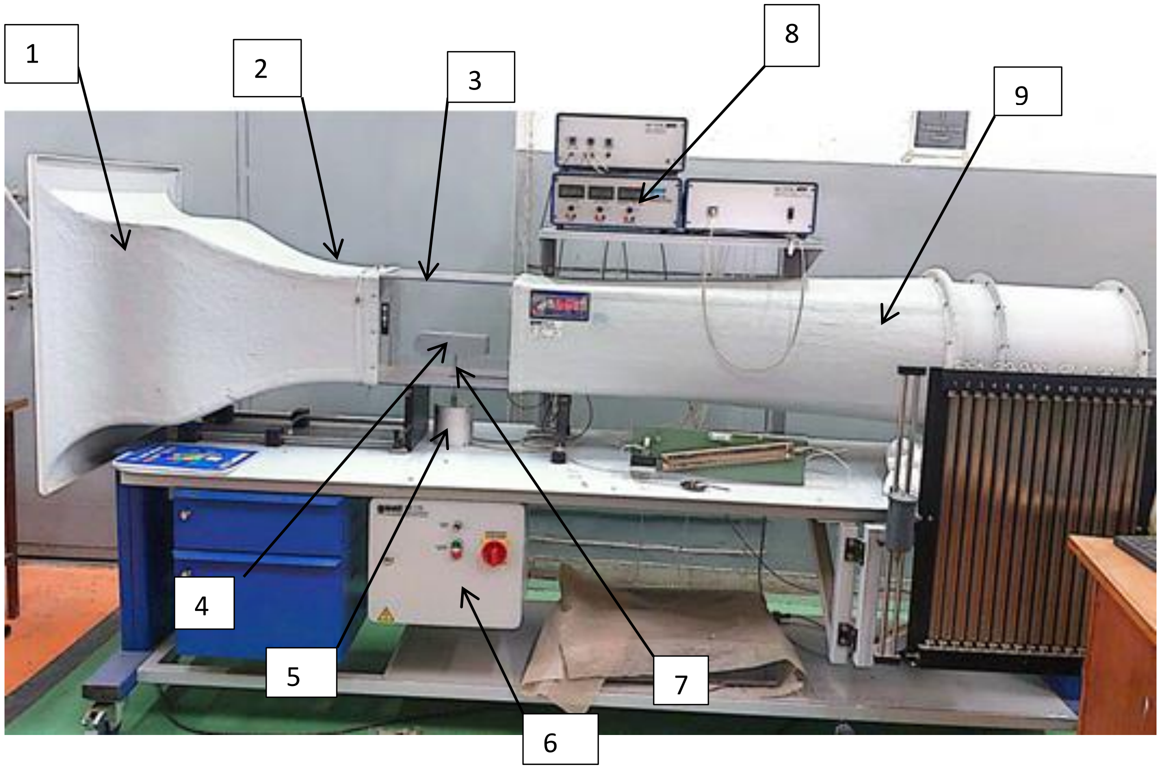

Figure 4. 20 HM170 educational wind tunnel and modified model mounted on it (Adama science and Technology University)

1. Funnel (inlet)

2. Jet

3. Measuring section

4. Bus

5. Force transducer

6. Speed adjuster and switch box

7. Model holder

8.Maesurement amplifier with force display

9. Diffuser

This machine (HM170 educational wind tunnel) is used to finding the lift force, drag force and moment of modified bus model. Wind tunnel testing closely simulates real-world driving conditions by adjusting wind speed and precisely managing environmental factors like temperature, humidity, and turbulence. Before starting the test the first step is measuring the relative humidity and temperature during testing time. The temperature and relative humidity of room is 25.8℃ and 60% respectively. To assess the aerodynamic performance of a test model, advanced instruments are used. Force balances accurately measure key aerodynamic forces such as drag, lift, and side force. The second is adjusting and tilting the modified model on model holder on force transducer.

Figure 4. 21 Zeroing the measuring amplifier

The third is to zeroing of the measured amplifier. The reading on amplifier must be zero before start running. The fourth is switch on the power and adjusting variable speed controller sequentially and recording data for each speed. Finally reduce speed to zero level and switch of the power.

CHAPTER FIVE

RESULTS AND DISCUSSION

5.1 Introduction

This chapter deals with more about results of computational fluid dynamics (CFD) analysis and validate with experimental tests. The analysis is done using ANSYS Fluent after the geometry importation into ANSYS work bench. Analysis is performed in two models (existing and modified models) at speeds of 80, 100 and 120 km. All research results are as follows:

5.2 Results of the Existing bus

The Computational Fluid Dynamics (CFD) analysis of a bus conducted at three different speeds: 80 km/h, 100 km/h, and 120 km/h. The analysis focused on evaluating the aerodynamic performance and stability of the existing scaled bus model and The following key parameters were investigated: Residual, drag coefficient, lift coefficient, drag force, lift force, pressure and velocity contour.

A. Residual history at 80km/h

The scaled existing model. This shows the convergence history of the Computational Fluid Dynamics (CFD) simulation for the scaled existing model. the first 200-300 iteration speed components show a rapid reduction. Subsequently, the rate of residual reduction slowed considerably for the remaining iterations. The simulation is carried out for 1000th iteration with residual of 10^{-5}. This low level of residue, achieved using the SST K-ω turbulence model along with the secondary sampling, is known as an increase in accuracy through minimal numerical diffusion. This provides strong confidence that the CFD analysis has achieved adequate convergence for the key flow parameters within the specified computational effort

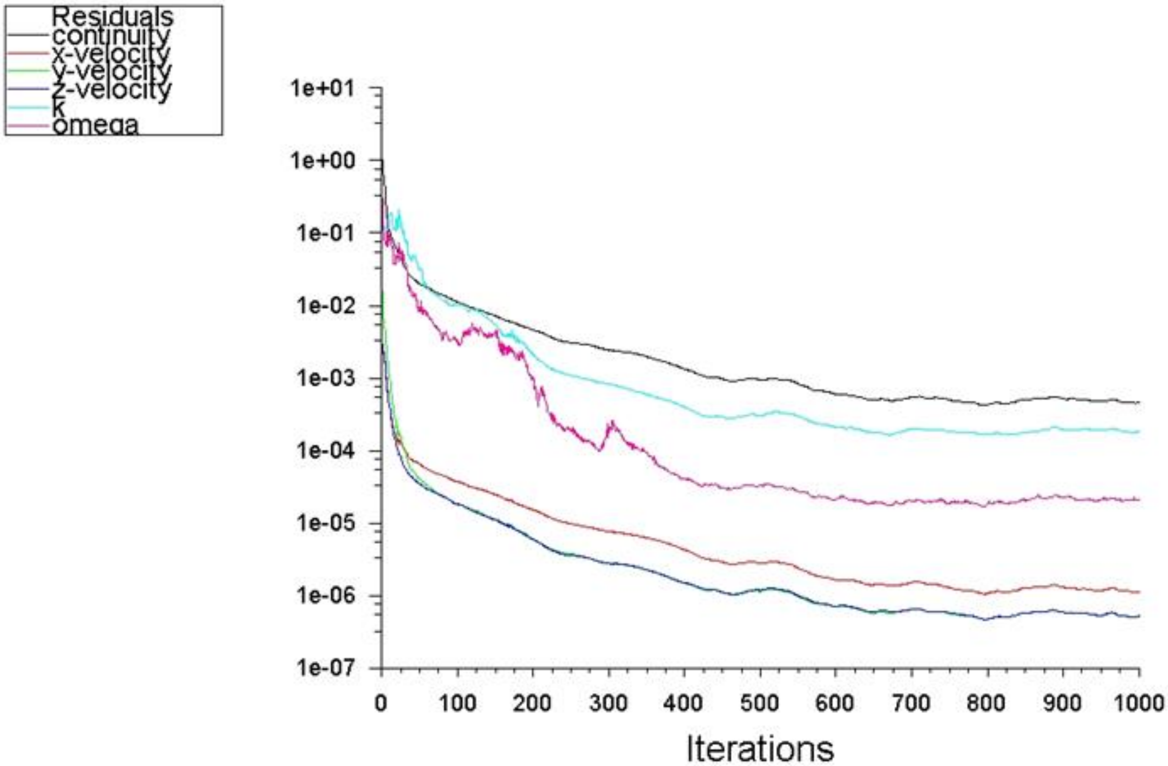

Figure 5. 1 The residual history of existing bus at 80km/h

C. Drag coefficient

Figure 5.2 -5.4 shows aerodynamic drag coefficients as a function of iteration. It is the result of computational fluid dynamics simulation. The x- axis represent the number of iteration or time steps the simulation was run. The progress continually iterate until the convergence solution was reached. Initially, the drag coefficient fluctuates significantly within the first 50- 100 iterations. Beyond this point, the drag coefficient stabilizes and converges to a relatively constant value, remaining nearly unchanged from approximately 100 to 1000 iteration. The y - axis represent the value of drag coefficient. This indicates that the simulation must have converged to a stable solution in terms of the drag force; In 80 km/h, 100 km/h and 120 km/h, the drag coefficient existing bus is 0.6473, 0.6442 and 0.6406, respectively. Considering this, about 0.64 was found if the average value.

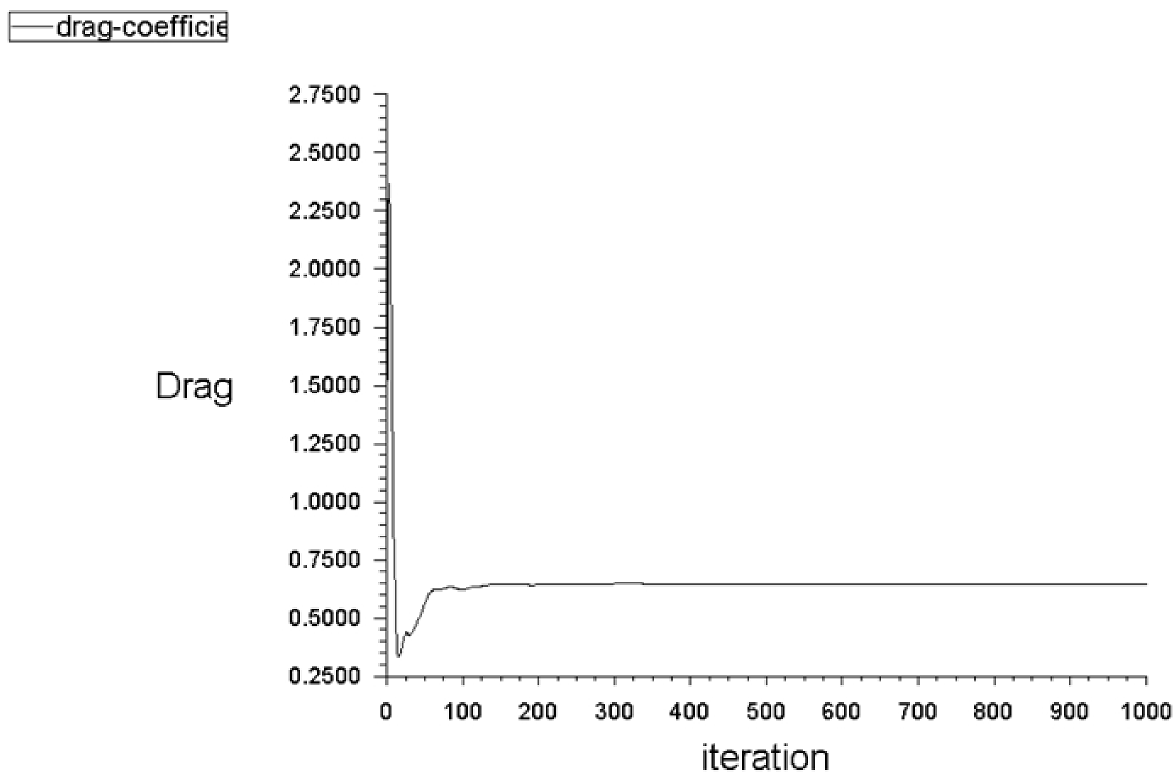

Figure 5. 2 Drag coefficient of existing bus at 80km/h

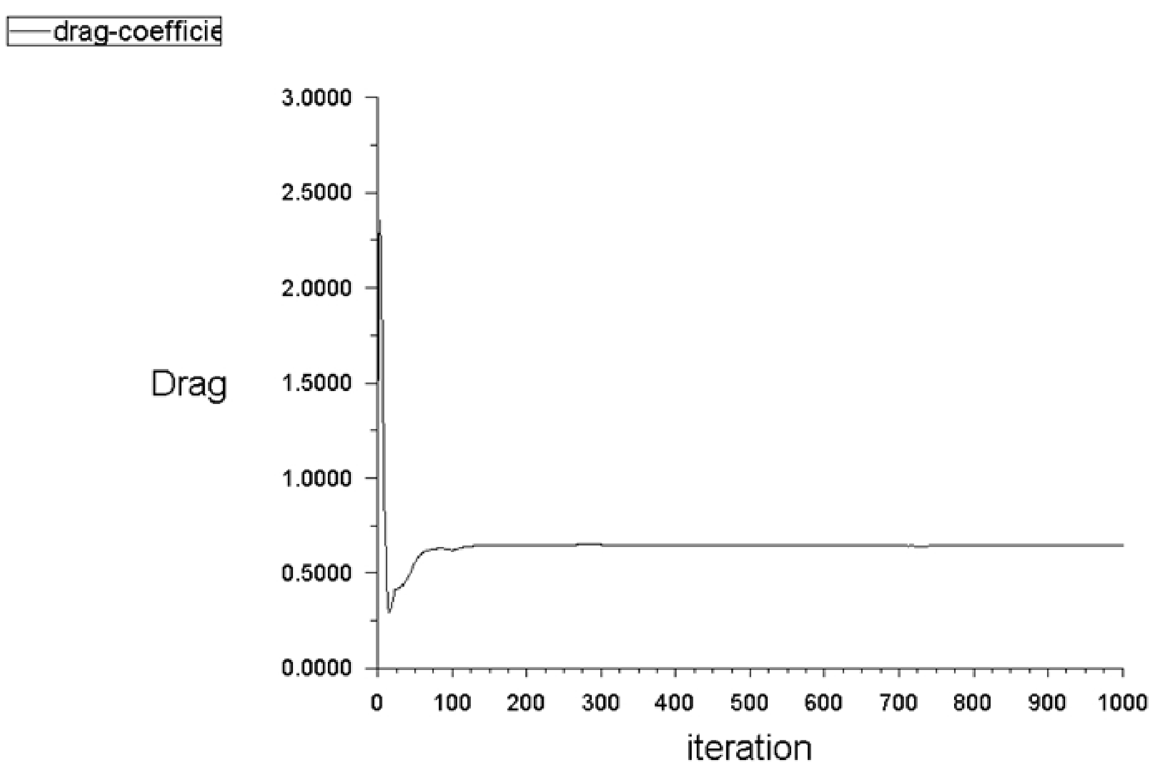

Figure 5. 3 Drag coefficient of existing bus at 100km/h

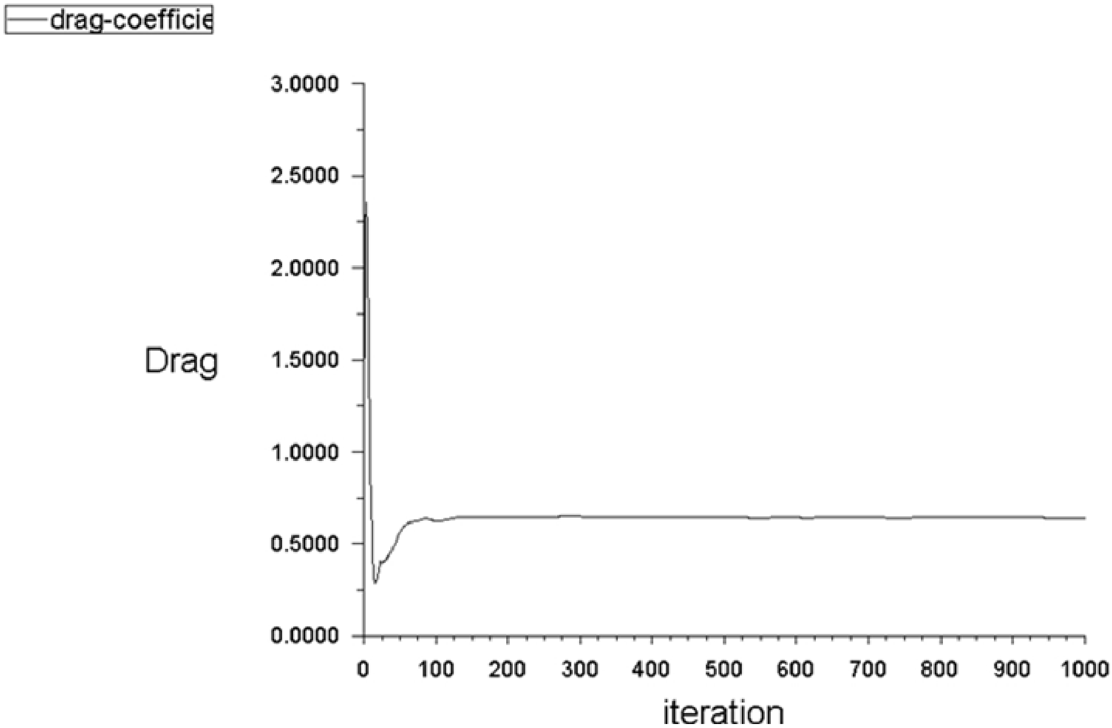

Figure 5. 4 Drag coefficient of existing bus at 120km/h

B. Lift coefficient

Figure 5.5 -5.7 shows aerodynamic lift coefficient as a function of iteration. It is the result of computational fluid dynamics simulation. The x- axis represent the number of iteration or time steps the simulation was run. The progress continually iterate until the convergence solution was reached. Initially, the lift coefficient fluctuates significantly within the first 50- 100 iterations. Beyond this point, the it stabilizes and converges to a relatively constant value, remaining nearly unchanged from approximately iteration 100 to 1000. The y - axis represent the value of lift coefficient. Their lift coefficient values obtained from computational fluid dynamics at velocities of 80 km/h, 100 km/h, and 120 km/h are: -0.1630, -0.1608, and -0.1605, respectively. The average value is – 0.16 approximately. This negative value shows that the lifting power acts to hold the wheel on the ground. This means that it is good results relative to stability of the bus.

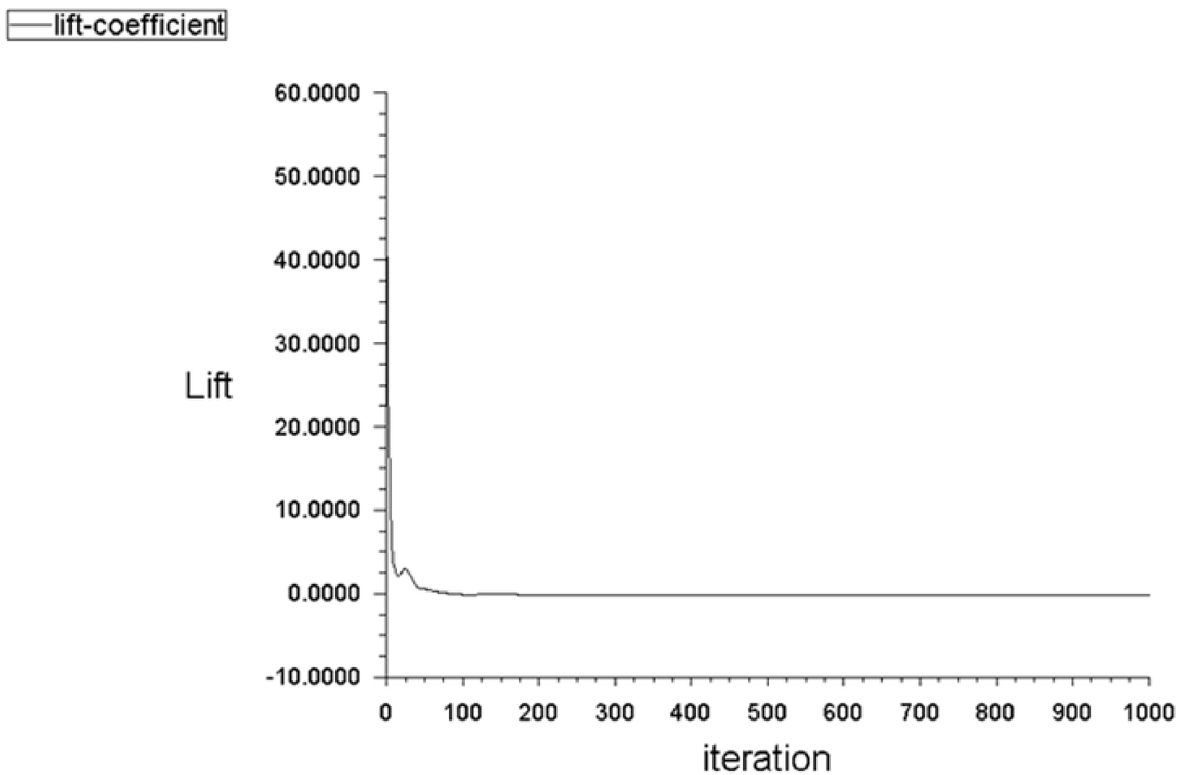

Figure 5. 5 coefficient of existing bus at 80km/h

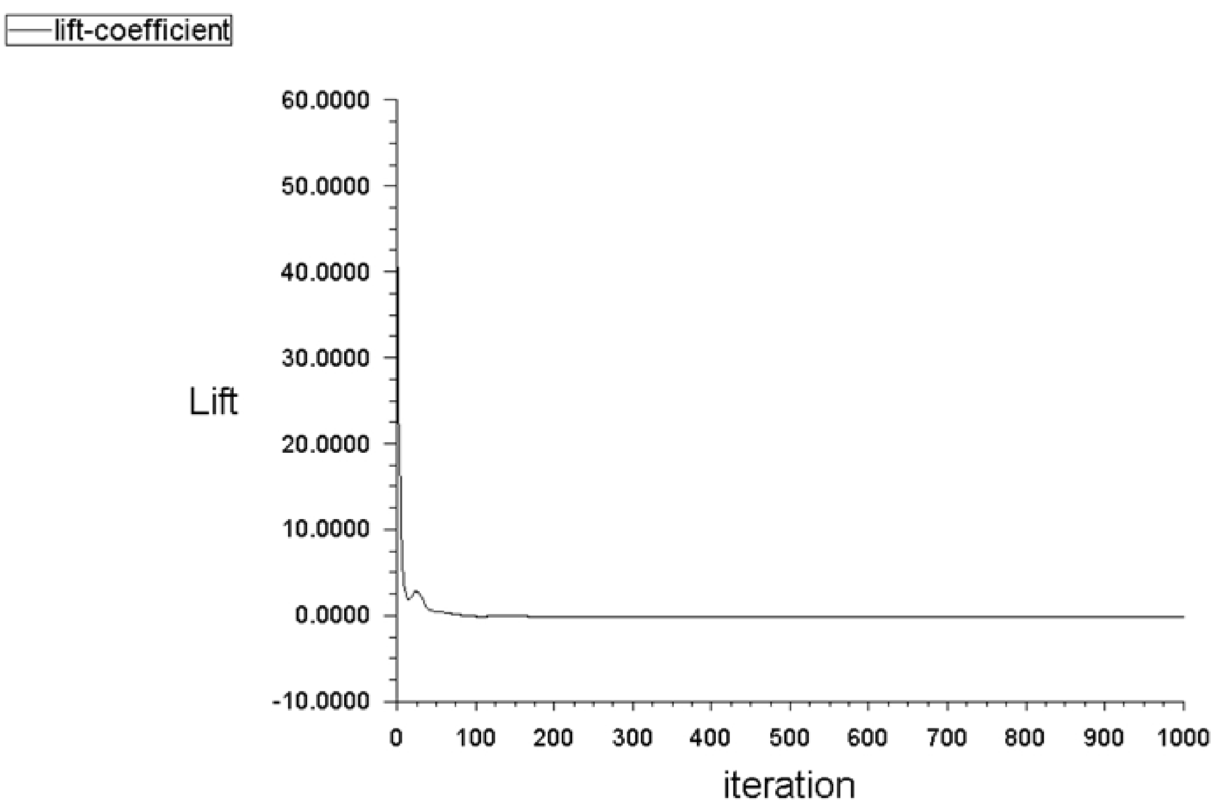

Figure 5. 6Lift coefficient of existing bus at 100km/h

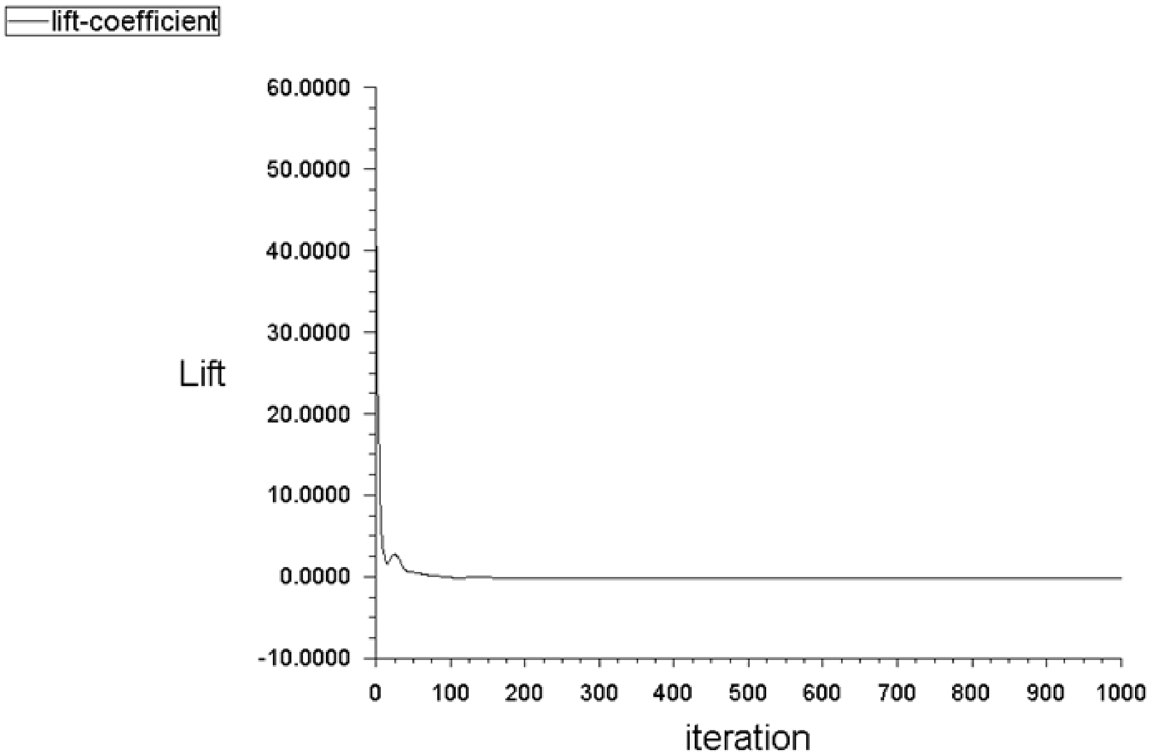

Figure 5. 7 Lift coefficient of existing bus at 120km/h

D. Pressure Contour

Figure 5.8 -5.10 shows the pressure contour of the existing bus. The legend on the left side of the figure indicated in different color the represents the value of pressure distribution surrounding the body of the bus. It is the output of the computational fluid dynamics simulation depends on the input given data. The results show that there is high pressure at stagnation point. There was high and low pressure zone as a legend indicated. The simulation carried out within 80km/h, 100km/h and 120km/h and the results indicates that the pressure distribution changes significantly with speed. The CFD simulation shows that the blue color indicates the region of negative pressure, while red indicates positive pressure, passing from bottom to top. The high-pressure front face of the bus, indicated in red on the front face, reveals the high positive pressure zone where the drag force acts. The yellow on the upper and side regions of the bus indicates low area pressure. The blue color shows a minimum pressure surface. As airspeed increases, so does the pressure magnitude, both positive and negative, on the surface area of the bus. Has less aerodynamic refinement. Because it have more sharp edges, protrusions (mirrors, lights), or flat surfaces. These features cause flow separation, vortices, and turbulent wakes, which degrade simulation clarity and pressure contour definition. The mesh resolution around complex surfaces (mirrors, grills, wheels) of the existing bus might be insufficient.

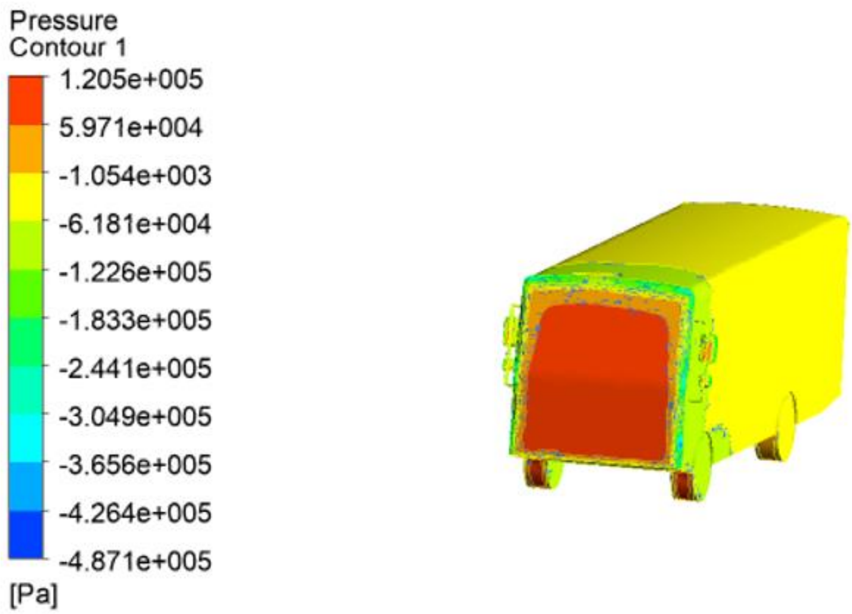

Figure 5. 8 pressure contour of Existing bus at 80km/h

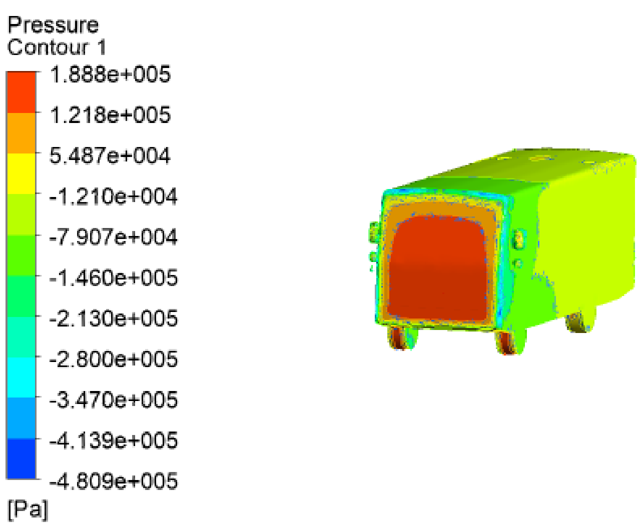

Figure 5. 9 pressure contour of Existing bus at 100km/h

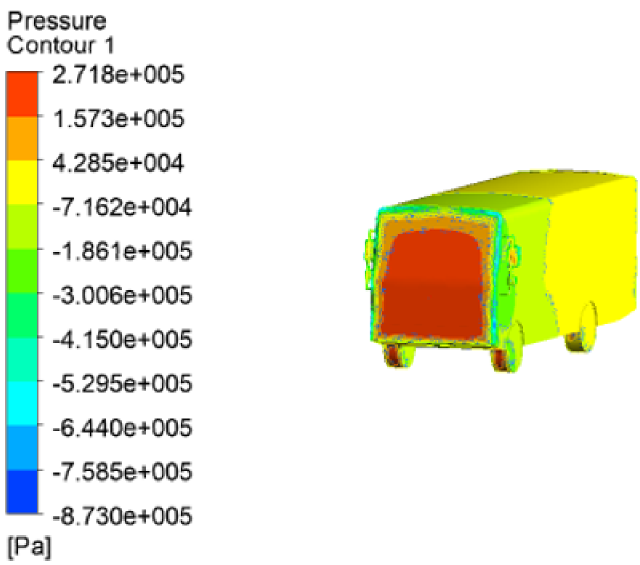

Figure 5. 10 pressure contour of Existing bus at 120km/h

The figure pressure reveals that the maximum pressure contour at speed of 80km/h, 100km/h and 120km/h is 120.5kpa, 188.8kpa and 271.8kpa respectively. The minimum pressure is -487.1kpa, -480.9kpa and -873kpa respectively.

D. Velocity Contour

Figures 5.11, 5.12, and 5.13 shows the velocity contours for bus model under airflow velocities of 80km/h, 100km/h, and 120 km/h, respectively. Various colors of the figure are different in the fluid speed around the bus. The low-velocity zone at the rear of the bus indicates that wake formation is taking place in this low-pressure zone. It's possible to observe intermediate flows around the object, whereas regions above and below the leading edge are the high fluid velocity areas. The front face of the bus is intended to be recognized as a zone of very high velocity.
However, the rear end of the bus is at a much lower velocity. This is because the air has already been disturbed by the passage of the vehicle. When the vehicle runs, most of the intermediate fluid velocities can be found throughout the main body, due to the fact that air does not pass through directly, but only deflects around their surfaces. On the other hand, the highest velocities persist almost everywhere above and below the front edges (front corners) of the bus, where the

flow accelerates around the curvature. These absolute values would increase for these regions at higher air speeds. All these aspects relating to velocity contours provide useful insight into the aerodynamic flow modalities around the bus.

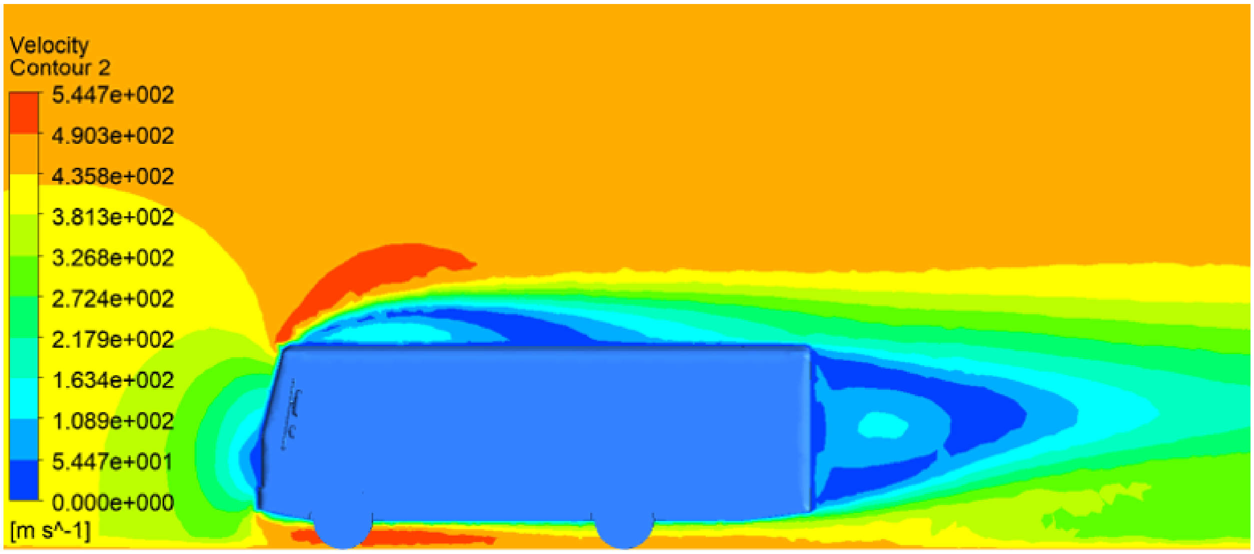

Figure 5. 11 velocity contour of Existing bus at 80km/h

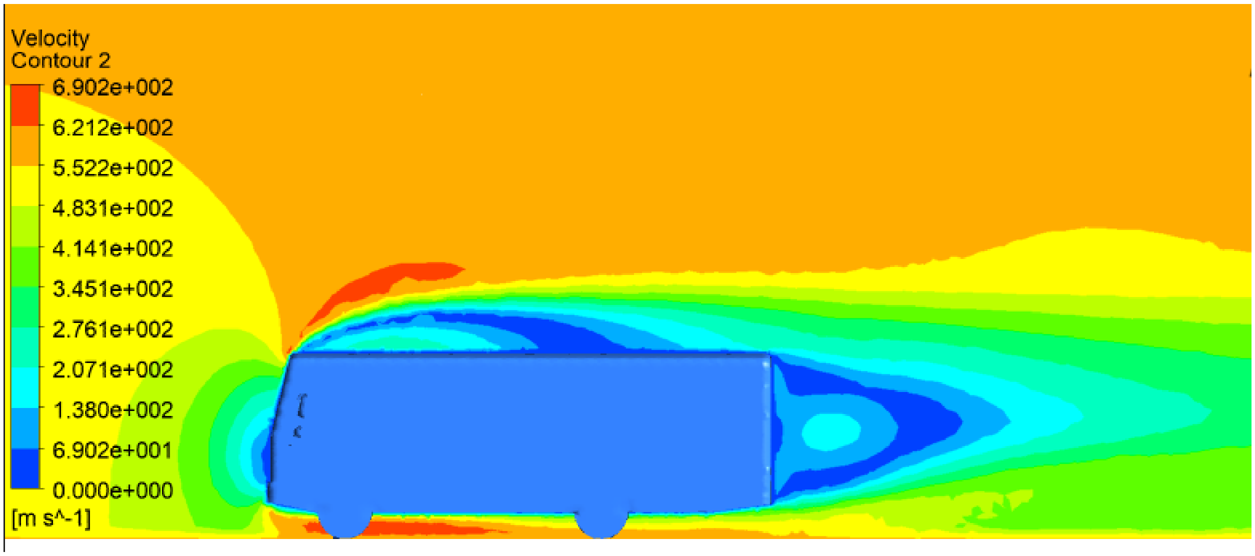

Figure 5. 12 velocity contour of Existing bus at 100km/h

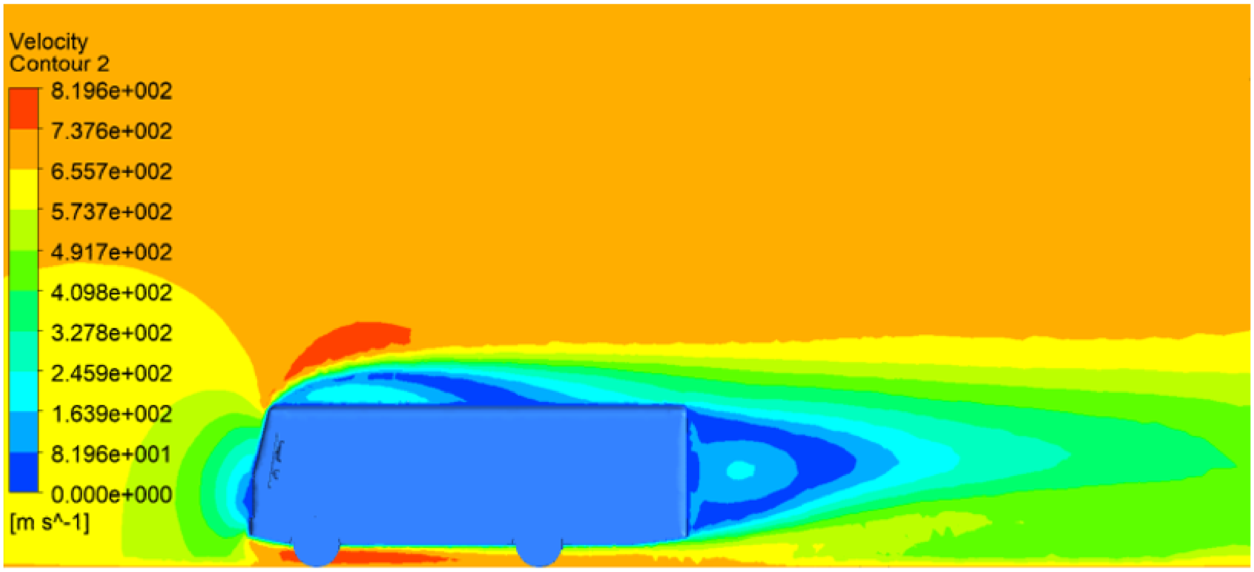

Figure 5. 13 velocity contour of Existing bus at 120km/h

Table 5.1 summarizes the results of scaled existing bus at different velocities of 80km/h, 100 km/h and 120km/h, respectively. The results in the table below reveals that the drag force increase as speed increase and when speed increase become with greater magnitude but in downward direction which increase contact between wheel and road.

Table 5. 1 The summery results of the existing model.

Frontal area of scaled existing bus(m^2)	**Speed (km/h)**	**Drag**		**Lift**	
		Drag coefficient	**Drag force**	**Lift coefficient**	**Lift force**
5.33	80	0.6473	1043.89	-0.1630	-262.87
	100	06442	1623.27	-0.1608	-405.32
	120	0.6406	2324.40	-0.1605	-582.60

5.3 Results of scaled modified bus

1. Residual history

The residual of scaled modified bus model at 80km/h, 100km/h and 120km/h indicate convergence situation of the analysis. The computational fluid dynamic simulation is carried out for 1000 iteration with second order discretization. Employing with second-order discretization, known for minimizing numerical diffusion, generally contributes to a more accurate solution. The figure illustrate that the rapid decreased up to 200-400 iteration approximately. Slowly decrease and converge after 400 iteration. , this residual plot suggests that the CFD analysis, utilizing the SST k-ω turbulence model with convergence order of 10^{-5}.

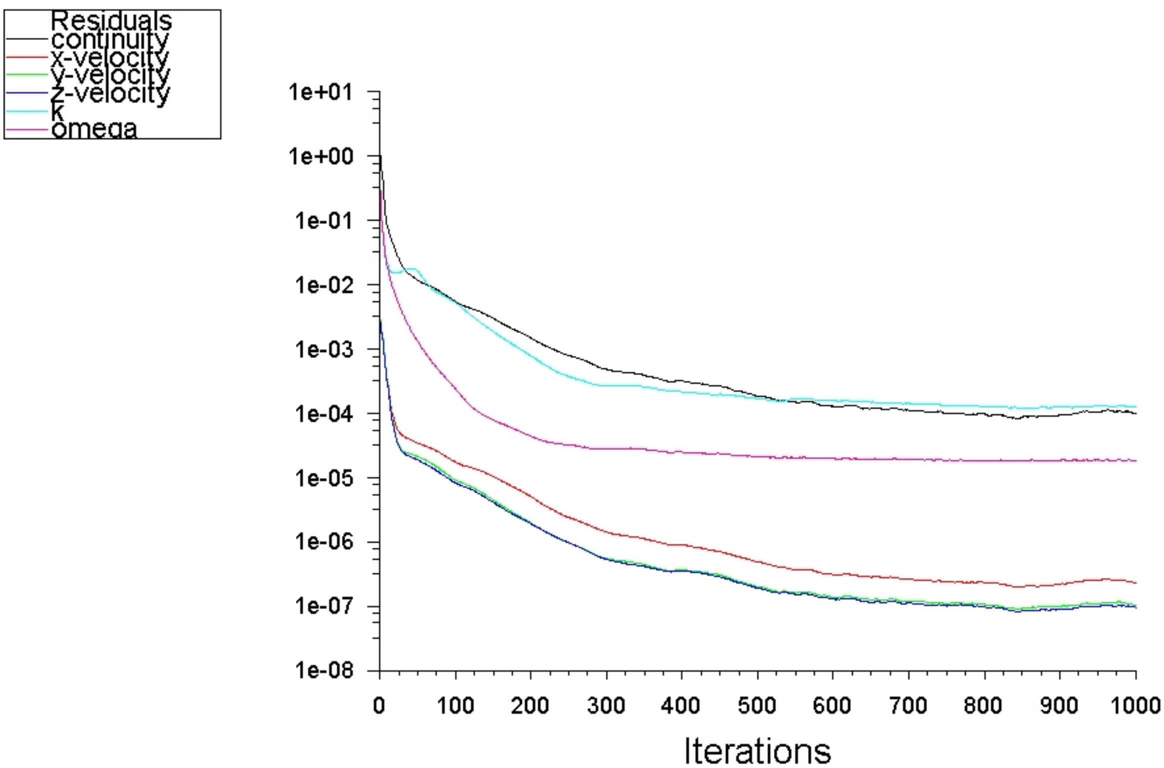

Figure 5. 14 The residual history of modified bus at 80km/h

2. Drag coefficient

The following figure 5.15 – 5.17 indicates the computational results of drag coefficients at speed of 80km/h, 100km/h and 120km/h is 0.4695, 0.4687, and 0.4678 respectively. This values closely the same so that the value is 0.468 approximately. The result indicates the improvement of the existing tire form that improves the resistance coefficient.

The drag coefficient for the existing bus converges to approximately 0.64. The drag coefficient for the modified bus converges to approximately 0.46. The provided data indicates that the modified bus has a significantly lower drag coefficient 0.46 compared to the existing bus 0.64. This reduction in drag is practically very significant due to its direct impact on fuel economy, performance, and environmental impact. The change are both statistically and practically significant.

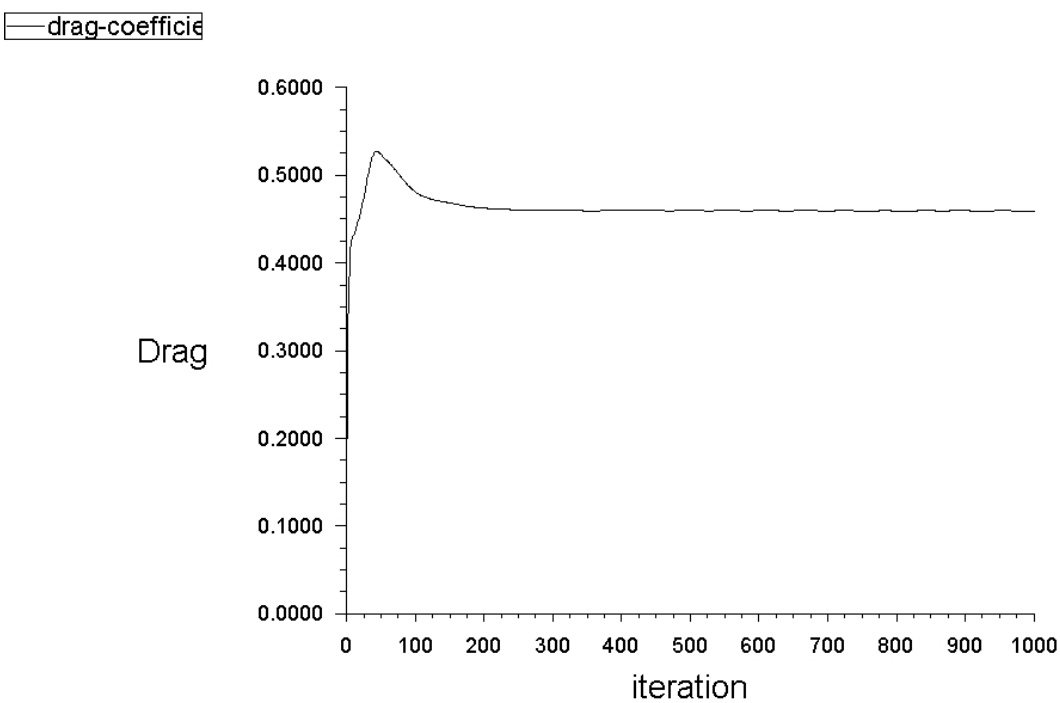

Figure 5. 15 Drag coefficient of modified bus at 80 km/h

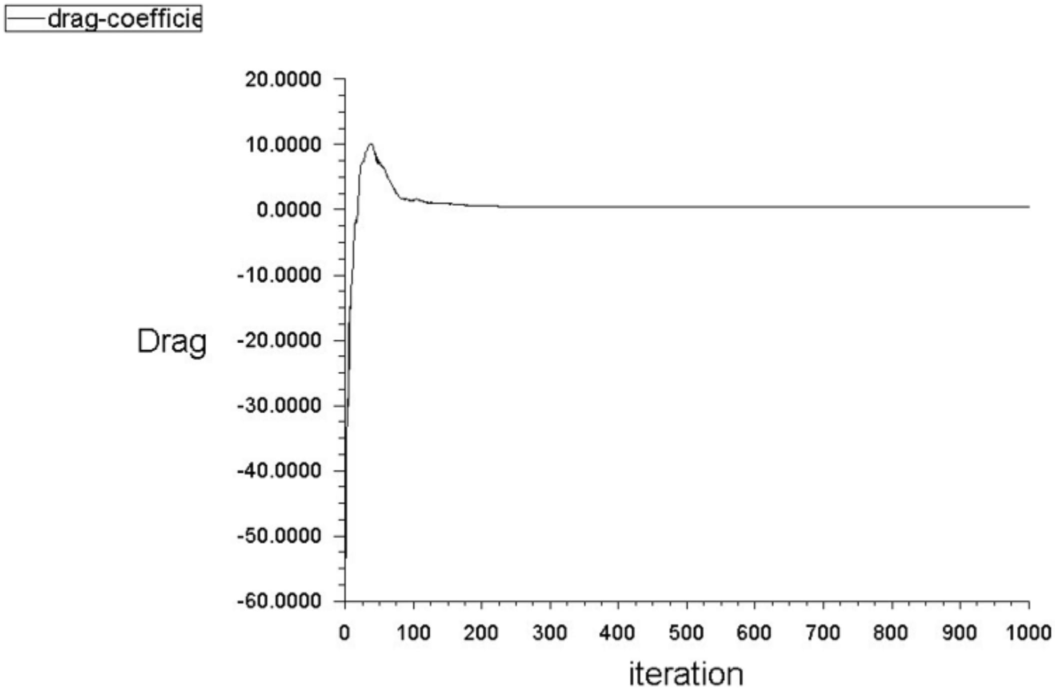

Figure 5. 16 Drag coefficient of modified bus at 100 km/h

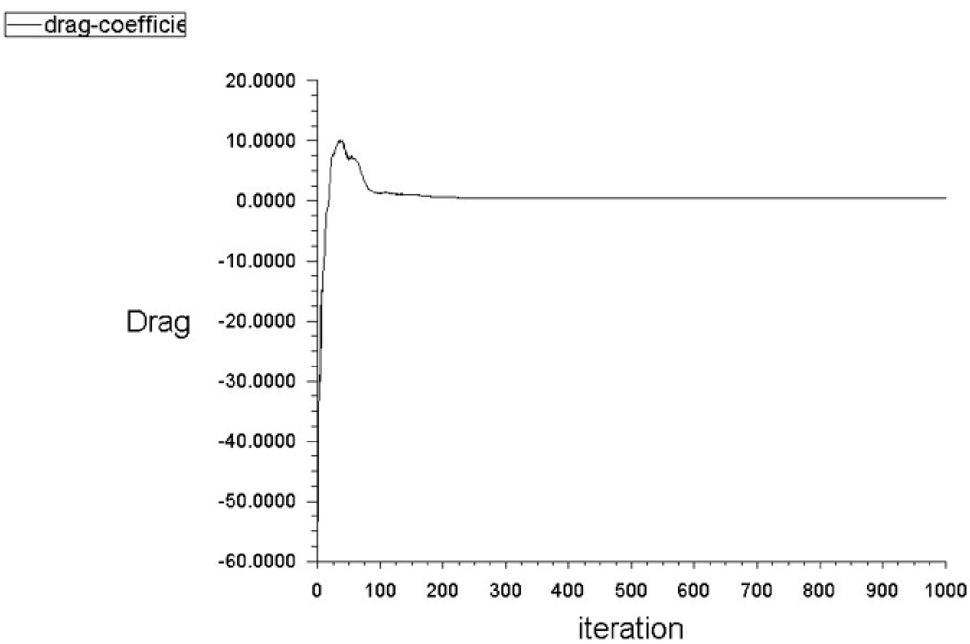

Figure 5. 17 Drag coefficient of modified bus at 120 km/h

3. Lift coefficient

The figures 5.18 - 5.20 below exhibit lift coefficient of scaled modified bus model. The value of the lift coefficient from the computing mechanics of the fluid at speeds of 80 km/h, 100 km/h and 120 km/h is -0.3327, -0, 3326 and -0.3319, respectively. The average value is -0.33 approximately. This negative value indicates that the instead of lifting upwards it is force to downwards which grip more the wheel to the ground. Therefore, the stability has is relatively improved. The lift coefficient for the existing bus converges too approximately -0.3319 to -0.3327. For most road vehicles, including buses, the goal for lift coefficient is to be as close to zero as possible. A positive lift coefficient indicates an upward force that can reduce tire grip, while a negative lift coefficient (downforce) can increase grip but also increases drag. The lift coefficient value of existing bus is -0.1630, -0.1608 and -0.1605 with respect to a given speed. This indicate that the lift of modified bus is greater in magnitude with negative results tales us the drag force is in downward direction which support for holding tire on the road. These helps to improve the stability of bus. The change is statistically and practically significant.

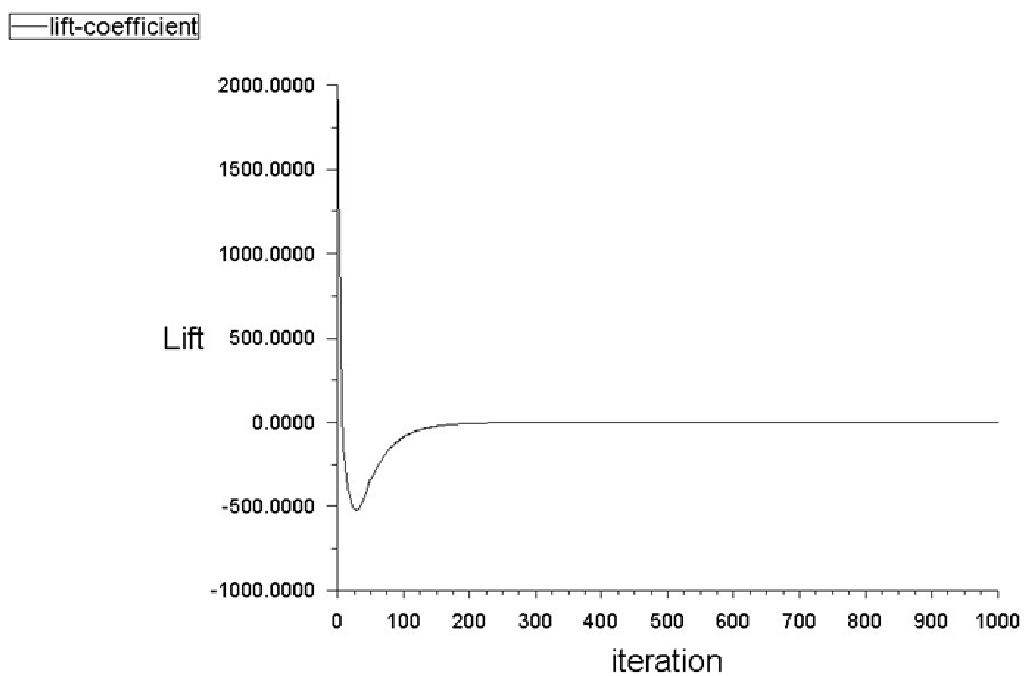

Figure 5. 18 Lift coefficient of modified bus at 80 km/h

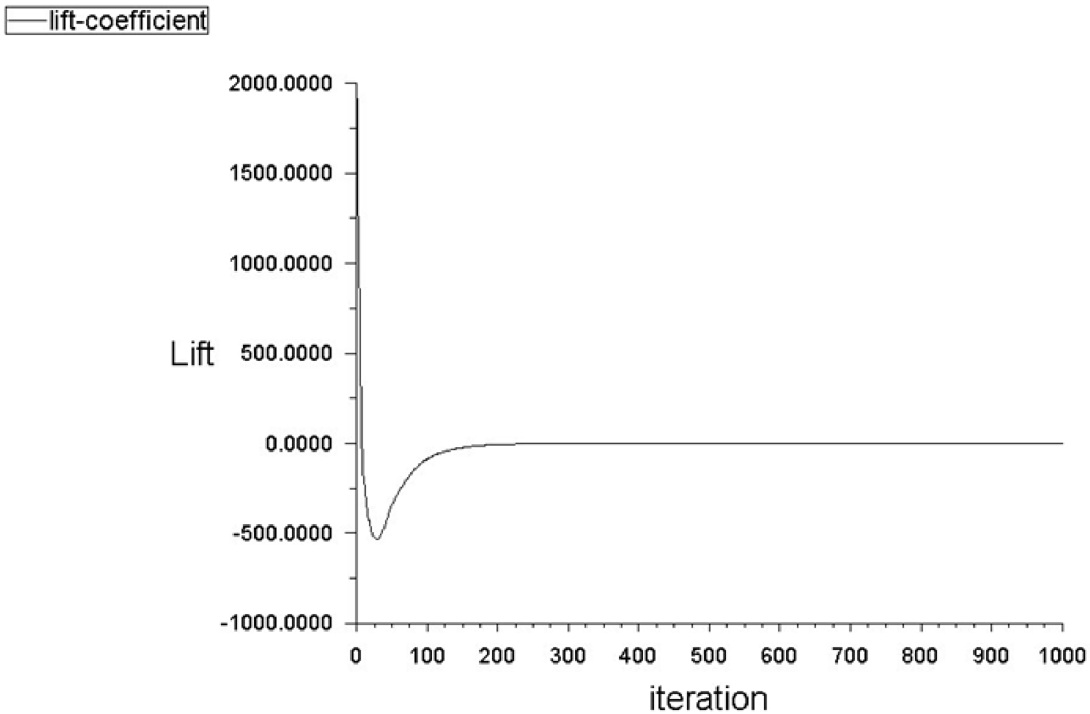

Figure 5. 19 Lift coefficient of modified bus at 100 km/h

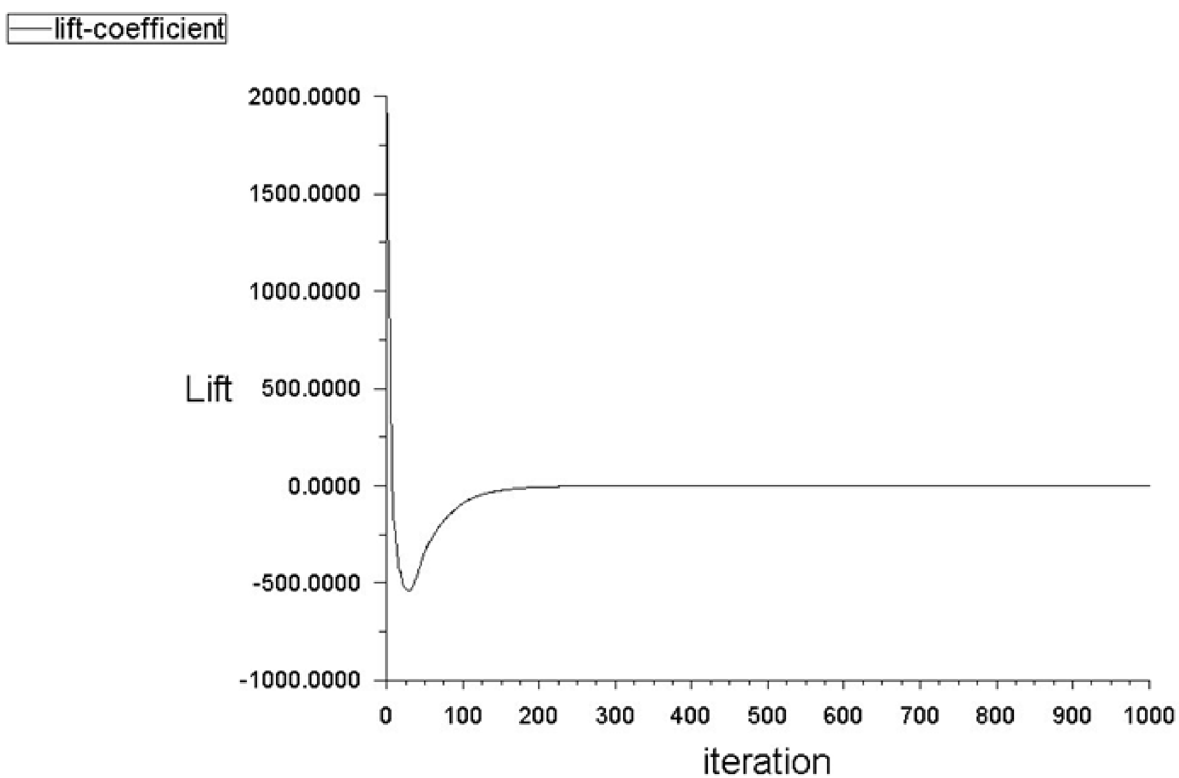

Figure 5. 20 Lift coefficient of modified bus at 120 km/h

4. Pressure contour

Pressure contour of modified bus in figure 5.21 - 5.23 obtained from CFD simulation, the blue color indicate negative pressure while the red color indicates positive pressure ranging from bottom to top. The red color on front face reveals a region with high positive pressure. Wherever the drag force acts on the bus, to the extent that the yellow color at the upper, and again toward the sides of the bus, is the color signifying a region of low area pressure. The blue color shows a minimum pressure surface. When speed of air increase the magnitude of pressure increase both in positive and negative region area of bus surface When compared to the existing model, there is slight improvement in high pressure regions, however, there is much better improvement in pressure when compared to the overall results.

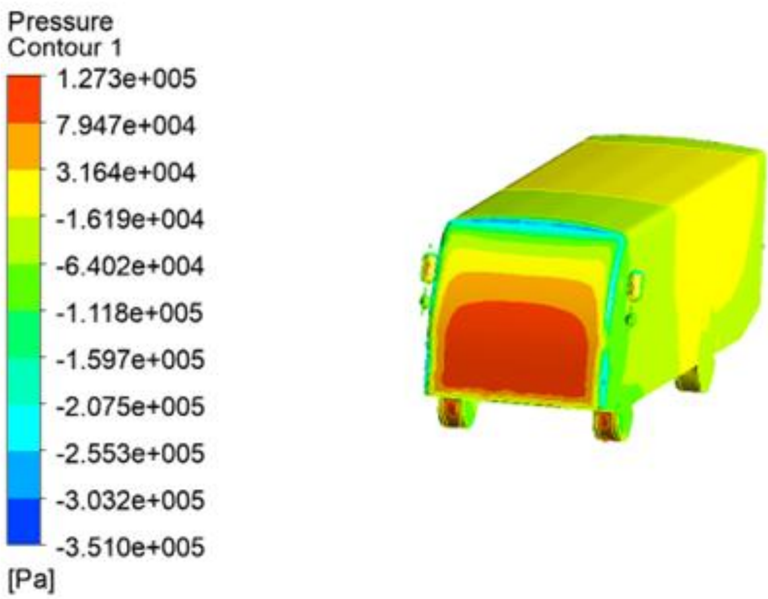

Figure 5. 21 pressure contour of modified bus at 80km/h

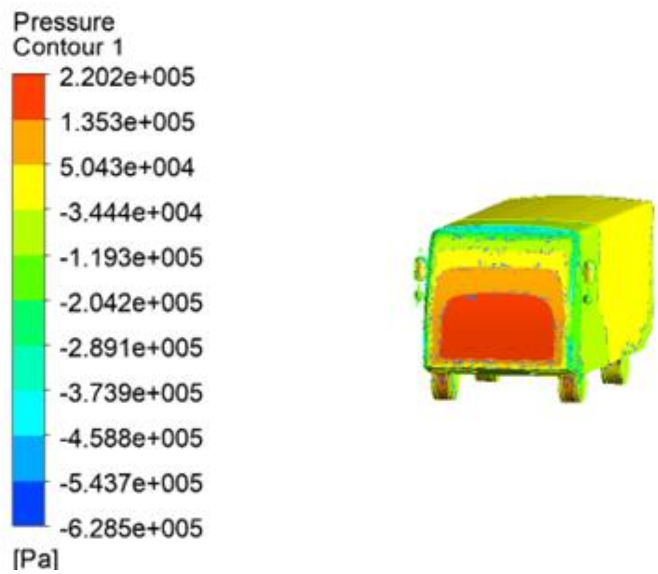

Figure 5. 22 pressure contour of modified bus at 100km/h

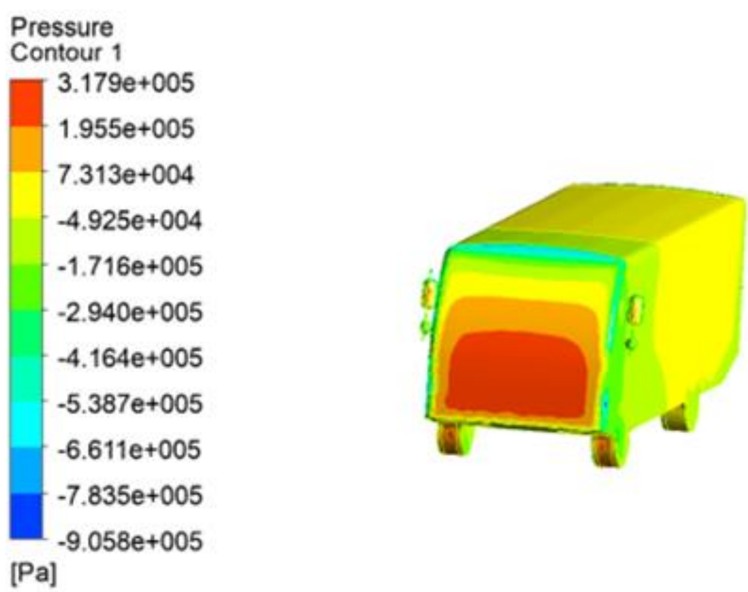

Figure 5. 23 pressure contour of modified bus at 120km/h

As shown on the above three figure the maximum pressure contour at speed of 80km/h, 100km/h and 120km/h is 127.3kpa, 220.2kpa and 317.9kpa respectively.

5. Velocity contour

The front shape of the existing bus is flat below the midpoint height of front face and inclined with small angle above midpoint of the bus small inclination angle. This flat front shape is not recommended from aerodynamic performance. In order to reduce the resistance area of the vehicle, it is very important to solve the problem by improving the curvature of the front type. Very important areas with low speeds occur behind the bus. The low velocity is noticed on the frontal face too. A distinct high-velocity zone is visible above the front of the bus. The concentration and relative magnitude of the high velocity in that specific region above the front of the bus seem to be greater.

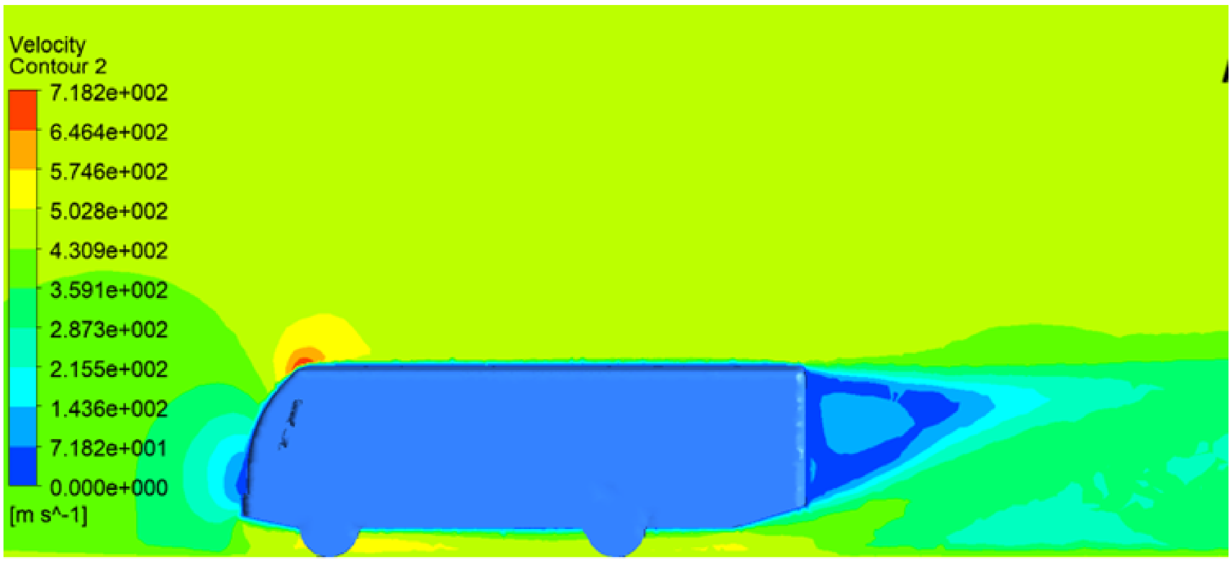

Figure 5. 24 velocity contour of modified bus at 80km/h

Figure 5. 25 velocity contour of modified bus at 100km/h

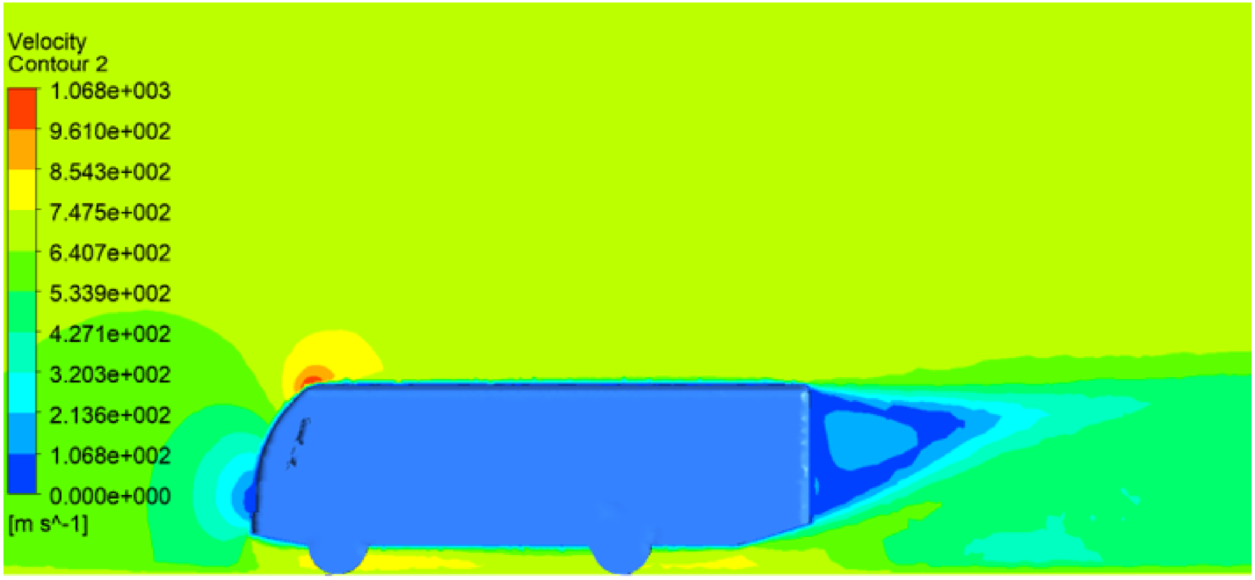

Figure 5. 26 velocity contour of modified bus at 120km/h

As indicated on the above figure 5. 24 – 5.26 the maximum velocity contour of scaled modified bus at 80km/h, 100km/h and 120km/h is 718.2m/s, 889.3m/s and 1068m/s respectively. The velocity of scaled existing bus is 544.2m/s, 690.2m/s and 819.6m/s respectively when comparing with the modified and existing model the velocity increase at modified bus model.

Table 5. 2 the summery results of the modified model.

Frontal area of scaled modified bus(m^2)	**Speed (km/h)**	**Drag**		**Lift**	
		Drag coefficient	**Drag force**	**Lift coefficient**	**Lift force**
4.88	80	0.4693	693.66	-0.3327	-491.51
	100	0.4687	1085.68	-0.3326	-767.78
	120	0.4678	1554.85	-0.3319	-1103.22

5.4 Comparison between of modified and existing bus

To investigate the aerodynamic effects of front shape on the existing bus, stability effect of previous modified bus CFD simulations are performed on a 1:10 scale model. Two distinct scenarios are analyzed to evaluate the impact of front shape on the bus's aerodynamic performance and stability improvement. The method provided control and systematic investigation of the influence of front-end shape on the aerodynamic characteristics of the bus; also with a view to investigating how the increment in height affects stability while providing useful parameters towards design enhancement.

A. Comparison in terms of frontal area

- **% Frontal area decrease =** $\frac{5.33-4.88}{5.33}$ x $100 = 8.44\%$

The frontal area of existing bus decrease by 8.44% when compared with modified one

- **Comparison with drag force**

% of drag force decrease at 80km/h, 100km/h and 120km/h

% of drag force at 80km/h $= \frac{1043.89 - 693.66}{1043.89} x\ 100$ = 33.55%

% of drag force at 100km/h = $\frac{1623.27 - 1085.68}{1623.27} x\ 100$ =33.11%

% of drag force at 120km/h = $\frac{2324.40 - 1554.85}{2324.40} x\ 100$ = 33.10%

The percentage decrease in drag force at 80km/h, 100km/h and 120km/h is 33.55%, 33.11% and 33.10% respectively.

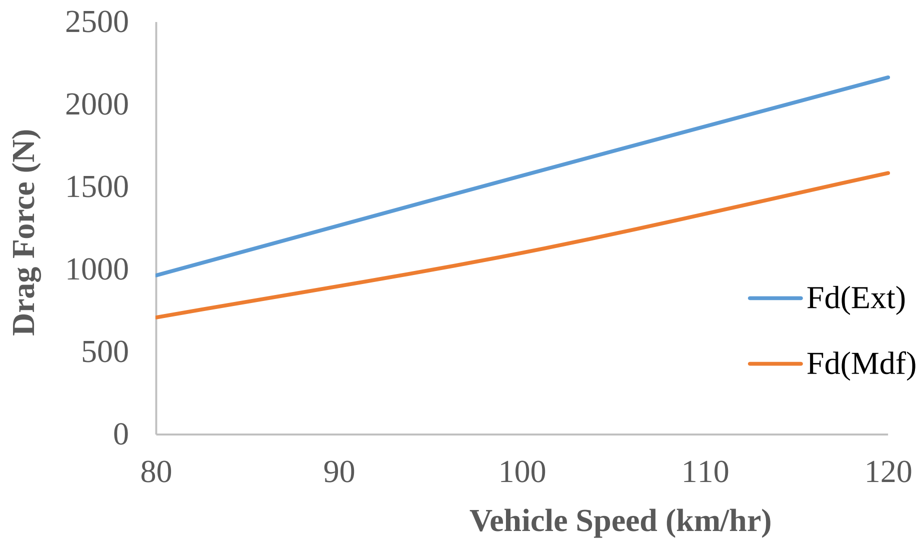

Figure 5. 27 Drag force comparison of existing and modified bus

Table 5. 3 The lift and drag coefficient of existing and modified bus

Bus	Frontal area (m^2)	Speed (km/h)	Drag		Lift	
			Drag coefficient	Drag force (N)	Lift coefficient	Lift force (N)
Existing bus model	5.33	80	0.6473	1043.89	-0.1630	-262.87
		100	0.6442	1623.27	-0.1608	-405.32
		120	0.6406	2324.40	-0.1605	-582.60
Modified bus model	4.88	80	0.4695	693.66	-0.3327	-491.51
		100	0.4687	1085.68	-0.3326	-767.78
		120	0.4678	1554.85	-0.3319	-1103.22

Table 5.3 shows that the drag coefficients measured for the existing buses are very similar. The frontal area of the modified bus is lesser than that of the existing bus. However, the drag

coefficient of the modified buses is lower than that of existing buses. Thus, ensuring that its drag force is low compared to the rest, because aerodynamic drag defines itself by both drag coefficient and projected frontal area of the body. Negative lift is preferable and increases the contact pressure acting between the wheels and the ground. "Negative" indicates the direction of the force. The table above depicts that additional lift created by the existing bus and modified bus would assist in tire road holding. The downward force on the bus increases with speed of the bus, which is a desirable feature for stability.

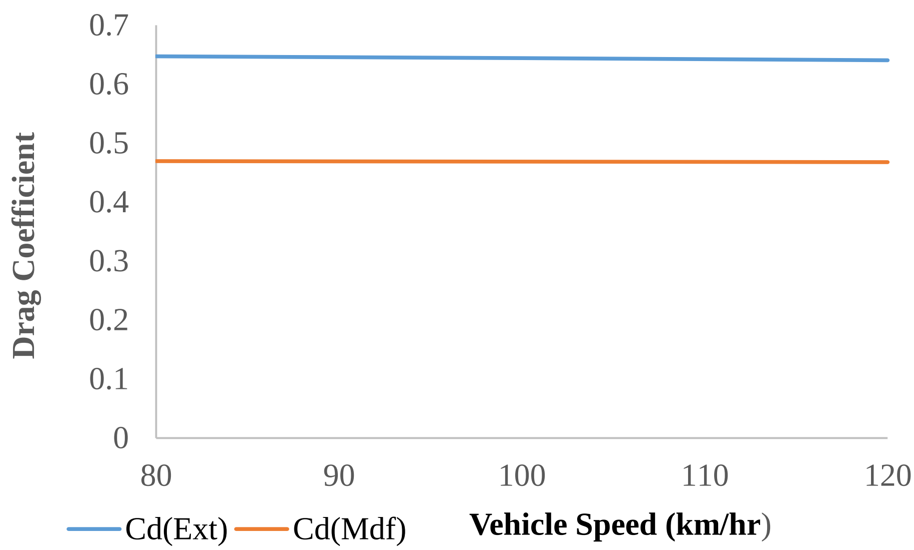

Figure 5. 28 Drag coefficient comparison of existing and modified bus

Table 5. 4 lift force and lift coefficient reduction

Bus	Frontal area (m^2)	Speed (km/h)	Lift		% of lift coefficient reduction	% of lift force reduction
			Lift coefficient	Lift force (N)		
Existing bus model	5.33	80	-0.1630	-262.87	_	_
		100	-0.1608	-405.32	_	_
		120	-0.1605	-582.60	_	_
Modified bus model	4.88	80	-0.3327	-491.51	-104.11	-87.23
		100	-0.3326	-767.78	-106.84	-89.42
		120	-0.3319	-1103.22	-106.79	-89.36

Tables 5.4 indicate lifting coefficient of two models at various speed studied in this thesis. For vehicle stability improvement at higher speeds, high down force is needed as a result of reduced lift coefficients. The modified model has the least lift coefficient making the existing model most stable at higher speeds. The reasoning for the results of lift coefficient being negative is that its lift force is directed downward, which works to hold the wheel on the ground. There is a percentage variation from existing model. Since the force is lift force downward it shows an improvement in stability of the bus. The reduction of lift coefficient at taken speed is -104.11%. -106.84% and – 106.79% respectively. The lift force is -87.97%, -89.42% and -89.36% respectively. Since the value is negative it indicates lift force is down ward direction that is used to wheel grip on road which increase the stability of the bus.

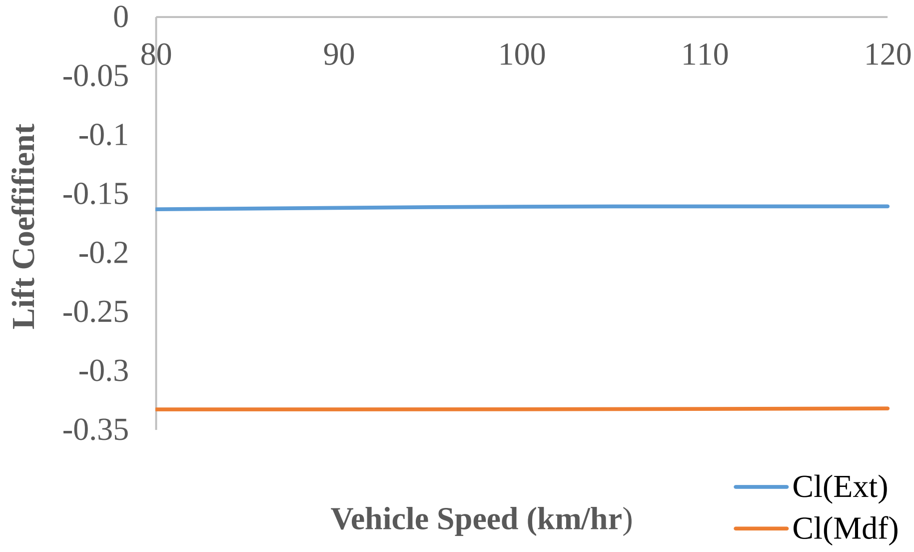

Figure 5. 29 Lift coefficient comparison of existing and modified bus

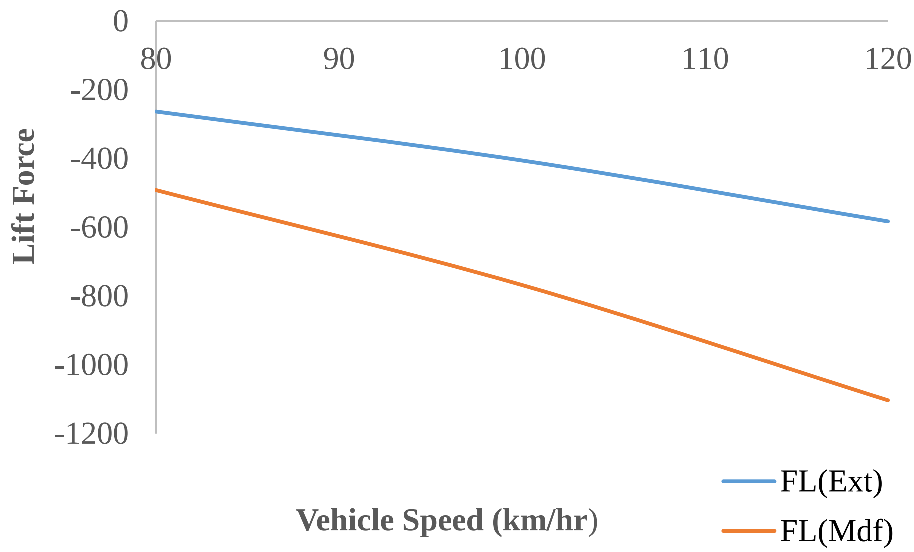

Figure 5. 30 Lift force comparison of existing and modified bus

5.5 Drag reduction in percentage

Table 5. 5 Comparison of existing and modified bus

Model	Speed (km/h)	Drag coefficient(Cd)	Drag force (Fd)	Percentage(%) of Cd reduction	Percentage(%) of Fd reduction
Existing bus	80	0.6473	1043.89	–	–
	100	0.6442	1623 27	–	–
	120	0.6406	2324.40	–	–
Modified bus	80	0.4695	693.66	27.46	33.55
	100	0.4687	1085.68	27.24	33.11
	120	0.4678	1554.85	26.97	33.10

The data depicted in Section 5.5 indicates a considerably lower drag force for the modified bus design, with this improvement entirely attributed to the small features modified at the aerodynamic configuration. The modified bus has, in fact, been found to have a drag coefficient 27% lower than that of the existing model, signifying a lesser degree of drag configuration and therefore somewhat more aerodynamic. The lessened drag coefficient affirms that the redesigned bus would cause lesser resistance by allowing smoother flow of air around the body. Another huge advantage to the modified bus over the existing bus is that it experiences a reduction of about 33.25% of the total drag under direct comparison, and this major reduction can be attributed mostly to the smaller frontal area of the modified bus, which is the main area facing the air resistance. The decrease in the frontal area reduces the amount of air in which the bus is replaced, indicating that obstacles will be less in the future.

Therefore, reduce resistance**.** The significant enhancement in aerodynamic performance of the modified bus through decreased drag coefficient and smaller frontal area corroborates the fact that aerodynamics really matters in improving vehicle efficiency.

5.6 Fuel consumption

The formula used to calculate the power and fuel saved due to the increased aerodynamic efficiency of the bus mainly from the reduced drag force (Kahsay and Zeleke, 2024).

5.6.1 Power and fuel saving

$$P_{sav} = (F_{D-\,Existing} - F_{D-\,Modified}) \text{ x } V_{bus} \text{-----------------------------------equ (5.1)}$$

Where, P_{sav} = power saved (W)

$F_{D\,-\,exsisting}$ = Drag force of existing bus (N)

$F_{D-\,modified}$ = Drag force of modified bus (N)

V_{bus} = velocity of bus (m/s)

$$\dot{m}_{fuel} = \frac{P_{sav}}{Q_{LHV} X \rho_{fuel}\, x \eta_{engine}} \text{----------------------------equ(5.2)}$$

$\dot{m}_{fuel}$ = mass flow rate (m^3/s)

Q_{LHV} = Lower heating value (Q_{LHV} of diesel 42.5MJ/kg)

ρ_{fuel} = density of fuel at ambient temperature (860kg/m^3)

η_{engine} = thermal efficiency of engine (thermal efficiency of engine 35%)

The unit of fuel consumption is m^3/s, 1m3/s =3.6 L/hr

Table 5. 6 Power saved

Model	Speed (km/h)	Drag force (F_d)	Power saved(w)	Fuel saved (L/h)
Existing bus	80	1043.89	−	
	100	1623 27	−	
	120	2324.40	−	
Modified bus	80	693.66	7782.11	2.19
	100	1085.68	14928.87	4.20
	120	1554.85	25649.10	7.21

Table 5.6 shows the amount of energy stored at speeds of 80 km/h, 100km/h and 120 km/h, 7782.11 w, 14928.87 W and 25649.1 w, respectively. The amount of fuel saved in 80 km/h, 100 km/h and 120 km/h is 2.19 l/h, 4.20 l/h and 7.21 l/h, respectively. So the result is that the power and fuel consumption are better with the modified tires than with the earlier models. At the same time increase in vehicle speed, air resistance also increases.

Therefore, to maintain this fast speed more engine power requires (Kahsay and Zeleke, 2024)

5.6.2 Reduced fuel consumption

Fuel reduction percentage rate = 3/5 (CD total reduction percentage rate)

Table 5. 7 Fuel consumption reduction

Model	Speed (km/h)	Drag coefficient(C_d)	Percentage(%) of C_d reduction	Percentage(%) of fuel saved
Existing bus	80	0.6473	−	−
	100	0.6442	−	−
	120	0.6406	−	−
Modified bus	80	0.4695	27.46	16.47
	100	0.4687	27.24	16.34
	120	0.4678	26.97	16.18

According to data from table 5.7 the amount of fuel consumption reduction between existing and modified bus at velocity of 80km/h, 100km/h and 120km/h is 16.47%, 16.34% and 16.18% respectively. Therefore, the average amount of fuel reduction is 16.33%.

5.7 Experimental Results

Computational fluid dynamics is one of the methods used to analysis aerodynamic performance. The other method used to analyze the air flow over the surface of the body is HM170 educational wind tunnel test machine. This tunnel work with scale down 3D printed model. The test was done under speed of 14m/s, 19.6m/s and 25.2m/s respectively.

Drag coefficient depend on air velocity. In experimental tests the static ground is not similar to as real operating condition. That is due to the boundary layer at static ground that affects Reynolds number is because Reynolds number is a function of air velocity (Mario et. al, 2020).

Table 5. 8 the drag force 3D model at forward speed (straight)

Frontal area of scaled 3Dmodel (m^2)	**Wind speed (m/s)**	**Drag force (N)**
0.004347	14	0.26
	19.6	0.5
	25.2	0.81

The drag coefficient of this test is calculated by using the drag force value taken from measurement amplifier reading during test. The density of air at the room temperature condition is 1.172/m^3.

$$C_d = \frac{2F_{D-3D\ model}}{\rho V^2 A} \text{--equ(5.2)}$$

Where: - Cd = drag coefficient

F_D = Drag force

A = Frontal area

ρ = density of air

V = velocity of air

Table 5. 9 the drag coefficient of CFD Simulation (numerical) and Experimental result

Frontal area of 3D model (m^2)	**Speed (m/s)**	**Drag coefficient result**		**Deviation (%)**
		Numerical	**Experimental**	
0.004347	14	0.4695	0.52	10.9
	19.6	0.4687	0.511	9
	25.2	0.4678	0.50	7

The result from the above table indicate the percentage increase of experimental results from numerical results are 10.9%, 9% and 7% respectively at speed of 14m/s, 19.6m/s and 25.2m/s respectively. The reason for the increase in percentage is because of variation in speed, vibration of small scale model and operating condition. However considering the data from the previous research the above result is acceptable.

5.8 Conclusion and recommendation

Conclusion

Most of the previous research shows ISUZU passenger bus is inefficient in fuel consumption and unstable due to aerodynamically inefficient design of exterior shape, height of the bus and overloading. The objective this study is to reduce aerodynamic drag and improve the stability of the ISUZU passenger bus. To address these issue design improvement of front end shape and headroom of ISUZU is studied under this thesis. The front end shape is modified with curvature shape with radius of 180mm and their effect on drag and stability are studied. Also the minimum headroom height is studied depending different anthropometric data and reference of past studied. According to the results from computational fluid dynamics (CFD) and experimental test the drag coefficient are decreased and the stability is improved. The overall efficiency of aerodynamic performance is increased.

Drag

- ✓ Improving the front-end shape leads to a reduction in frontal area and drag coefficient, this increases aerodynamic efficiency.
- ✓ The drag coefficient of the modified bus at speeds of 80 km/h, 100 km/h, and 120 km/h improved by 27.22% compared to the existing bus.
- ✓ The drag force of the modified bus was reduced by 33.25% compared to the existing model.
- ✓ These aerodynamic improvements contribute to fuel savings of 16.47% at 80 km/h when comparing the modified bus to the existing design.

Lift

The lift force of the modified bus increased in -89.85%**,** indicating a significant increase in downward force (the negative sign shows the direction is downward).

- ✓ This increase in **downforce** helps grip the wheels to the ground, contributing to improved stability.
- ✓ Changing the diffuser angle from 7.24° to 17.5° altered the lift coefficient, resulting in more downward force and better tire contact with the road surface.

Stability

- ✓ The increased downward lift force enhances wheel grip, which improves the stability of the bus, especially at higher speeds.
- ✓ Reduction in vehicle height lowers the center of gravity, which plays a significant role in improving stability.
- ✓ A lower center of gravity also reduces the risk of rollover or accidents.

5.9 Recommendation

- ✓ The locally manufacturing company of modified ISUZU bus must be aware of the aerodynamic impact on fuel consumption.
- ✓ The manufacturing companies of this bus have to work with aerodynamically skilled person and it should implement a continuous improvement process of aerodynamics.

REFERENCES

Chen et al. (2019). Research and Optimization of Vehicle Handling Stability Based on Multi - body Dynamics.

P Chirinda & Matope. (2020). The Lighter the Better: Weight Reduction in the Automotive Industry and its Impact on Fuel Consumption and Climate Change.

Thakur et al. (2020). A Study of Cross Wind Effect on Bike's Aerodynamic.

A study of wake effects on the drag of Ahmed′s squareback model at the industrial scale. (2015).

Effects of Aerodynamic downforce on Vehicle Control and Stability. (2021).

A.Muthuvel et al. (2013). Aerodynamic Exterior Body Design of Bus.

Abdullah. (2021). *The Effect of Automotive Aerodynamics in Fuel Consume.* International Journal.

Agarwal. (2020). AERODYNAMICS OF VEHICLES.

Arabaci. (2022). Aerodynamic Design of Buses Inspired by Beluga Whales .

Arteaga et al. (2020). Aerodynamic optimization of the body of a bus.

Ashagrie et al. (2017). A Study on Driving Stability of Bus Using Computational Fluid Dynamics (CFD).

Chinta & Rao . (2014). A New Design and Analysis of BUS Body Structure .

Chowdhury et al. (2012, July 26). Impact of Vehicle add-ons on Energy Consumption and Greenhouse Gas Emissions. *www.scienceDirect.com*.

Damissie et al. (2017). *Aerodynamic Drag Reduction on Locally Built Bus Body using Computational Fluid Dynamics (CFD): A Case Study at Bishoftu Automotive Industry.* Adama: International Journal.

Digssie et al. (2016). Developing an equation for estimating body height from linear body measurements of Ethiopian adults.

Fridman & Napper. (2016). An analysis of bus interior headroom for future design applications.

Fridman and Napper . (2016). An analysis of bus interior headroom for future design applications.

G/yesus et, al. (2013). Ergonomics Assessment of Passenger Seats of Mini-Buses in Ethiopia.

Grandemange et al. (2015). A study of wake effects on the drag of Ahmed′s squareback model at the industrial scale.

Hagnell et al. (2020). From aviation to automotive - a study on material selection and its.

Howell et al. (2021). Ssome Observations on Shape Factors Influencing Aerodynamic Lift on Passenger Cars.

Iresha et al. (2021). *Effects of Crosswind on an Automobile Under Dynamic Conditions.* Sri Lanka.

Kahsay and Zeleke. (2024, March). Aerodynamic design optimization of locally built FSR Isuzu bus through numerical simulation. *European Journal of Mechanics - B/Fluids 85:181-192*.

kamur et al,. (2019). *Analysis of Subjective Qualitative Judgement of Passenger Vehicle High Speed Drivability due to Aerodynamics.* Chalmers: DOI:10.3390/en12142839.

kamur et al. (2019). Analysis of Subjective Qualitative Judgement of Passenger Vehicle High Speed Drivability due to Aerodynamics.

Kapote. (2024). Aerodynamic Drag Reduction of Heavy Vehicle Using Computational Fluid Dynamics (CFD).

Khademian et al. (2020). Lightweight materials (LWM) in transportation especially application.

Kim et al. (2017). Salient drag reduction of a heavy vehicle using modified cab-roof fairings.

M. Palanivendhan et al. (2021). Reduction in aerodynamic drag acting on a commercial vehicle by using a dimpled surface.

Manigandan. (2024). Design and Analysis of a Car Body Using aerodynamic model.

Mario et. al. (2020). Numerical and experimental analysis of drag force in medium speedtrain design.

Mcarthur et al. (2018). An experimental characterisation of the wake of a detailed heavy vehicle in cross-wind.

Minh Hoang Trinh et al. (2022). Study on the Dynamic Instability of a Bus in Crosswind Conditions.

Mirmahdi et al. (2021). *The Effect of Aerodynamic Forces on Automotive Design and Reducing Fuel Consumption.*

Mukut & Abedin. (2019). Review on Aerodynamic Drag Reduction of Vehicles.

Nizom. (2011). Study of Aerodynamics of Double Decker Bus for Driving Stability.

R.Jadhav & P.Chorage. (2020). Modification in commercial bus model to overcome aerodynamic drag effect by using CFD analysis.

Raj et al. (2020). STRUCTURAL ANALYSIS OF BUS BODY FRAME USING FEA FOR STATIC.

Reddy & R. Locanadham. (2017). *CFD ANALYSIS ON AERODYNAMIC EFFECTS ON A PASSENGER CAR.*

Reddy et al. (2016). DESIGN AND ANALYSIS OF BUS BODY SUPERSTRUCTURE.

Ribeiro et al. (2022). Drag reduction of a commercial bus with add-on aerodynamic devices.

Roy & Sharma. (2021). Effects of Aerodynamic downforce on Vehicle Control and Stability.

Roy et al. (n.d.). Effects of Aerodynamic downforce on Vehicle Control and Stability.

S.Nath et al. (2021). Drag reduction by application of aerodynamic devices in a race car.

Sikder & Abedin. (2023). 1. Experimental investigation for reducing aerodynamic drag and fuel consumption in a passenger bus.

song, l. &. (2015). *Structural local analysis and optimization of bus body skeleton.*

Szodrai. (2022, Maya 9). Numerical Assessment of Side-Wind Effects on a Bus in Urban Conditions. *https://doi.org/10.3390/app12115688*.

Tafesse et al. (2018). Design and Analysis of Body Structure: a Case of Locally Built Isuzu Passenger Bus.

Tam et al. (2023). Optimization of frame structure coach 29/34 seats in static durability state.

Tirfe et al. (2021). Investigating the Aerodynamic Effect of Rooftop Cargo Compartment – a Case of Modified Intercity Bus.

UI Hoque et al. (2018). Aerodynamic Shape Optimization of Vehicles Using CFD Simulation.

yang & deny. (2015). *Structural local analysis and optimization of bus body skeleton.*

yang et al. (2021). Aerodynamic Shape Optimization Method of Non-Smooth Surfaces for Aerodynamic Drag Reduction on A Minivan.

Yuan and Wang. (2017). Effect of underbody structure on aerodynamic drag and optimization.

yudianto et al. (2021). Aerodynamics of Bus Platooning under Crosswind.

Zhang et al. (2020). Numerical investigation on aerodynamic performance and stability of a sedan under wind–bridge–tunnel road condition.

Zhou et al. (2022). Analysis of the aerodynamic characteristics of the outflow. *Guangzhou Automobile Group Co., Ltd Automotive Engineering Institute,*.

APPENDIX

Appendix A: ANSYS RESULT DATA

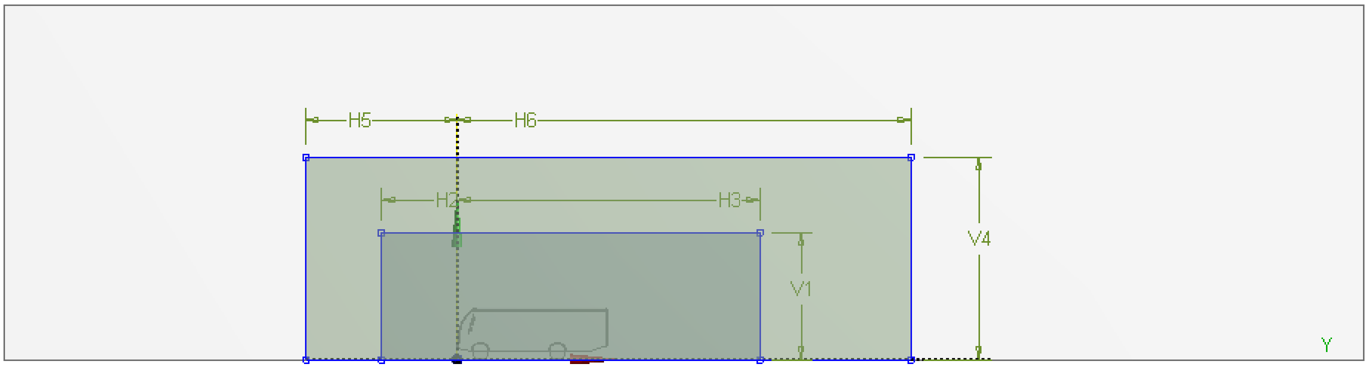

Figure A -1 Geometry of modified bus inside enclosure and two inner box

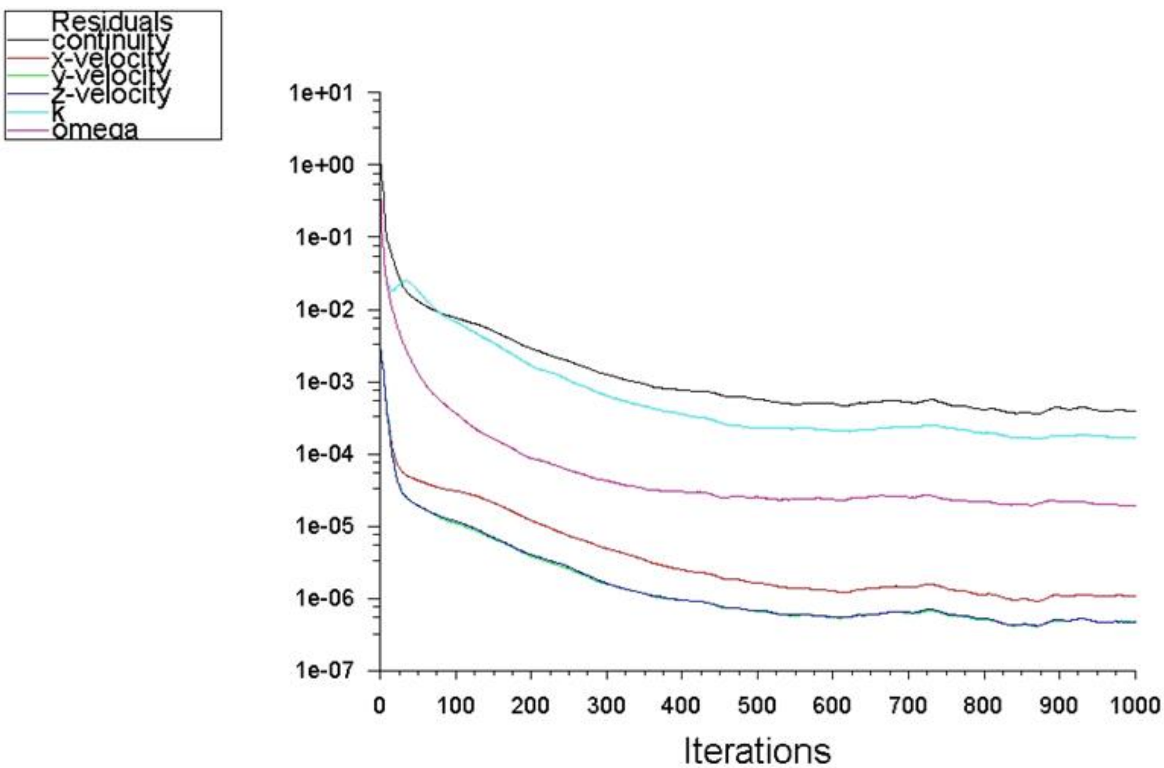

Figure A -2 Residual history of existing bus at 100km/h

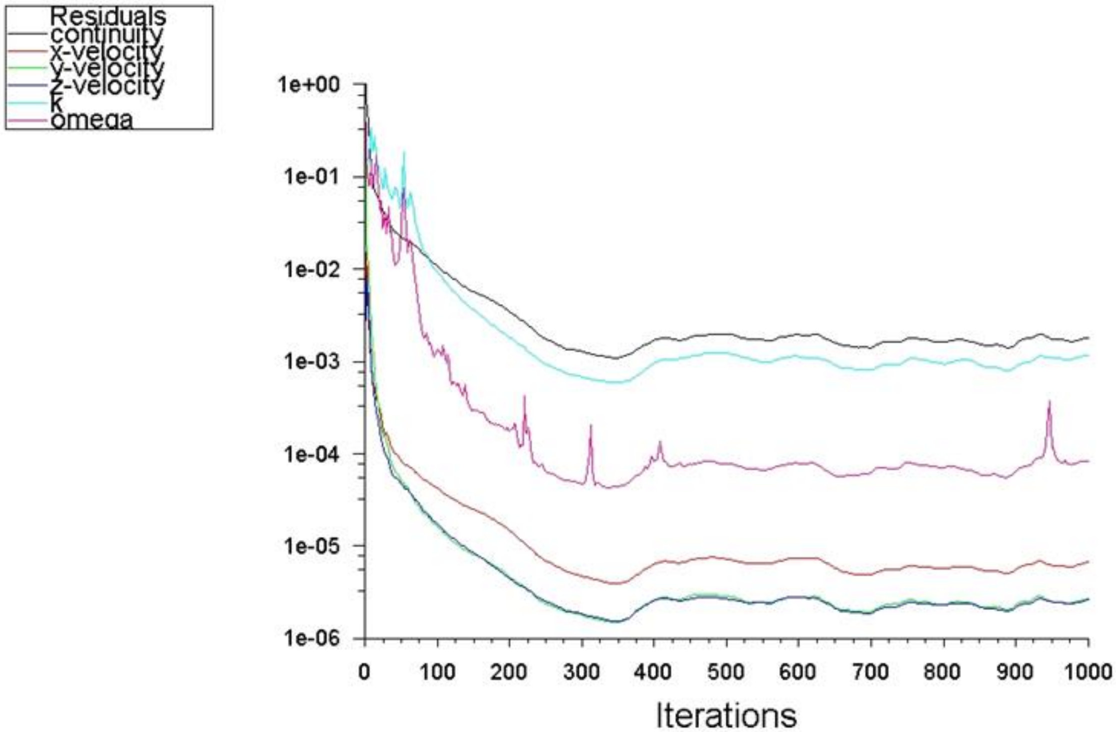

Figure A – 3 Residual history of existing bus at 120km/h

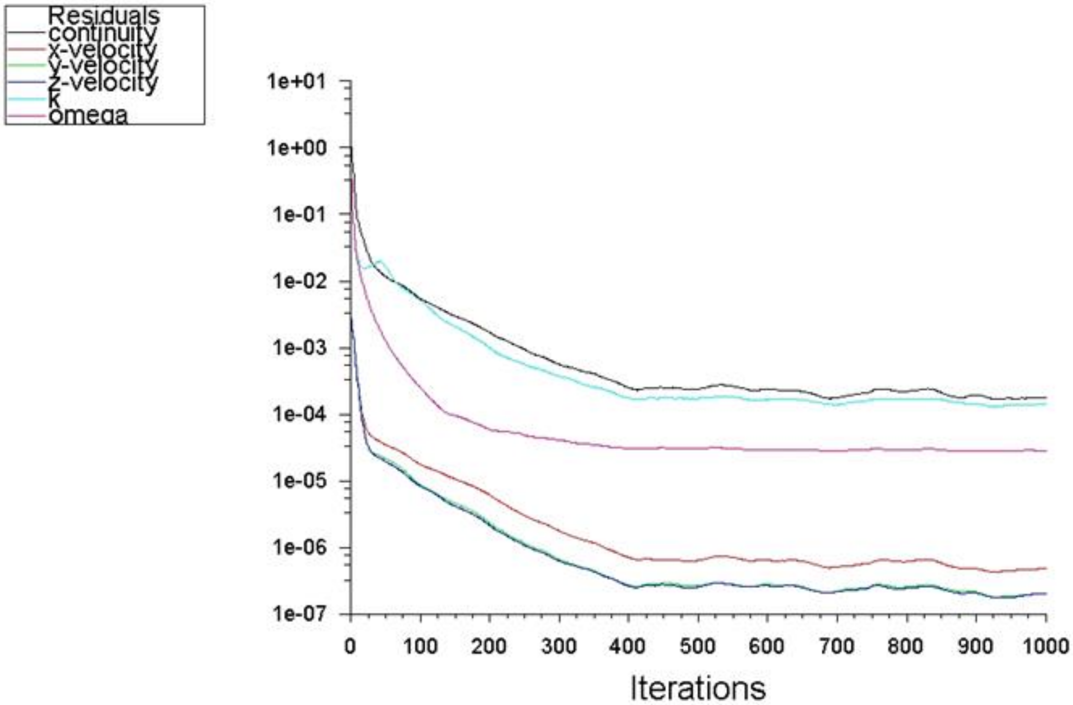

Figure A-4 Residual history of modified bus at 100km/h

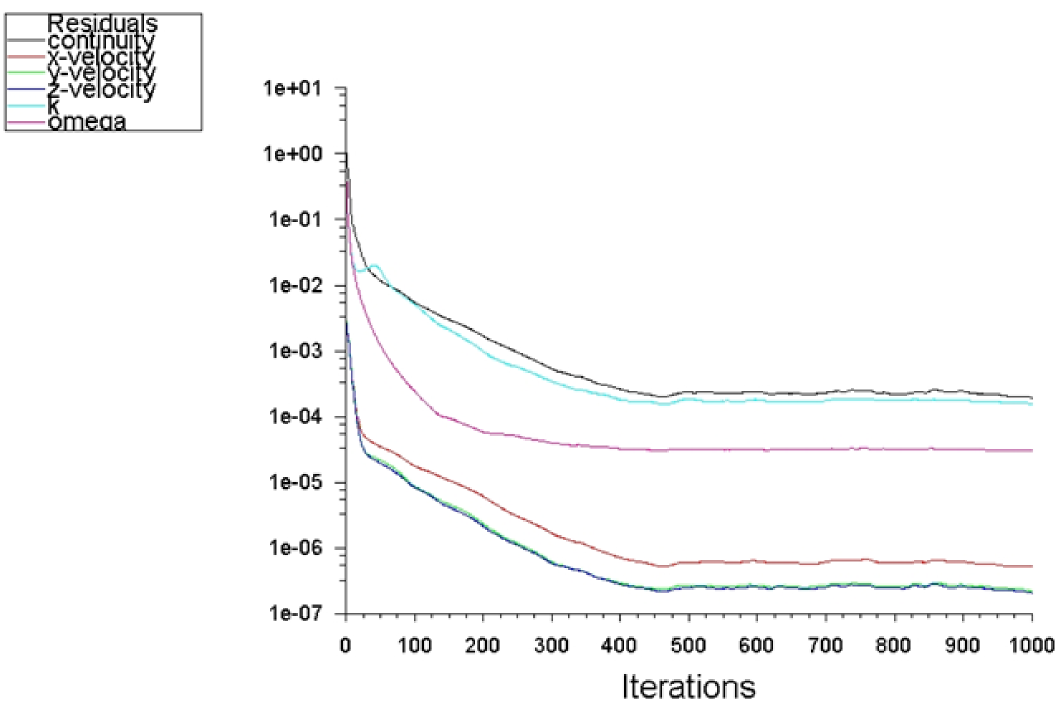

Figure A-5 Residual history of modified bus at 120km/h

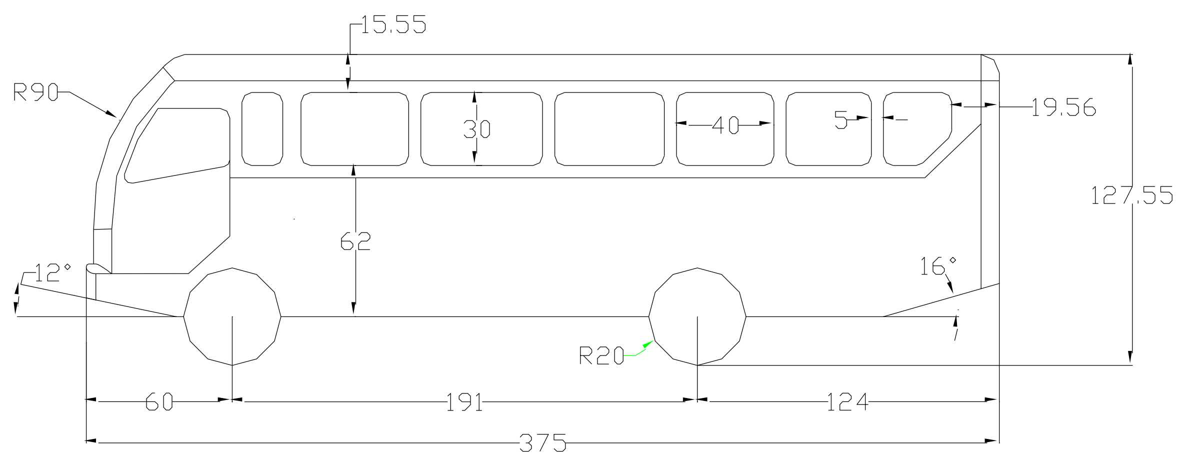

Right side view of the scaled modified bus	ASTU			
Drawn By Alemashet lemi	Drawing Title Right side view			
Advisor Alemayehu wakjira(PhD)	Size A3	Drawing Number 1		
	Scale 1:20	Sheet 1/1		

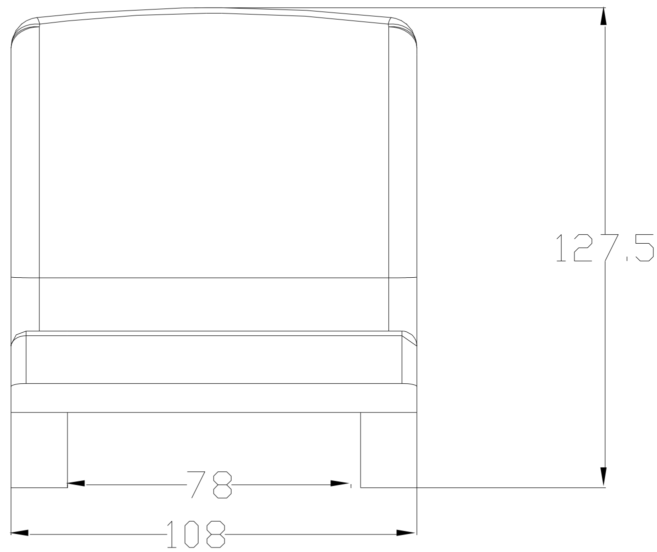

Front view of the scaled modified bus	ASTU	
Drawn By Alemashet lemi	Drawing Title: Front view	
Advisor Alemayehu wakjira(PhD)	Size A3	Drawing Number 2
	Scale 1:20	Sheet 1/2

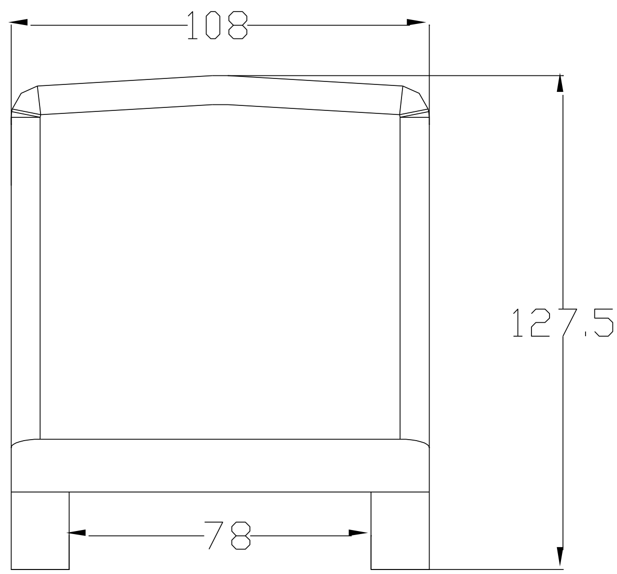

Rear view of the scaled modified bus	ASTU		
Drawn By Alemashet lemi	Drawing Title Rear view		
Advisor Alemayehu wakjira(PhD)	Size A3	Drawing Number 3	
	Scale 1:20	Sheet 1/3	

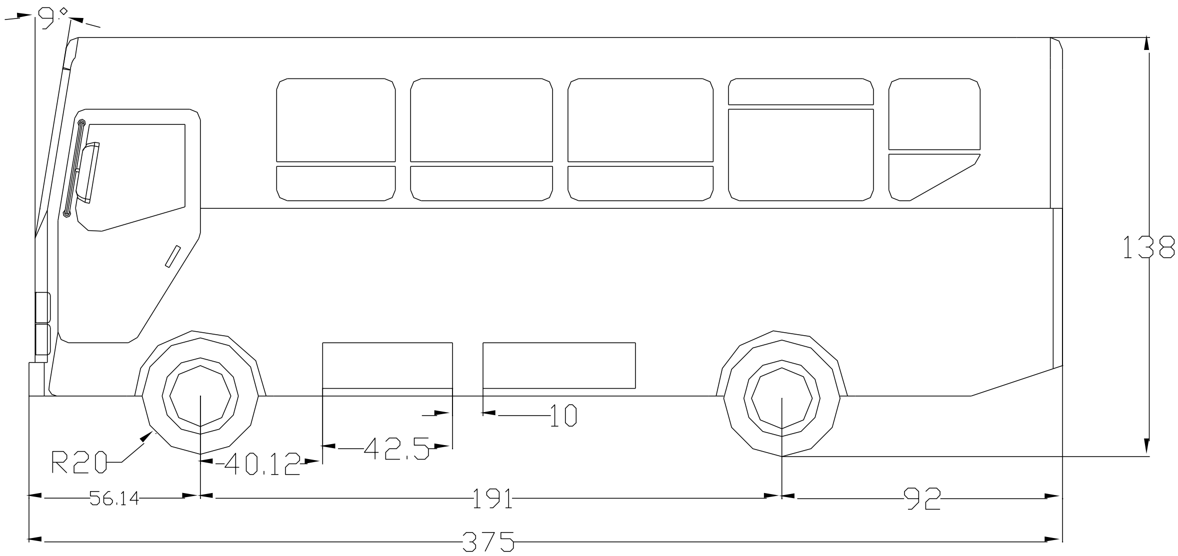

Right side view of the scaled existing bus	ASTU		
Drawn By Alemashet lemi	Drawing Title: Right side view		
Advisor Alemayehu wakjira(PhD)	Size A3	Drawing Number 4	
	Scale 1:20	Sheet 1/4	

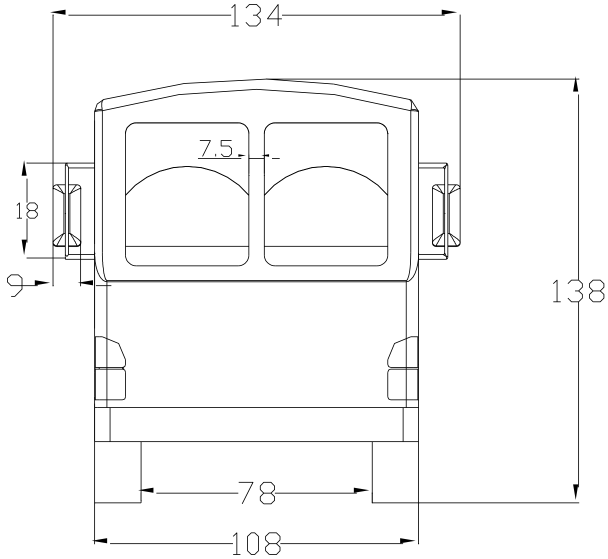

Front view of the scaled existing bus	ASTU		
Drawn By Alemashet lemi	Drawing Title Front view		
Advisor Alemayehu wakjira(PhD)	Size A3	Drawing Number 5	
	Scale 1:20	Sheet 1/5	

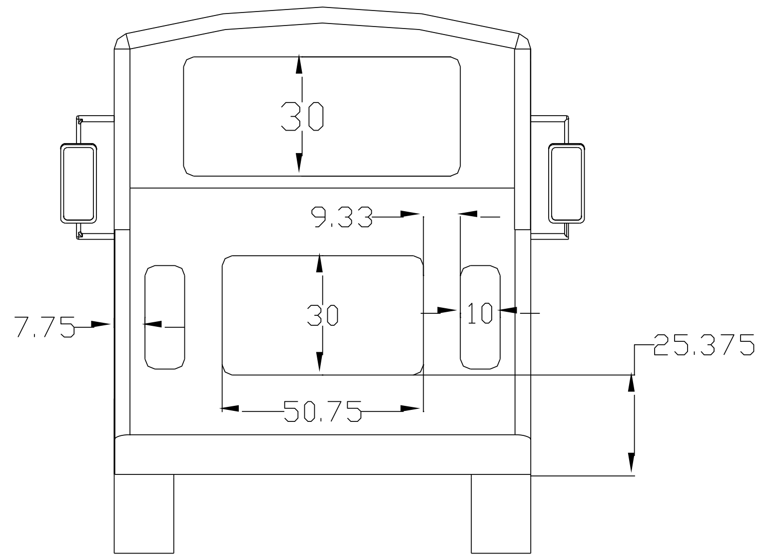

Rear view of the scaled existing bus	ASTU	
Drawn By Alemashet lemi	Drawing Title Rear view	
Advisor Alemayehu wakjira(PhD)	Size A3	Drawing Number 6
	Scale 1:20	Sheet 1/6

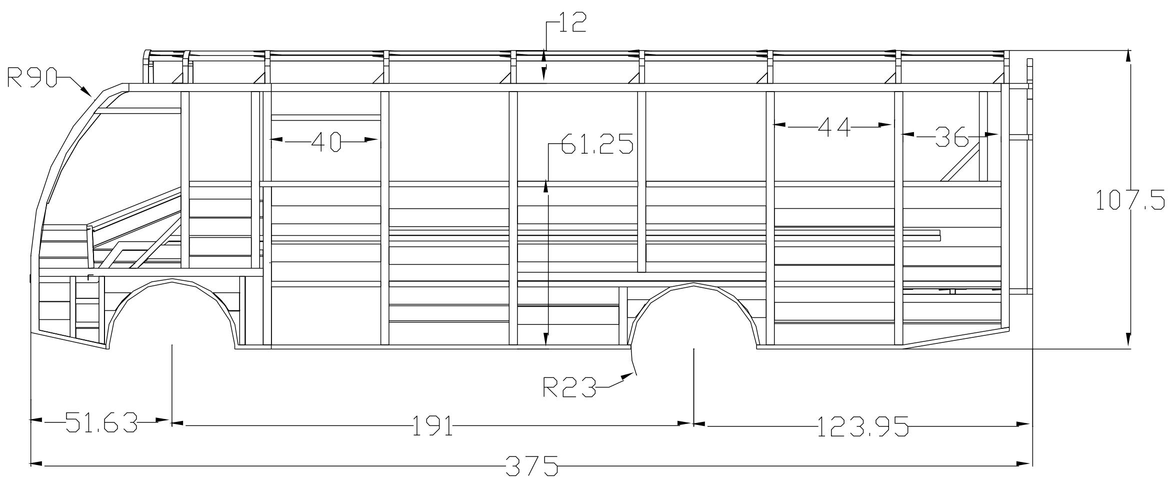

Right side view of the scaled structural skeleton	ASTU	
Drawn By Alemashet lemi	Drawing Title Right side view	
Advisor Alemayehu wakjira(PhD)	Size A3	Drawing Number 1
	Scale 1:20	Sheet 1/2

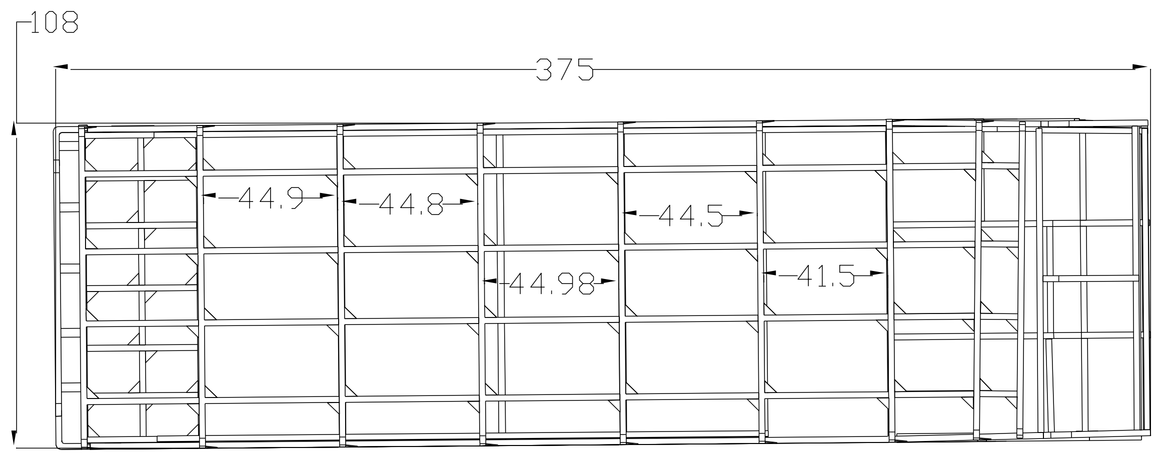

Top view of the scaled structural skeleton	ASTU		
Drawn By Alemashet lemi	Drawing Title Top view		
Advisor Alemayehu wakjira(PhD)	Size A3	Drawing Number 1	
	Scale 1:20	Sheet	1/9

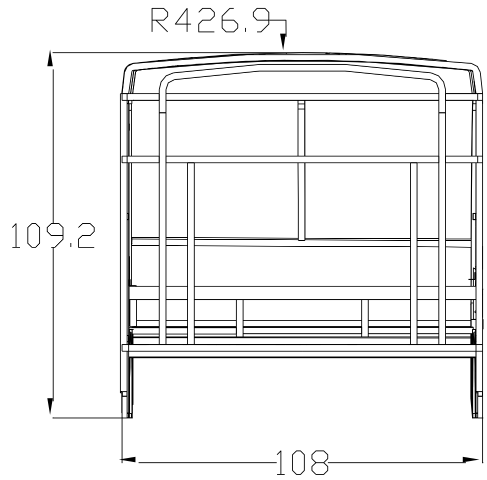

Rear side view of the scaled structural skeleton	ASTU	
Drawn By Alemashet lemi	Drawing Title Rear side view	
Advisor Alemayehu wakjira(PhD)	Size A3	Drawing Number 1
	Scale 1:20	Sheet 1/8